Advances in Materials Science and Engineering

Advanced Composites with Natural Reinforcement

Guest Editors: Jim Low, Ian J. Davies, Yu Dong, Shaikh Faiz Uddin Ahmed, Hao Wang, and Hazizan Md Akil

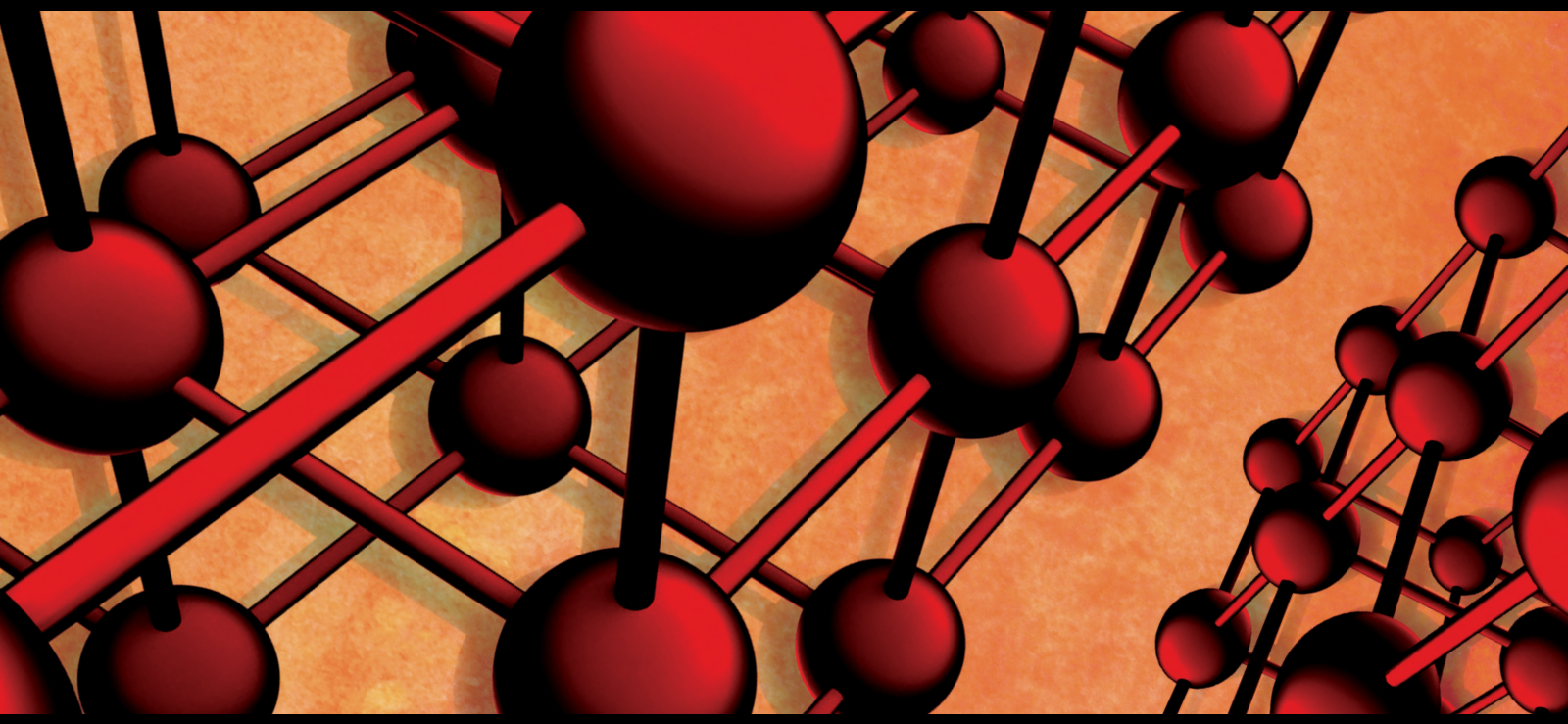

Advanced Composites with Natural Reinforcement

Advances in Materials Science and Engineering

Advanced Composites with Natural Reinforcement

Guest Editors: Jim Low, Ian J. Davies, Yu Dong,
Shaikh Faiz Uddin Ahmed, Hao Wang, and Hazizan Md Akil

Editorial Board

Contents

Hindawi Publishing Corporation
Advances in Materials Science and Engineering
Volume 2014, Article ID 376351, 2 pages
http://dx.doi.org/10.1155/2014/376351

Editorial

Advanced Composites with Natural Reinforcement

Jim Low,[1] Ian J. Davies,[2] Yu Dong,[2] Shaikh Faiz Uddin Ahmed,[3] Hao Wang,[4] and Hazizan Md Akil[5]

[1] *Department of Applied Physics, Curtin University, G.P.O. Box U1987, Perth, WA 6845, Australia*
[2] *Department of Mechanical Engineering, Curtin University, G.P.O. Box U1987, Perth, WA 6845, Australia*
[3] *Department of Civil Engineering, Curtin University, G.P.O. Box U1987, Perth, WA 6845, Australia*
[4] *Centre of Excellence in Engineered Fibre Composites (CEEFC), University of Southern Queensland, Toowoomba, QLD 4350, Australia*
[5] *School of Materials and Mineral Resources Engineering, Universiti Sains Malaysia, 14300 Nibong Tebal, Penang, Malaysia*

Correspondence should be addressed to Jim Low; j.low@curtin.edu.au

Received 12 December 2013; Accepted 12 December 2013; Published 22 April 2014

The strict environmental regulations and depletion of petroleum resources urge the use of alternative eco-friendly natural reinforcements to produce advanced composites. These natural fillers or fibres such as sisal, coir, basalt, hemp, flax, and wool offer great renewability, biodegradability, abundance, cost effectiveness, and low specific gravity as opposed to synthetic fibres like glass and carbon. Composite industry realises enormous advantages of their composites in better functional or structural properties over synthetic counterparts despite not having relatively high mechanical performance.

The popular research theme for composites with natural reinforcements generally covers polymer composites, geopolymer composites, ceramic composites reinforced with natural fibres and fillers (including some nano- or micro-fillers), fibre surface modification for the optimisation of mechanical properties, and processing of natural, renewable, and biodegradable reinforcements. This special issue aims to provide a platform for scientists, material engineers, researchers, and composite industrialists to exchange and share ideas and findings in this exciting field. There are totally six papers contained in this special issue to deal with the processing, characterisation, and properties of composites reinforced with various forms of natural fibres and fillers. The synopsis of each paper is as follows.

In *"Effect of zeolite modification via cationic exchange method on mechanical, thermal, and morphological properties of ethylene vinyl acetate/zeolite composites,"* surface modification of zeolite by organic modifier was found to be capable of improving the properties of EVA/zeolite composites.

In *"Pretreatment of woven jute FRP composite and its use in strengthening of reinforced concrete beams in flexure,"* woven jute fibre reinforced polymer composite was shown to be a suitable material which could be used for flexural upgradation of reinforced concrete beams.

In *"Efficacy of thermally conditioned sisal FRP composite on the shear characteristics of reinforced concrete beams,"* woven sisal fibre reinforced polymer composite was found to impart ductile failure and increased the shear strength and initial crack load of reinforced concrete beams.

In *"Nanofibre electrospinning poly (vinyl alcohol) and cellulose composite mats obtained by use of a cylindrical electrode,"* submicron PVA fibre mats reinforced with cellulose nanofibres were successfully prepared by the electrospinning of aqueous PVA solutions.

In *"Improvement of mechanical properties of noil hemp fiber reinforced polypropylene composites by resin modification and fiber treatment,"* resin modification and fibre treatment have been shown to be effective in improving interfacial bonding and enhancing the mechanical properties of composites.

In *"Investigation of mechanical and structural properties of blend lignin-PMMA,"* lignin was found to increase the impact strength but reduce the transverse strength and elastic modulus of PMMA resin.

Acknowledgments

We would like to thank all the authors who have submitted their papers to this special issue and also to all the reviewers for their invaluable contributions to the reviewing process.

Jim Low
Ian J. Davies
Yu Dong
Shaikh Faiz Uddin Ahmed
Hao Wang
Hazizan Md Akil

Hindawi Publishing Corporation
Advances in Materials Science and Engineering
Volume 2013, Article ID 435260, 6 pages
http://dx.doi.org/10.1155/2013/435260

Research Article

Investigation of Mechanical and Structural Properties of Blend Lignin-PMMA

Koray Soygun,[1] Selçuk Şimşek,[2] Ersen Yılmaz,[2] and Giray Bolayır[1]

[1] *Department of Prosthodontics, Faculty of Dentistry, Cumhuriyet University, 58140 Sivas, Turkey*
[2] *Department of Chemistry, Cumhuriyet University, 58140 Sivas, Turkey*

Correspondence should be addressed to Koray Soygun; koraysoygun@hotmail.com

Received 24 September 2013; Accepted 26 November 2013

Academic Editor: Jim Low

This *in vitro* study investigated the mechanical and structural characteristics of lignin-added PMMA resin composites at concentrations of 1, 3, and 5% by weight. Four sample groups were formed. For the transverse strength test, the specimens were prepared in accordance with ANSI/ADA specification number 12, and for the impact test ASTM D-256 standards were used. With the intent to evaluate the properties of transverse strength, the three-point bending ($n = 10$) test instrument (Lloyd NK5, Lloyd Instruments Ltd., Fareham, Hampshire, UK) was used at 5 mm/min. A Dynatup 9250 HV (Instron, UK) device was employed for the impact strength measurements ($n = 10$). All resin samples were tested by using a thermomechanical analyzer (Shimadzu TMA 50, Shimadzu, Japan). Mechanical tests revealed that, although the control group was found to have the value of highest transverse strength, the highest impact strength was observed in the PMMA-L-1 group. Upon examining the thermomechanical analysis data, it could be seen that the E value of the control sample was higher than that of all the other samples. Adding lignin powder into PMMA performs plasticizer effect on resin matrix.

1. Introduction

Polymethyl metacrylate (PMMA) resin is commonly used in the construction of denture base. The fracture of the denture base is a common clinical occurrence in prosthodontic service but still remains adamantly an unsolved problem [1–4]. In prosthodontics literature many studies [1–7] have proposed to improve the physical and mechanical properties of PMMA resin. Among the various reinforcement approaches, the incorporation of fibers such as glass [2, 5, 6, 8], carbon [9], polyester [2, 10], nylon [2, 8] and wood [11, 12] fibers into the polymer matrix has been found to considerably improve many mechanical and physical properties of denture base resins.

There are many studies which added natural polymers to reinforce different resin matrix, of which lignin is included [11–14]. Lignins (Figure 1) are one of the high molecular weight components of wood and occupy the second place regard to their abundance throughout the world as organic polymeric substances of natural origin [15]. Lignin has long been of interest as a source of inexpensive and renewable adhesives and thermoplastics [16, 17]. However, the commercial utilization of lignin has not been met with success. Lignin is often thought of as a waste product of the paper making process and in the conversion of cellulosics to ethanol. However, it is a potential valuable source of aromatic chemicals, biodegradable polymers, and carbon fibers [18]. Lignins were first used as reinforcing fillers in natural and cured rubbers [19]. Lignins were employed as a reinforcing agent in elastomeric polyethers, polyester amid and polyalkylene glycols [14]. Physico-mechanical properties were reported to be improved for the final product by using lignin [11, 13, 14].

The aim of the present study was to determine the mechanical and structural properties of lignin powder that was added into PMMA.

2. Materials and Methods

Acrylic resin was obtained (Meliodent, Bayer Dental, Newbury, Berkshire, UK) and Kraft Lignin (Lignin, Kraft;

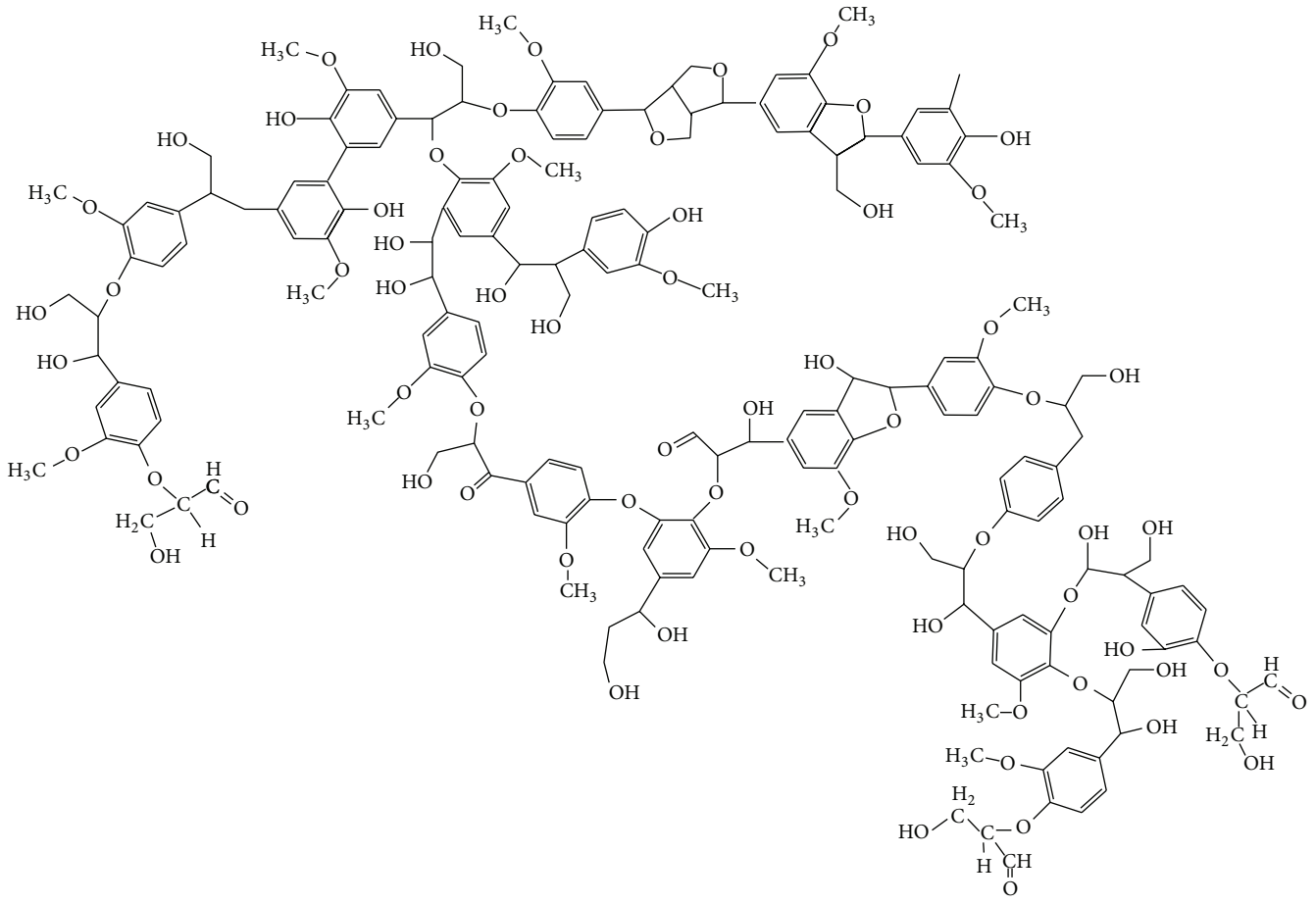

Figure 1: Structure of lignin molecule.

INDULIN at; $\{(CH_3O)(OH)Ar(C_3H_4O)\}_x$) was kindly supplied by MeadWestvaco Corp. (USA). All experiments were always performed in duplicates. ±5% was the limit of experimental error of each of the duplicates, and any experiment that resulted in a value higher than this limit was repeated.

Acrylic resin specimens were prepared at a powder/liquid ratio of 2.34 g/mL in accordance with the manufacturer's instructions. After 1-minute mixing and following a dough time of 6 min, the acrylic resin was molded into moulds which had been prepared in advance. After the molding procedure was completed, 5 min pressure was applied onto the molds under a hydraulic press (Rucker PHI, Birmingham, UK). The molds were then transferred into a 70°C water bath for 1 h, and, after that, the polymerization action was performed immediately by keeping them in the boiling water for 30 min. Upon completion of polymerization, the flasks were left to cool at ambient temperature before being opened. Deflasked specimens were manually polished with a 600-grit water-proof silicon carbide paper under tap water.

PMMA-L composites were prepared at three different concentrations by weight. Four sample groups were constituted as PMMA-L-1 (1% wt), PMMA-L-2 (3% wt), and PMMA-L-3 (5% wt). Four groups, each of which consisted of 10 specimens, were formed for each test. The transverse and impact strength tests were applied as mechanical tests.

Transverse strength was determined by three-point bending test method. The specimens for this test were prepared in $65 \times 10 \times 2.5\,mm^3$ dimensions in accordance with ADA standard number 12. In preparing the test specimens, a stainless steel mould was used. The standard wax specimens were obtained by pouring the melted pink plate waxes (Modelling Wax, De Trey S.A, Bios Colombes, France) into the isolated mold. The prepared wax specimens were taken into the mold and these wax specimens were removed by melting them and then the molds were made ready for acrylic molding.

Transverse strength was determined by the three-point flexure test in a computer-aided universal test device (Lloyd NK5, Lloyd Instruments Ltd., Fareham, Hampshire, UK). The specimens were placed on supports, located at 50 mm intervals, and a 5 mm/min cracking speed was applied. This amount of speed is enough to crack the specimens. The degree of bending before the cracking occurred was recorded (NEXYGEN, Lloyd Instruments Ltd., Fareham, Hampshire, UK).

Transverse strength values were calculated in N/mm^2 (MPa) by using the following formula:

$$T_s = \frac{3Fl}{2bd^2}, \tag{1}$$

where T_s = transverse strength (N/mm^2); F = applied load (N); l = distance between supports (mm); b = specimen width (mm); d = specimen thickness (mm).

The specimens for the impact strength test were obtained in accordance with ASTM D256 standards and prepared in metal moulds in $55 \times 10 \times 10$ mm^3 dimensions. The specimens had a V-shaped notch in the middle, with 2 mm width and 2.54 mm depth. The specimens were also siliconized (Imprex putty, Arma, Turkey). Polymerization procedures were as described previously. Upon completion of polymerization, the flasks were left to cool at ambient temperature before being opened. Deflasked specimens were manually polished as described above. Impact strength was determined in a Charpy type impact test device (Dynatup 9250 HV, Instron, UK). A drop weight of 7.3 kg (which was equivalent to 12-J energy) was applied to the specimens on the unnotched side.

After the data collection, mean value and standard deviation were calculated with a SPSS statistical software program (14.0 version, SPSS Inc., Chicago, USA). Data were then analyzed by Kruskall-Wallis and Tukey tests for pairwise comparisons of the groups at the 0,05 level of significance.

Following the mechanical tests applied to all the specimen groups, the fractured surfaces were examined under SEM, in the specimens whose acrylic part was broken and 2 mm sections were obtained by using a water-cooled sectioning device (Buehler IsoMet, Low Speed Saw, USA). The section specimens were then made conductive under the vacuum of 4×10^{-2} mbar in a Polaron SC7620 Sputter Coater device by coating with Au-Pd for 15 s (3 Angstrom coating per second, in total 45 Angstrom). The interface of powder-resin was visualized by surface scanning electron microscope (LEO 440 Scanning Electron Microscope, UK).

The fractured surface of one specimen from each group was also investigated spectroscopically, in order to evaluate the chemical interactions between the materials, by a FTIR spectrometer (Bruker, Vertex 70, Bruker Optics Inc., Ettlingen, Germany). The FTIR spectrometer was used with a diamond crystal Pike MIRacle ATR unit. Fifty scans were obtained and averaged to a resolution of 4 cm^{-1}.

TMA test samples were prepared at $20 \times 5 \times 1$ mm dimensions as recommended by the manufacturer of the instrument (Shimadzu TMA 50, Shimadzu, Japan). Curves demonstrating changes in thermal-mechanical properties with temperature were obtained by using the values produced by the TMA instrument. The stress-strain curves were obtained under nitrogen atmosphere at a heating rate of 10°C min^{-1} and at a loading rate of 10 g min^{-1}.

3. Results and Discussion

FT-IR spectra of PMMA resin and PMMA-L composite samples are represented comparatively in Figure 2. Upon examining the FT-IR spectra, all of the PMMA-L composite samples showed an O–H stretching peak at 3397 cm^{-1} and a C=O streching peak at 1721 cm^{-1}. As the lignin content increased, the intensity of the C=O peaks decreased while the intensity of the O–H peaks increased. These intensity changes can be attributed to hydrogen bonds that formed between the lignin and carbonyl groups of PMMA. The absorption peaks at 2920, 1386, and 750 cm^{-1} belong to aliphatic C–H, C–O, and aromatic rings, respectively.

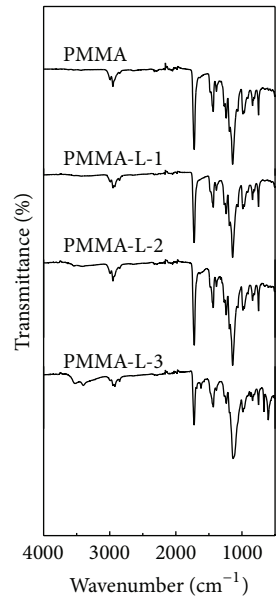

Figure 2: The FTIR spectra of composite samples.

Structural images of the specimens were obtained by using surface scanning electron microscope. The assessments in lignin-added specimens were made in terms of lignin-resin connection and lignin distribution (Figures 3 and 4). PMMA (control) group (Figure 3(a)) has a smooth and compact structure; however, the lignin powder has a spherical structure (Figure 3(b)). In the PMMA-L specimens group (Figures 4(a) and 4(c)), lignin was not spread homogeneously and had no interfacial adhesion with the resin and many gaps between the lignin and the resin matrix were observed. Some cavities appeared to have formed on the interface with the resin matrix. On inspecting (Figures 4(a)–4(c)), a crack line in the lignin powder was observed.

Stress-strain curves of PMMA and lignin-PMMA composites are given in Figure 5. Elastic modulus (E) obtained from these stress-strain curves of PMMA and the prepared composites are listed in Table 1. Below the yield point, elastic modulus (E) can be considered as a criterion for elasticity of a polymer. As seen in Table 1, while the lignin content increases, the elastic modulus of the polymers decreases. Since the elastic modulus and elasticity are inversely related it could be argued that the addition of lignin decreases the elastic modulus of composite resins and hereby improves its plastic properties.

Values obtained from the transverse and impact strength tests were analyzed and the results of statistical evaluation were presented (Table 2). Transverse strength, maximum deflection, and absorbed energy values groups were compared using the Kruskal-Wallis test, and the difference between the groups was found to be significant ($P < 0.05$).

In the present study, when the transverse strength of PMMA and PMMA-L sample groups was compared, it was

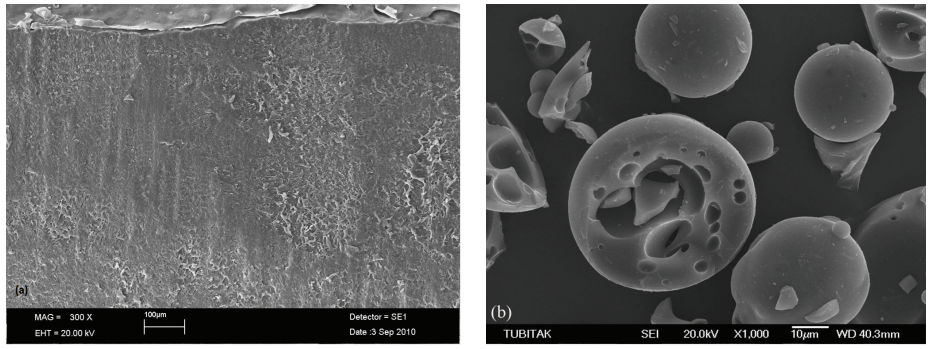

(a) (b)

Figure 3: SEM image; (a) PMMA (b) lignin.

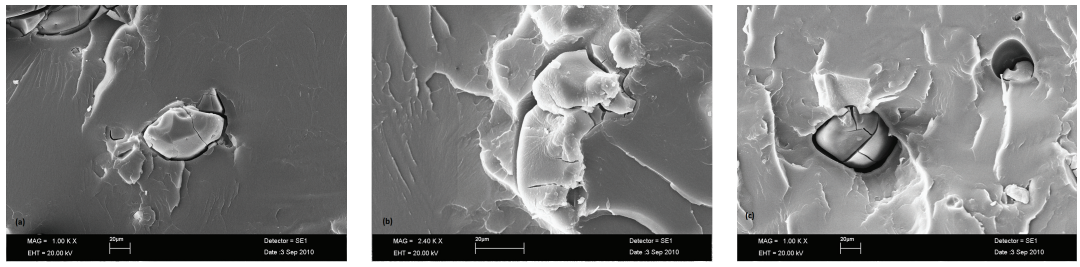

(a) (b) (c)

Figure 4: SEM image. (a) PMMA-L-1; (b) PMMA-L-2; (c) PMMA-L-3.

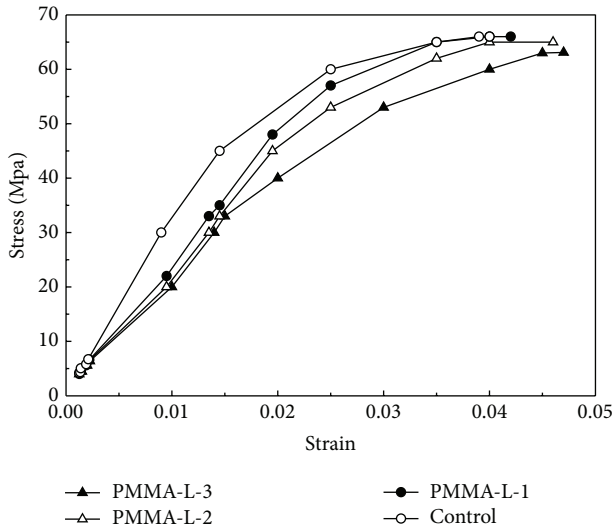

Figure 5: Stress-strain curve of composite samples.

found that PMMA (control) sample group had the highest transverse strength (80.24 ± 8.69 MPa).

Among the PMMA-L groups, the PMMA-L-1 group had a higher transverse strength than the other PMMA-L groups. As the amount of added lignin increased, it was observed in Table 2 that the value of transverse strength decreased. When deflection of the sample groups was evaluated, PMMA-L-3 had the highest value (7.73 ± 1.35 mm). According to deflection and transverse test, an increase in lignin content led to increasing deflection values but also a decrease in transverse strength values of the composites. As seen in SEM images (Figures 4(a)–4(c)), these results could be explained by poor adhesions between the added lignin and the polymer matrix.

Table 1: Value of elastic modulus of composite samples derived from TMA test.

Specimen	Elastic modulus (MPa)
Control	2873
PMMA-L-1	2739
PMMA-L-2	2631
PMMA-L-3	2533

In a previous study, wood fiber was added to PMMA at different ratios. It was observed that the control group has better mechanical strength than the fiber added group. Then, by adding binding agent to the fiber added PMMA group, it was observed that their mechanical strength was improved [11].

It has been reported that the mechanical strength of wood fiber added into PMMA resin is not higher than PMMA resin but that of wood fiber treated with bonding agent. Because of increased link between resin matrix and fill, it was emphasized that using improved agent of adhesion between them is needed [20–22]. In the present study, it is considered, that in the specimens to which lignin was added, cavities

Table 2: Value of transverse and impact strength of composite samples.

	Transverse strength*	Maximum deflection*	Absorbed energy*
Control	80.24 ± 8.69	3.38 ± 0.77	0.26 ± 0.04
PMMA-L-1	70.92 ± 5.17	4.97 ± 0.79	0.89 ± 0.09
PMMA-L-2	57.63 ± 5.54	5.15 ± 0.61	0.87 ± 0.05
PMMA-L-3	39.09 ± 1.38	7.73 ± 1.35	0.83 ± 0.09
	KW = 17.10	KW = 14.82	KW = 11.64

*Significant at $P < 0.05$ for coefficient of correlation. $n = 10$.

in between lignin-PMMA could be decreased by bonding agents.

Many researchers have used the impact strength tests in order to test acrylic resin and to determine the effects of environmental conditions or continuous, trimmed fibers. This test has also been used for the comparison of different denture base resins. The impact strength is not the real property of a material because the dimension of the specimen is dependent on factors such as the existence and depth of the notches, the loading configuration, and the speed of impact. The frenulum areas damaging the integrity of acrylic dentures are the ones where the stress concentration is high. In order to stimulate this, the specimens of impact test are prepared in notches [23]. In our study, we also prepared the specimens for impact test according to the Charpy test method.

According to impact test results, the control group specimens have the lowest energy absorption value (0.26 ± 0.04 J) and these values were significantly much higher in lignin-added specimens. As seen in the table PMMA-L-1, which contained 1% lignin by weight, has the highest energy absorption value (0.89 ± 0.09 J) and, as the lignin content increased, the energy absorption values decreased. Although higher lignin content decreases the energy absorption values of the specimens, the decrease was not statistically significant ($P > 0.05$). Increasing energy absorption values at lignin-added groups could be explained by hydrogen bonds that formed between lignin and matrix.

4. Conclusions

In spite of the fact that added lignin powder, increases the impact strength of PMMA resin matrix, it causes a decrease in transverse strength and elastic modulus. It could be clearly seen that lignin performs a plasticizer effect on PMMA resin matrix. Furthermore, advanced clinical grade investigations are required.

References

[1] D. C. Jagger, R. G. Jagger, S. M. Allen, and A. Harrison, "An investigation into the transverse and impact strength of "high strength" denture base acrylic resins," *Journal of Oral Rehabilitation*, vol. 29, no. 3, pp. 263–267, 2002.

[2] O. M. Doğan, G. Bolayir, S. Keskin, A. Doğan, B. Bek, and A. Boztuğ, "The effect of esthetic fibers on impact resistance of a conventional heat-cured denture base resin," *Dental Materials Journal*, vol. 26, no. 2, pp. 232–239, 2007.

[3] H. D. Stipho, "Effect of glass fiber reinforcement on some mechanical properties of autopolymerizing polymethyl methacrylate," *The Journal of Prosthetic Dentistry*, vol. 79, no. 5, pp. 580–584, 1998.

[4] M. K. Marei, "Reinforcement of denture base resin with glass fillers," *Journal of Prosthodontics*, vol. 8, no. 1, pp. 18–26, 1999.

[5] M. Nakamura, H. Takahashpi, and I. Hayakawa, "Reinforcement of denture base resin with short-rod glass fiber," *Dental Materials Journal*, vol. 26, no. 5, pp. 733–738, 2007.

[6] T. Kanie, K. Fujii, H. Arikawa, and K. Inoque, "Flexural properties and impact strength of denture base polymer reinforced with woven glass fibers," *Dental Materials*, vol. 16, no. 2, pp. 150–158, 2000.

[7] D. L. Gutteridge, "The effect of including ultra-high-modulus polyethylene fibre on the impact strength of acrylic resin," *British Dental Journal*, vol. 164, no. 6, pp. 177–180, 1988.

[8] O. M. Doğan, G. Bolayır, S. Keskin, A. Doğan, and B. Bek, "The evaluation of some flexural properties of denture base resin reinforced with various aesthetic fibers," *Journal of Materials Science*, vol. 19, pp. 3343–3348, 2008.

[9] C. K. Shreiber, "Polymethyl metacrylate reinforced with carbon fibers," *British Dental Journal*, vol. 130, pp. 29–30, 1971.

[10] S. Y. Chen, W. M. Liang, and P. S. Yen, "Reinforcement of acrylic denture base resin by incorporation of various fibers," *Journal of Biomedical Materials Research*, vol. 58, pp. 203–208, 2001.

[11] D. Maldas, B. V. Kokta, and C. Deneault, "The mechanical properties of wood fiber-reinforced polymethylmetacrylate," *International Journal of Polymeric Materials and Polymeric Biomaterials*, vol. 12, pp. 297–323, 1989.

[12] S. Mishra and J. B. Naik, "Mechanical properties of wood polymer composites prepared from agro-waste and HDPE," *Polymer*, vol. 44, no. 3, pp. 511–522, 2005.

[13] H. D. Rozman, R. N. Kumar, M. R. M. Adlli, A. Abusamah, and I. Z. A. Mohd, "The effect of lignin and surface activation on the mechanical properties of rubberwood-polypropylene composites," *Journal of Wood Chemistry and Technology*, vol. 18, no. 4, pp. 471–490, 1998.

[14] D. K. Setua, M. K. Shukla, V. Nigam, H. Singh, and G. N. Mathur, "Lignin reinforced rubber composites," *Polymer Composites*, vol. 21, no. 6, pp. 988–995, 2000.

[15] F. S. Chakar and A. J. Ragauskas, "Review of current and future softwood kraft lignin process chemistry," *Industrial Crops and Products*, vol. 20, no. 2, pp. 131–141, 2004.

[16] J. F. Kadla and S. Kubo, "Lignin-based polymer blends: analysis of intermolecular interactions in lignin-synthetic polymer blends," *Composites A*, vol. 35, no. 3, pp. 395–400, 2004.

[17] R. Pucciariello, V. Villani, C. Bonini, M. D'Auria, and T. Vetere, "Physical properties of straw lignin-based polymer blends," *Polymer*, vol. 45, no. 12, pp. 4159–4169, 2004.

[18] D. R. Crist, R. H. Crist, and J. R. Martin, "A new process for toxic metal uptake by a kraft lignin," *Journal of Chemical Technology and Biotechnology*, vol. 78, no. 2-3, pp. 199–202, 2003.

[19] E. G. Lyubeshkina, "Lignins as components of polymeric composite materials," *Russian Chemical Reviews*, vol. 52, pp. 1196–1224, 1983.

[20] O. Karacaer, A. Doğan, O. M. Doğan, and A. Usanmaz, "Dynamic mechanical properties of dental base material reinforced with glass fiber," *Journal of Applied Polymer Science*, vol. 85, no. 8, pp. 1683–1697, 2002.

[21] G. S. Solnit, "The effect of methyl methacrylate reinforcement with silane-treated and untreated glass fibers," *The Journal of Prosthetic Dentistry*, vol. 66, no. 3, pp. 310–314, 1991.

[22] P. K. Vallittu, "Comparison of two different silane compounds used for improving adhesion between fibres and acrylic denture base material," *Journal of Oral Rehabilitation*, vol. 20, no. 5, pp. 533–539, 1993.

[23] G. Zappini, A. Kammann, and W. Wachter, "Comparison of fracture tests of denture base materials," *The Journal of Prosthetic Dentistry*, vol. 90, no. 6, pp. 578–585, 2003.

Hindawi Publishing Corporation
Advances in Materials Science and Engineering
Volume 2013, Article ID 394656, 9 pages
http://dx.doi.org/10.1155/2013/394656

Research Article

Effect of Zeolite Modification via Cationic Exchange Method on Mechanical, Thermal, and Morphological Properties of Ethylene Vinyl Acetate/Zeolite Composites

N. D. Zaharri, N. Othman, and Z. A. Mohd Ishak

School of Materials and Mineral Resources Engineering, Engineering Campus, Universiti Sains Malaysia, 14300 Nibong Tebal, Penang, Malaysia

Correspondence should be addressed to N. Othman; srnadras@eng.usm.my

Received 25 July 2013; Revised 16 October 2013; Accepted 19 October 2013

Academic Editor: Jim Low

In this research, organozeolite filled ethylene vinyl acetate (EVA) composites were prepared in a melt-mixing process and followed by compression molding using hot press machine according to standard test specimen. Prior to mixing process, zeolite was modified via cationic exchange of alkylammonium ions. The effect of zeolite or organozeolite loading from 5 up to 25 volume percentages on the properties of EVA/zeolite composites was evaluated. A combination of Fourier Transform Infrared Radiation (FTIR) and scanning electron microscopy (SEM) coupled with energy dispersive X-ray (EDX) analysis were done to characterize the resultant organoclay. Tensile test was performed in order to study the mechanical properties of the composites. EVA filled with organozeolite showed better tensile properties compared to EVA filled with unmodified zeolite, which might be an indication of enhanced dispersion of organophilic clay in the composites. Meanwhile, morphological study using SEM revealed the fibrillation effect of organozeolite. Besides, thermal properties of the composites were also characterized by using thermogravimetric analysis (TGA) and differential scanning calorimetry (DSC). The results showed that the application of the cation exchange treatment increases both decomposition and melting temperature of EVA/zeolite composites.

1. Introduction

There has been intensive research on layered silicate filled polymer composites recently. Several different layered silicates for polymer composites, for example, kaolinite, montmorillonite, hectorite, illite, muscovite, sepiolite, and hectorite, have been identified [1]. However until now, not much study has been done on natural zeolite, particularly mordenite type zeolite. Zeolite is another type of layered silicate material which can be classified into three groups according to Si/Al ratio in their frameworks, which are "low silica" zeolites, "intermediate silica" zeolites and also "high silica" zeolites [2]. Zeolites form a large group of hydrous silicates that show close similarities in composition, association, and mode of occurrence. The zeolite family includes mordenite, clinoptilolite, faujasite, chabazite, heulandite, and mazzite. They are framework aluminosilicates with exchangeable cations and highly variable amounts of H_2O in the generally large voids of the framework.

In this study, mordenite type zeolite is used as filler in polymer composites. Mordenite is classified into "intermediate silicate" zeolite where the Si/Al ratio is found to be between 4.5 and 5.5 [2]. Mordenites have been classified as "large-port" or "small-port," depending on whether or not they adsorb large molecules such as benzene and cyclohexane. Ever since mordenite was synthesized, it has been known that some synthetic mordenite can accept cations or molecules larger than 4.5 Å, while natural mordenite cannot. Explanations for small-port mordenite have remained controversial [3]. Further varieties of mordenite can be produced by removing aluminum from the structure by strong acid treatment with hydrochloric acid [4].

Zeolites are widely known as microporous materials where each type of zeolite exhibits different pore structural characteristics. In the case of mordenite zeolite, the pore structure is complicated since the mordenite presents two types of porous channels. Figure 1 represents the channel

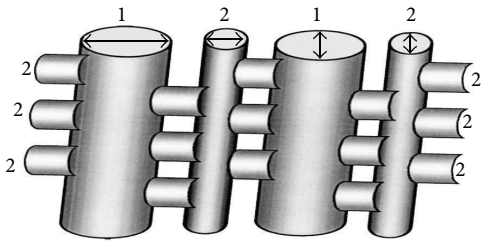

Figure 1: Channel structure of mordenite type zeolite [5].

structure of mordenite type zeolite. By referring to the figure, channel 1 is formed by the assemblage of 12-membered rings, each of which is having 12 oxygen atoms. Meanwhile channel 2 is made of 8-membered rings in which there are 8 oxygen atoms. Cation sites are located in the centers of this 8-membered rings channel [5]. The porous structure of mordenite consists of a channel system in which 8- and 12-membered ring channels run parallel to the [001] or *c*-axis and 8-membered run ones parallel to [010] or *b*-axis. Free diameters of the 12-membered rings are 0.65×0.70 nm, while free diameters of the 8-membered rings are 0.26×0.57 nm. Channels 1 and 2 are interconnected via perpendicular channel 2 tubes, in the form of small side pockets along the [010] axis. Thus the channel system is essentially a 2-dimensional network with elliptical 12-ring apertures and a limiting diffusion in the [010] or b direction [6].

However, the hydrophilic nature of inorganic mineral, including zeolites, limits its compatibility with polymer matrix. Hence, surface modification of filler needs to be done prior to compounding process in order to change the nature of filler from hydrophilic to hydrophobic. Enhancement of the polymer-filler interfacial adhesion by surface modification has become one of the popular evolutionary steps in polymer industry as well as in academic field. Compared to the unmodified composites, the composites filled with treated or modified filler exhibit increased mechanical properties, reduced gas permeability, and enhanced thermal stability and flame retardancy [7, 8].

In this study, method of cation exchange with alkylammonium ions was performed since it is the easiest way to make mineral fillers become hydrophobic yet effective in enhancing the properties of composites [9]. This cation exchange method does not only alter the surface polarity of the filler but also expand its intergallery distance, and thus it enables the polymer to penetrate more easily into the galleries. In the past several years, variety of fillers especially clays such as montmorillonite (MMT) [10], layered double hydroxides (LDH) [11], bentonite [12], and α-zirconium phosphate (α-ZrP) [13] have been ionic exchanged before being incorporated into polymer matrix in order to obtain optimal properties of composites.

However, there are only a few studies dealing with mordenite type zeolite modified by cationic exchange method in polymer composites. Zeolites are extensively used all over the world due to their ion exchange properties [14]. Due to this, zeolites can be easily modified using ion exchange treatment in order to change their nature from hydrophilic to hydrophobic hence improving the compatibility between the inorganic filler particles and polymer matrix. In this treatment, the intercalated ions of zeolite are exchanged with the ions of organic surfactant which consequently alters the surface properties of zeolite to be hydrophobic. Among the widely used organic surfactants are phosphonium, imidazolium, stibonium compounds, and organic amines such as octadecylamine, hexadecylamine, dodecylamine, and octylamine. The swelling of mineral filler in aqueous surfactant, such as organic amine consisting alkylammonium ions, might lead to an extension of the interlayer galleries due to the hydration of inorganic ions contained in these galleries, allowing the alkylammonium ions to intercalate between them. However, some mineral fillers such as illites and kaolinites do not have expandable galleries due to strong interlayer interactions.

All clay minerals including zeolites show a main preference for larger over smaller inorganic cations. This tendency, referred to as "fixation" in the soil science literature, becomes more pronounced as layer charge increases. For smectites, this preference (for larger cations) follows the orders of $Cs^+ > Rb^+ > K^+ > Na^+ > Li^+$ and $Ba^{2+} > Sr^{2+} > Ca^{2+} > Mg^{2+}$. Meanwhile at higher layer charge (vermiculites), as in the case of mordenite type zeolite, the preference is $Mg^{2+} > Ca^{2+} \approx Sr^{2+} \approx Ba^{2+}$. The preference of clay minerals for certain cations is caused by several other effects. These include hydration of the cations at the surface and in solution (entropy), electrostatic cation-surface and cation-cation interactions, interaction between the water molecules and the surface, and the polarizability or hard and soft acid-base character of the cations [15].

The goal of this study was to improve the properties of EVA/zeolite composites by modifying the hydrophilic surface of zeolite using cation exchange method. FTIR and EDX analyses were done to elucidate the modification effect on the composites. The tensile properties and SEM analysis were evaluated in order to determine the mechanical and morphological properties of the composites, respectively. Also, thermogravimetric analysis (TGA) and differential scanning calorimetry (DSC) measurements were performed to characterize the thermal behavior of the EVA/zeolite composites.

2. Experimental

2.1. Materials. Ethylene vinyl acetate (EVA) containing 15% vinyl acetate was purchased from The Polyolefin Company (Singapore Pvt. Ltd. Cosmothene Eva H2020). The natural filler used was mordenite type of zeolite mineral species. The natural zeolite was mined in Indonesia. The chemical formula is Ca, Mg_2, K_2 $Al_2Si_{10}O_{24}$ $7H_2O$ with orthorhombic crystal system. It was provided in grains form and white color with density of 1.914 g/cm^3. This filler was modified with octadecylamine with the chemical formula of CH_3–$(CH_2)_{17}$–NH_2. This product was purchased from Aldrich and used without further purification.

2.2. Cation Exchange Process. The octadecylamine was dissolved in 1 liter of 0.01 M hydrochloric acid solution (based

on deionized water). The solution was stirred at 80°C for few hours. Then 10 grams of zeolite were added to the solution which was then stirred at the same temperature for few more hours. The solution was then filtered and washed with hot ethanol : water (1 : 1) mixture. Finally, the resulting organoclay was then dried at 85°C for 36 hours and kept dry in a desiccator.

2.3. Preparation of the Composite. Prior to mixing process, zeolite was grinded into powder form using a ring mill machine. After grinding process, the exact particle size was determined by Malvern Mastersizer particle size analyzer. The result obtained was 5.62 μm. Then, the zeolite powder and EVA were dried in oven at 80°C for 24 hours. The compounding process was done by using an internal mixer Thermo Haake Polydrive with Rheomix, R600/610 model. The amounts of EVA and zeolite were calculated accurately according to Rules of Mixtures formula as shown in (1) [16].

Consider the following:

$$V_f = \frac{\rho_m W_f}{\rho_f W_m + \rho_m W_f}, \quad (1)$$

where V_f is volume percentage of filler and W_f and W_m are weight fraction of filler and matrix, respectively while ρ_f and ρ_m are density of filler and matrix, respectively.

The processing conditions were set at 130°C with 7 min of mixing time and 50 rpm of rotor speed. After compounding, the unmodified and modified zeolite filled composites were compression molded into 1 mm of sample thickness. The samples were preheated at 130°C for 8 minutes followed by compression for 2 minutes. Finally, the samples were cold pressed for 4 minutes.

2.4. Characterization. FTIR, PerkinElmer Spectrum One model machine, was used to investigate the presence of functional groups in zeolite, organozeolite, EVA/zeolite composite, and also EVA/organozeolite composite samples. The range of wavelength was 550–4000 cm^{-1} with 4 scan times. The standard spectrum was obtained from the FTIR machine in order to determine the involved functional groups.

The molded tensile test sheet for tensile testing was cut into five dumbbell-shaped samples using Wallace die cutter. The thickness of each dumbbell-shaped sample was measured. The tensile properties were determined using electromechanical Instron machine, model 3366according to ASTM D 638 with a crosshead speed of 50 mm/min. The tensile mechanical properties such as tensile strength, elongation at break, and Young's modulus were obtained by calculating the average values of the five tested dumbbell-shaped samples.

Scanning electron microscopy/energy dispersive X-ray (SEM/EDX) analysis was performed using Leica Cambridge Ltd. model S360to study the composites morphology. The morphology study was done on the fractured surface of the composite samples due to tensile testing. Samples were examined after sputter coating with gold to avoid electrostatic charging and poor image resolution. The relative amounts of occurrence elements in both unmodified and modified zeolite powder were measured using the energy dispersive X-ray analyzer facility of the microscope.

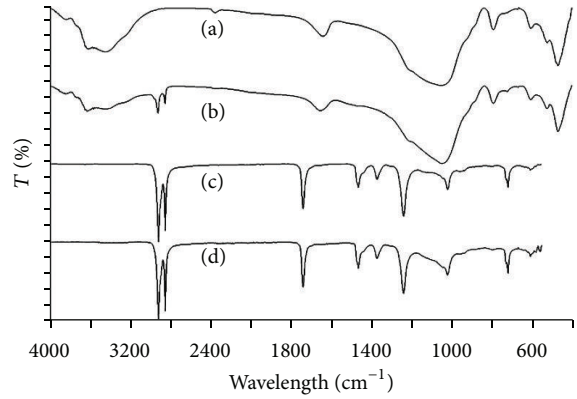

Figure 2: FTIR spectra of (a) zeolite, (b) organozeolite, (c) EVA/zeolite composite, and (d) EVA/organozeolite composite.

A PerkinElmer Pyris TGA-6 thermogravimetric analyzer was used to measure the weight losses and decomposition temperature of the EVA/zeolite composites in the temperature range of 20–600°C with a heating rate of 20°C/min and under a flow of nitrogen.

DSC was carried out with a PerkinElmer Pyris DSC-6 instrument to determine the crystallinity and melting temperature of the composites. Samples of EVA/zeolite composites were weighed to be approximately 5 mg and placed in an aluminum pan. DSC scans were obtained from 30–190°C at a rate of 10°C/min. The crystallinity degree for the composites is determined by the ratio $\Delta H_m/\Delta H_{m100}$, where ΔH_m is the heat of fusion in joule per gram polyethylene segments in the EVA samples, while ΔH_{m100} is the heat of fusion in joule per gram pure polyethylene with 100% crystallinity. The ΔH_{m100} is 281 joule per gram pure polyethylene with 100% crystallinity [17].

3. Results and Discussion

3.1. FTIR Analysis. FTIR spectra of unmodified and organomodified zeolite are illustrated in Figure 2. The common features in the FTIR spectra for zeolite and organozeolite are the presence of characteristics bands at around 3620, 1051, and 470 cm^{-1} which correspond to –OH stretching of structural hydroxyl group, Si–O stretching, and Al–O stretching, respectively. However, there are four new peaks present in the FTIR spectrum of organozeolite compared to the unmodified zeolite. The new peaks are 2918 and 2852 cm^{-1} which assigned to C–H asymmetric and symmetric stretching vibrations of surfactant, respectively meanwhile the new bands around 1468 and 3250 cm^{-1} are attributed to CH_2 methylene (scissoring) vibration and N–H stretching of alkyl ammonium, respectively. In addition, a reduction in intensity at 3620 cm^{-1} (–OH stretching peak) for organozeolite FTIR spectrum indicates that the zeolite becomes more organophilic or hydrophobic after the surface modification. For EVA/organozeolite composites, the spectrum shows a new broad absorption band at around 1070–1150 cm^{-1} in

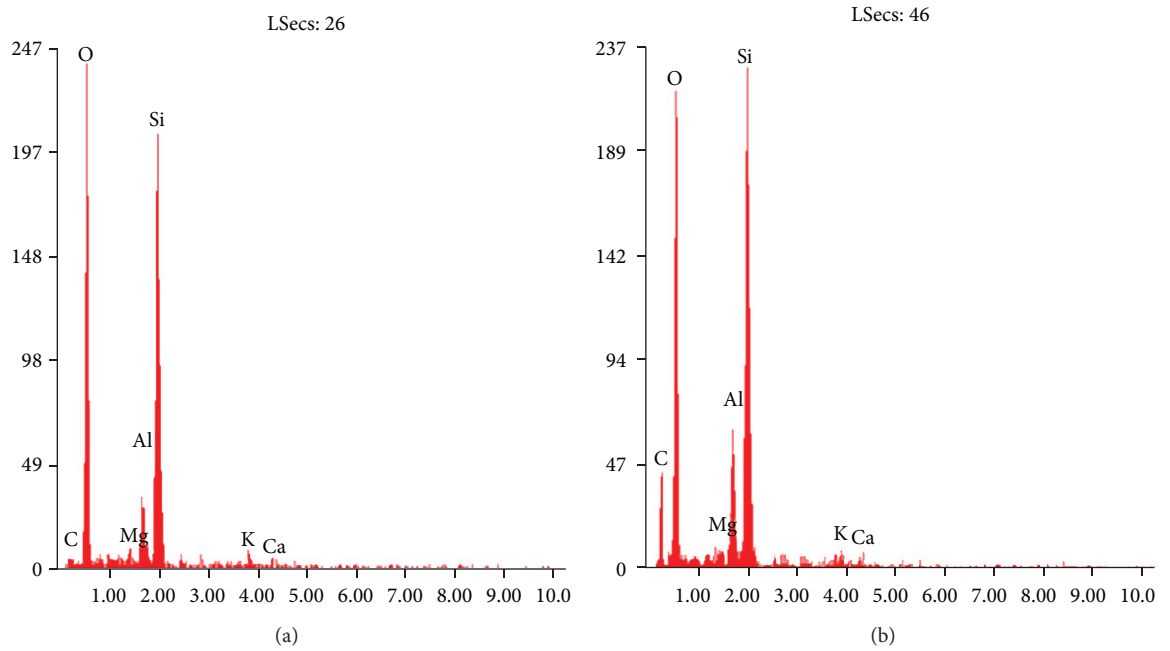

Figure 3: Semiquantitative elemental analysis provided by EDX.

Table 1: Weight percentages of occurrence elements in zeolite before and after modification.

Elements	Wt%	
	Zeolite	Organozeolite
O	42.34	34.81
Al	7.44	7.46
Si	41.31	32.62
C	3.66	21.20
Mg	1.53	0.73
K	2.56	1.62

comparison with EVA/zeolite composites. This new band which corresponded to the C–O–C group suggests the presence of possible reactions between acetate group of EVA and methyl group of octadecylamine. These prove that zeolite is successfully modified by the organic modifier (octadecylamine) and thus organozeolite is formed.

3.2. EDX Analysis. The semiquantitative elemental analysis provided by EDX detected several elements involved in creating the structure of zeolite which are Si, Al, O, C, Mg, and K as shown in Figures 3(a) and 3(b). It can be seen from the EDX spectrum that the bands of Mg and K reduced after surface modification. Moreover, the atomic ratio of C/Si changes from 0.0886 to 0.6499 in consequence of performing the cation exchange method. These clearly suggest the success of ion exchange on the expense of Mg^{2+} and K^{+} cations and also the increment of C/Si atomic ratio. Table 1 represents the weight percentages of occurrence elements in unmodified and organozeolite powder.

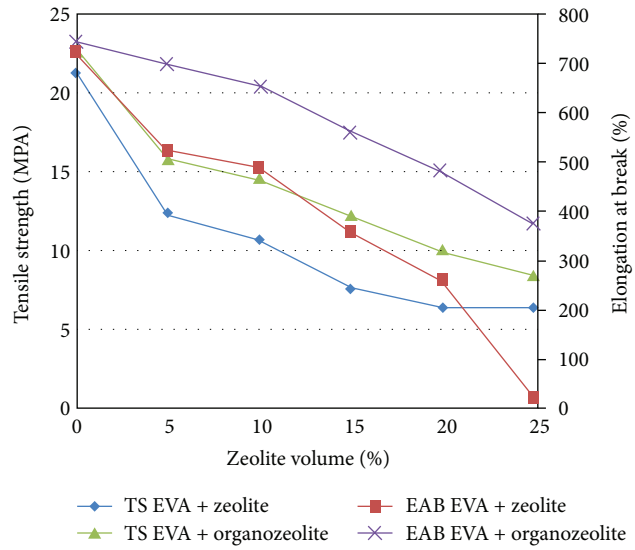

Figure 4: Tensile strength and elongation at break of zeolite and organozeolite EVA composites.

3.3. Tensile Properties. The tensile behavior of unmodified and organozeolite filled EVA composites at various zeolite content is presented in Figures 4 and 5. Figure 4 shows that tensile strength of both unmodified and modified composites decreased as the zeolite content was increased. This is due to the hydrophilic nature of zeolite which is incompatible with the hydrophobic EVA matrix. This leads to agglomeration and poor dispersion of zeolite in the EVA matrix hence reduced the composites strength at higher zeolite loading.

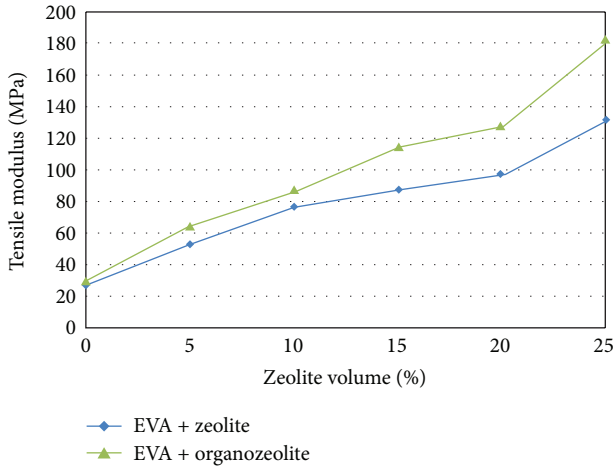

Figure 5: Tensile modulus of zeolite and organozeolite EVA composite.

Greater tensile strength can be observed for the composites filled with organozeolite compared to that of unmodified zeolite. The enhancement in tensile strength for organozeolite/EVA composites is attributed to the improved interaction between organozeolite and EVA matrix resulting from the cationic exchange reaction which has hydrophobilized the zeolite (as proved by FTIR and EDX results) hence enable it to be dispersed within the EVA matrix. It can also be inferred that this modification method has opened up the interlayer spaces of zeolite thus facilitating EVA matrix to penetrate between the layers. Furthermore, good interphase interaction between the dispersed zeolite and EVA matrix is believed to facilitate stress transfer from the continuous phase of EVA to the reinforcement phase of zeolite, hence allowing for tensile improvements. Similar results were reported by Velmurugan and Mohan for epoxy nanocomposites containing clay modified with alkyl quaternary ammonium [18].

Figure 4 also indicates that the elongation at break of EVA composites decreases with increasing zeolite content. This is probably due to the fact that ductility decreases when stiffness is increased by the incorporation of zeolite into the EVA matrix. However, the incorporation of organozeolite into EVA matrix results in higher elongation at break than that of unmodified zeolite at similar loading. This can be a consequence of enhanced adhesion between the organozeolite and EVA matrix thus increasing the ability of the composites to elongate before failure. The enhanced zeolite-EVA adhesion after the modification has also minimized the formation of voids, and hence deformations could not start so easily [19].

The addition of zeolite into EVA matrix significantly increases the tensile modulus of the composites as illustrated in Figure 5. This is due to the inherent properties of inorganic filler, which is rigid and has been proven to be efficient in stiffening polymers [20]. The tensile modulus of EVA/organozeolite composites is higher than that of EVA/zeolite composites at all filler content. This infers that organozeolite is more compatible within EVA matrix compared to unmodified zeolite, which consequently increases the stiffness of the composites.

3.4. Morphology Study. Figures 6 and 7 show the tensile fracture surfaces of unmodified and organozeolite filled EVA composites, respectively. By comparing Figures 6(a) and 7(a), more extensive fibril structure morphology with minimal voids or cavities can be observed on the fractured surface of EVA/organozeolite composites. This indicates better adhesion and interfacial interaction formed between EVA matrix and organozeolite. Besides, the formation of fibrilous morphology indicates a more ductile failure compared to the unmodified composites [21]. This proves that, during deformation, the organozeolite absorbs more stress before fracture hence results in the significant improvement in tensile strength and elongation at break for the EVA/organozeolite composites. This result is in perfect agreement with those reported by Kocsis et al. (2004). At high zeolite loading (25 vol.%), the morphology of unmodified zeolite filled composites as shown in Figure 6(b) exhibits several agglomerations and voids which originate from poor interface adhesion between EVA matrix and zeolite [22]. Unlike Figure 7(b), almost no agglomeration and very little voids can be noticed in the morphology of EVA/organozeolite composites even at high zeolite loading (25 vol.%). This suggests that the surface modification of zeolite with octadecylamine is capable of increasing the compatibility between EVA matrix and organozeolite. These observations validate the results of tensile tests discussed earlier.

3.5. Thermogravimetric Analysis (TGA). Figures 8 and 9 illustrated the TGA and differential thermogravimetry (DTG) curves of EVA and its composites, respectively. The weight loss and derivative weight of EVA/zeolite composites caused by thermal degradation are monitored as a function of temperature. In general, the curve of thermal degradation of EVA is almost similar to that corresponding to its composites where 2 steps are presented. The first one is attributed to the vinyl acetate loss or deacetylation and the second one is associated with the decomposition of polyethylene chains resulting from the first process. As expected, the percentage of residue of zeolite content at completion of EVA degradation was found to increase with increasing zeolite loading in the matrix. It is also noted that EVA/zeolite composites exhibit higher weight loss at 600°C than that of EVA/organozeolite composites. This is because, at this temperature, the weight loss is corresponding to the dehydroxylation of zeolite [23]. This result also suggests that the EVA/organozeolite composite has been well hydrophobilized by cation exchanged method as shown by the lower reduction of weight at 600°C owing to the dehydroxylation process. Table 2 summarizes the selected parameters of thermal characteristics such as onset temperature, T_5 are taken as the point at which 5% degradation occurs, T_{90} indicating the temperature at 90% weight loss, and also T_{100} representing

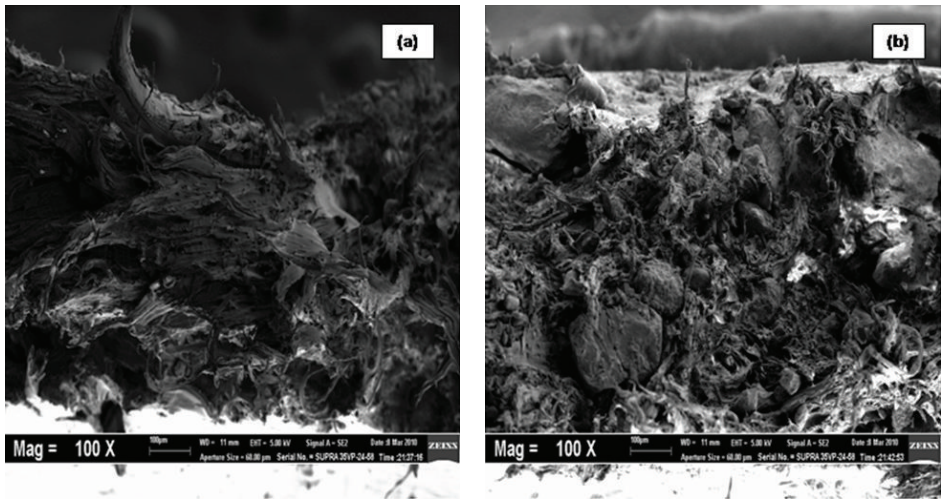

(a) (b)

Figure 6: Tensile fracture surfaces of (a) 5 wt% EVA/zeolite and (b) 25 wt% EVA/zeolite.

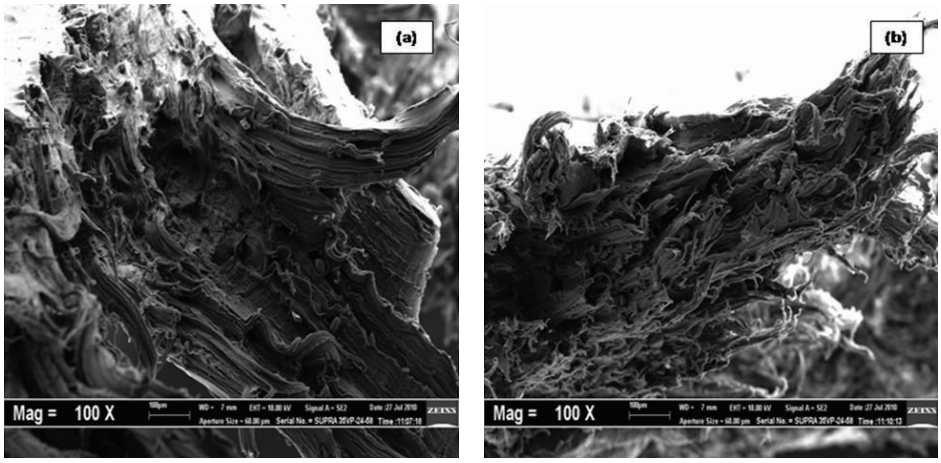

(a) (b)

Figure 7: Tensile fracture surfaces of (a) 5 wt% EVA/organozeolite composite and (b) 25 wt% EVA/organozeolite composite.

the maximum degradation temperature of EVA and its composites. Surprisingly, the results demonstrate that the thermal stability of EVA decreased in the presence of both unmodified and organozeolite. This is in contrast with those reported by Alexandre and Dubois [24]. However, the reduction in T_5, T_{90}, and also T_{100} with increasing zeolite content could be explained by the possibility of zeolite to accumulate heat and then be transformed as a heat source hence promotes an acceleration of the decomposition process in combination with the heat flow supplied by the outside heat source [25].

EVA/organozeolite composites exhibit greater T_5 and T_{90} compared to that of EVA/zeolite composites suggesting better interfacial interaction between EVA and organomodified zeolite. Also, the maximum degradation temperature (T_{100}) of organozeolite filled EVA composites is higher than that of unmodified composites. These results prove that the filler-matrix adhesion and also dispersion of filler within polymer matrix are important factors governing the thermal stability of the composites. Similar results were obtained by Zhang et al. (2003) where they reported that the well-dispersed filler in the polymer matrix could be more effective in

Table 2: TGA results of EVA matrix and its composites.

Composites system	T_5 (°C)	T_{90} (°C)	T_{100} (°C)
EVA	367	447	497
5% EVA/zeolite	328	440	488
15% EVA/zeolite	293	412	458
25% EVA/zeolite	247	397	441
5% EVA/organozeolite	338	447	496
15% EVA/organozeolite	321	416	462
25% EVA/organozeolite	315	401	445

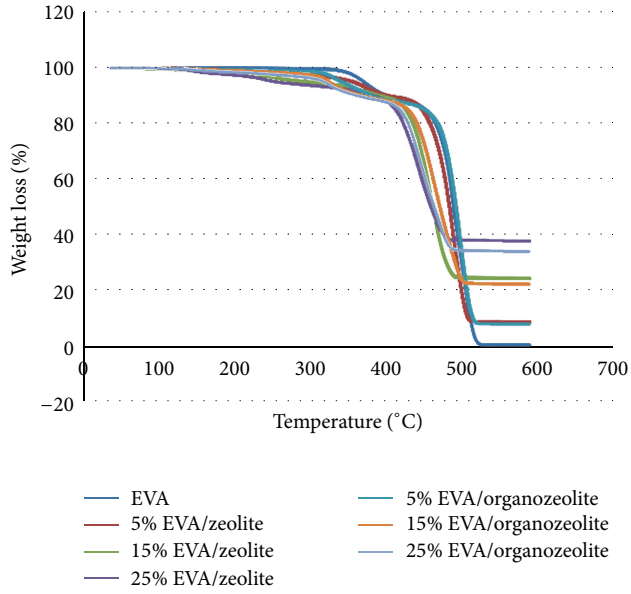

Figure 8: TGA curves of zeolite and organozeolite EVA composites.

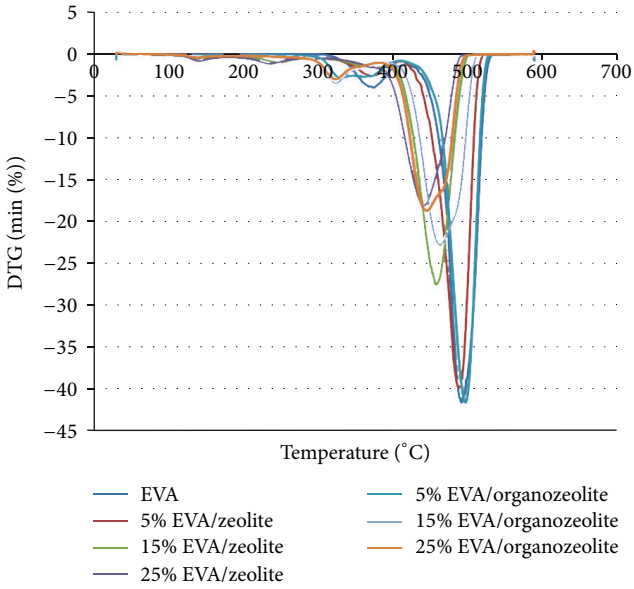

Figure 9: Thermogravimetry (DTG) curves of zeolite and organozeolite EVA composites.

hindering the diffusion of volatile decomposition products hence leading to the improved thermal stability [26].

3.6. Differential Scanning Calorimetry (DSC). Figure 10 indicates the DSC thermograms of unmodified and organozeolite filled EVA composites with different zeolite contents. As shown in the figure, pure EVA is melted at 91.46°C and the melting temperature decreased with the addition of zeolite. The same reason as explained in the result of TGA could be used to account for the decreased thermal

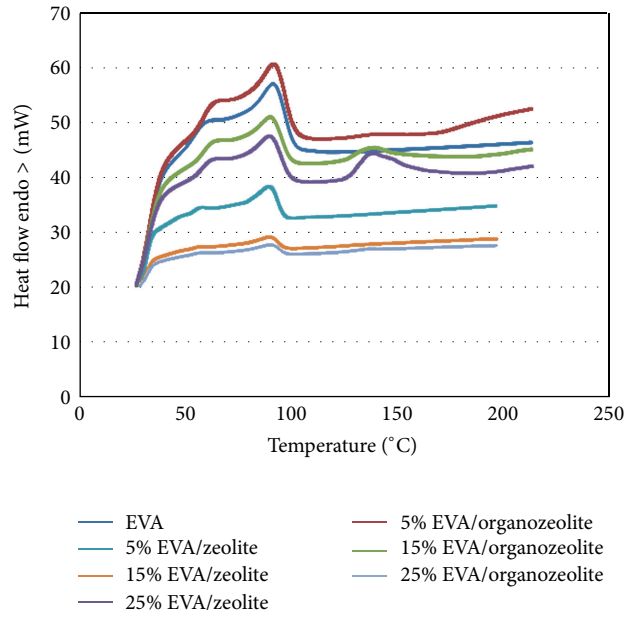

Figure 10: The DSC thermograms of unmodified and organozeolite filled EVA composites with different zeolite contents.

Table 3: DSC results of EVA matrix and its composites.

Composites system	Melting temperature (°C)	Enthalpy of fusion (J/g)	Degree of crystallinity (%)
EVA	92	29	10
5% EVA/zeolite	89	27	10
15% EVA/zeolite	89	19	7
25% EVA/zeolite	89	16	6
5% EVA/organozeolite	92	21	7
15% EVA/organozeolite	90	19	7
25% EVA/organozeolite	90	15	5

stability in the presence of zeolite. However, the reduction in melting temperatures with increasing zeolite loading is not significant. The DSC measurements show that the incorporation of organozeolite into EVA matrix results in higher melting temperature relative to the unmodified zeolite filled EVA composites. This is believed to be due to the improved interfacial interaction between EVA and organozeolite, resulting from the cation exchange method treatment. Table 3 lists the melting temperature and the degree of crystallinity of EVA composites. Poly (vinyl acetate) segment in the EVA copolymer is assumed to be noncrystalline in the calculation of the percent crystallinity of the sample. Apparently, the incorporation of both unmodified and organozeolite into EVA matrix reduced the heat of fusion which leads to lower degree of crystallinity. Probably, this is due to the presence of zeolite causing physical hindrance to the motion of EVA molecular chains hence retarding the crystallization of polymer phase of the composites which consequently reduces the degree of crys-

tallinity [27]. It can also be seen from the table that EVA/organozeolite composites possess lower crystallinity than that of EVA/zeolite composites. This might be attributed to the improved interaction between EVA and organozeolite providing greater effect in imparting physical hindrance to restrict the molecular chain mobility of EVA.

4. Conclusions

It can be concluded that the surface modification of zeolite by organic modifier (octadecylamine) is capable of improving the properties of EVA/zeolite composites. FTIR and EDX results revealed that zeolite has been successfully modified via cation exchange method. Incorporation of both unmodified and organozeolite increased the stiffness but decreased the strength and ductility of EVA matrix. However, EVA/organozeolite composites show higher value of tensile strength, elongation at break, and tensile modulus than those of unmodified zeolite filled EVA composites. This might be attributed to the improved compatibility between EVA and organomodified zeolite. SEM micrographs also supported the finding of improved compatibility for the EVA/organozeolite through a better dispersion of the organozeolite within EVA matrix hence gives an improvement in the composites properties. TGA and DSC results indicate that the thermal properties of EVA decreased in the presence of both zeolite and organozeolite. Organozeolite filled EVA composites exhibit higher melting and thermal decomposition temperature compared to that of unmodified zeolite filled EVA composites.

Acknowledgments

The authors thank Universiti Sains Malaysia for a Research University Grant (no. 1001/PBAHAN/8033027) which financially supported this work. Gratitude is also expressed to all the academic and nonacademic staff in the School of Materials and Mineral Resources Engineering for their support and contribution to the project.

References

[1] S. M. Auerbach, K. A. Carrado, and P. K. Dutta, *Handbook of Layered Materials*, CRC, 2004.

[2] F. R. Ribeiro, *Zeolites—Science and Technology*, vol. 80, Springer, 1984.

[3] L. B. Sand, "Synthesis of large-port and small port mordenites," in *Molecular Sieves*, Society of Chemical Industry, London, UK, 1968.

[4] M. M. Dubinin, "Porous structure of adsorbents and catalysts," *Advances in Colloid and Interface Science*, vol. 2, no. 2, pp. 217–235, 1968.

[5] K. Ssing, D. Everett, R. Haul et al., "Reporting physisorption data for gas/solid system," *Pure and Applied Chemistry*, vol. 57, no. 4, pp. 603–619, 1985.

[6] P. A. Jacobs and J. A. Martens, *Synthesis of High-Silica AluminoSilicate Zeolites*, vol. 33, Elsevier Science Limited, 1987.

[7] A. Usuki, A. Koiwai, Y. Kojima et al., "Interaction of nylon 6-clay surface and mechanical properties of nylon 6–clay hybrid," *Journal of Applied Polymer Science*, vol. 55, no. 1, pp. 119–123, 2003.

[8] E. M. Araújo, R. Barbosa, A. W. B. Rodrigues, T. J. A. Melo, and E. N. Ito, "Processing and characterization of polyethylene/Brazilian clay nanocomposites," *Materials Science and Engineering A*, vol. 445, pp. 141–147, 2007.

[9] G. Lagaly, "Characterization of clays by organic compounds," *Clay Minerals*, vol. 16, no. 1, pp. 1–21, 1981.

[10] S. Chuayjuljit, R. Thongraar, and O. Saravari, "Preparation and properties of PVC/EVA/ organomodified montmorillonite nanocomposites," *Journal of Reinforced Plastics and Composites*, vol. 27, no. 4, pp. 431–442, 2008.

[11] M. Badreddine, A. Legrouri, A. Barroug, A. de Roy, and J. P. Besse, "Ion exchange of different phosphate ions into the zinc-aluminum-chloride layered double hydroxide," *Materials Letters*, vol. 38, no. 6, pp. 391–395, 1999.

[12] S. Chandramouleeswaran and S. T. Mhaske, "Novel tailored polymeric surfactant for dispersing clay into the non polar polymer," *Journal of Dispersion Science and Technology*, vol. 29, no. 7, pp. 1024–1028, 2008.

[13] H. Wu, C. Liu, J. Chen, Y. Yang, and Y. Chen, "Preparation and characterization of chitosan/α-zirconium phosphate nanocomposite films," *Polymer International*, vol. 59, no. 7, pp. 923–930, 2010.

[14] G. P. Tsintskaladze, A. R. Nefedova, Z. V. Gryaznova, G. V. Tsitsishvili, and N. G. Gigolashvili, "Active centres of decationated zeolites in oxidative transformation of methanol," *Petroleum Chemistry*, vol. 25, no. 3, pp. 160–165, 1985.

[15] M. Auboiroux, F. Melou, F. Bergaya, and J. C. Touray, "Hard and soft acid-base model applied to bivalent cation selectivity on a 2:1 clay mineral," *Clays and Clay Minerals*, vol. 46, no. 5, pp. 546–555, 1998.

[16] M. Xanthos, *Functional Fillers for Plastics*, Wiley-Vch, 2010.

[17] R. Z. Greenley, J. Brandrup, and E. Immergut, "Polymer handbook," in *Polymer Handbook*, pp. 267–274, 1989.

[18] R. Velmurugan and T. P. Mohan, "Room temperature processing of epoxy-clay nanocomposites," *Journal of Materials Science*, vol. 39, no. 24, pp. 7333–7339, 2004.

[19] H. Demir, D. Balköse, and S. Ülkü, "Influence of surface modification of fillers and polymer on flammability and tensile behaviour of polypropylene-composites," *Polymer Degradation and Stability*, vol. 91, no. 5, pp. 1079–1085, 2006.

[20] J. Wang and R. Pyrz, "Prediction of the overall moduli of layered silicate-reinforced nanocomposites-part I: basic theory and formulas," *Composites Science and Technology*, vol. 64, no. 7, pp. 925–934, 2004.

[21] P. W. Balasuriya, L. Ye, and Y.-W. Mai, "Morphology and mechanical properties of reconstituted wood board waste-polyethylene composites," *Composite Interfaces*, vol. 10, no. 2-3, pp. 319–341, 2003.

[22] W. S. Chow, Z. A. M. Ishak, U. S. Ishiaku, J. Karger-Kocsis, and A. A. Apostolov, "The effect of organoclay on the mechanical properties and morphology of injection-molded polyamide 6/polypropylene nanocomposites," *Journal of Applied Polymer Science*, vol. 91, no. 1, pp. 175–189, 2004.

[23] H. van Olphen and J. Fripiat, *Data Handbook for Clay Minerals and Other Non-Metallic Materials*, Pergamon Press, New York, NY, USA, 1979.

[24] M. Alexandre and P. Dubois, "Polymer-layered silicate nanocomposites: preparation, properties and uses of a new class of materials," *Materials Science and Engineering R*, vol. 28, no. 1, pp. 1–63, 2000.

[25] S. S. Ray and M. Okamoto, "Polymer/layered silicate nanocomposites: a review from preparation to processing," *Progress in Polymer Science*, vol. 28, no. 11, pp. 1539–1641, 2003.

[26] W. Zhang, Y. Liang, W. Luo, and Y. Fang, "Effects of clay-modifying agents on the morphology and properties of poly(methyl methacrylate)/clay nanocomposites synthesized via γ-ray irradiation polymerization," *Journal of Polymer Science A*, vol. 41, no. 21, pp. 3218–3226, 2003.

[27] H. M. Jeong, B. C. Kim, and E. H. Kim, "Structure and properties of EVOH/organoclay nanocomposites," *Journal of Materials Science*, vol. 40, no. 14, pp. 3783–3787, 2005.

Hindawi Publishing Corporation
Advances in Materials Science and Engineering
Volume 2013, Article ID 128158, 15 pages
http://dx.doi.org/10.1155/2013/128158

Research Article

Pretreatment of Woven Jute FRP Composite and Its Use in Strengthening of Reinforced Concrete Beams in Flexure

Tara Sen[1] and H. N. Jagannatha Reddy[2]

[1] *Department of Civil Engineering, National Institute of Technology, Agartala, Barjala, Tripura (West), Jirania, Pin 799055, India*
[2] *Department of Civil Engineering, Bangalore Institute of Technology, K. R. Road, V. V. Puram, Bangalore, Pin 560004, India*

Correspondence should be addressed to Tara Sen; tarasen20@gmail.com

Received 30 May 2013; Revised 18 August 2013; Accepted 27 August 2013

Academic Editor: Shaikh Faiz Uddin Ahmed

Environmental awareness motivates researchers worldwide to perform studies of natural fibre reinforced polymer composites, as they come with many advantages and are primarily sustainable. The present study aims at evaluating the mechanical characteristics of natural woven jute fibre reinforced polymer (FRP) composite subjected to three different pretreatments, alkali, benzyl chloride, and lastly heat treatment. It was concluded that heat treatment is one of the most suitable treatment methods for enhancing mechanical properties of jute FRP. Durability studies on Jute FRP pertaining to some common environmental conditions were also carried out such as effect of normal water and thermal aging on the tensile strength of jute FRP followed by fire flow test. The heat treated woven jute FRP composites were subsequently used for flexural strengthening of reinforced concrete beams in full and strip wrapping configurations. The study includes the effect of flexural strengthening provided by woven jute FRP, study of different failure modes, load deflection behavior, effect on the first crack load, and ultimate flexural strength of concrete beams strengthened using woven jute FRP subjected to bending loads. The study concludes that woven jute FRP is a suitable material which can be used for flexural upgradation of reinforced concrete beams.

1. Introduction

A structure is designed for a specific life span, and depending on the nature of the structure, its purpose, and its usability, its design life varies. For a domestic building, this design life could be thirty to forty years, whereas for a public building, it could be fifty to sixty years. Deterioration in concrete structure is a major challenge faced by the infrastructure and bridge industries worldwide. The deterioration can be mainly due to environmental effects, which include corrosion of steel, gradual loss of strength with aging, repeated high intensity loading, variation in temperature, freeze-thaw cycles, contact with chemicals and saline water and exposure to ultraviolet radiations, and also deterioration due to exposure to an aggressive environment and accident events such as earthquakes. That is why reinforced concrete structures often have to face modifications and improvements of their performance during their service life. When possible, it is often better to repair or upgrade the structure by retrofitting which is prestrengthening a structure before its failure. The most common and advanced material used worldwide for structural strengthening is FRP (fibre reinforced polymer) composites, which are used for the strengthening purposes be it in flexure or shear or the ductility parameter or even confinement, and is successfully used all over the world the said purpose [1–4]. FRPs help to increase strength and ductility without excessive increase in stiffness and self weight, as they are very light materials. FRPs have various advantages such as, high strength, low weight, corrosion resistance, high fatigue resistance, easy and rapid installation and minimal change in structural geometry, and better mechanical and chemical performance. Beams are the critical structural members subjected to bending, torsion, and shear, and they are one of the most important load carrying elements in a structural system. Therefore, extensive research works are being carried out throughout the world on the retrofitting of concrete beams with externally bonded FRP composites. The most common FRP materials used for retrofitting

and rehabilitation of concrete members include carbon, glass, and aramid FRPs. It has been experimentally proved that when concrete beams and columns are retrofitted with carbon-fibre-reinforced polymer (CFRP) composites, then there is an enhancement in the flexural strength, shear strength, and torsional strength [5–9]. Also glass fibre reinforced polymer (GFRP) composites have been very successful in improving the flexural strength, shear strength, torsional strength, and so forth of concrete structures. [10–12]. All these FRPs mentioned above are artificial fibres or man-made fibres, which involve large manufacturing and production units with high processing costs. One of the main disadvantages of using man-made fibres as FRPs for strengthening is that beams or columns strengthened with FRP can fail in a brittle manner due to FRP debonding or FRP rupture, at the FRP-concrete interface. This type of brittle failure is very significant and common when carbon FRP or glass FRP materials are used for strengthening. FRPs are a major source of CO_2 emissions, most of which arise during their processing and manufacturing. FRPs use large amounts of energy for their production and transport, this is known as the "embodied energy" of the material. Most of this energy is produced by the burning of fossil fuels, which increases the amount of carbon dioxide (CO_2) in the atmosphere. Crop-derived materials can be used in making FRPs, which have performance attributes that can improve the "in-use" energy profile of buildings and cut down the inherently embodied energy. The present trend of using bio or crop or plant based products for FRP fabrication has been influenced by a number of factors, including increased environmental and health concerns, more sustainable methods of manufacturing and reduced energy consumption, supporting a desire for lighter weight structures, the use of sustainable material in building constructions, and the use of sustainable materials and green material for manufacturing of FRPs. A natural-based material can be defined as a product made from renewable agricultural and forestry feedstock, including crops and crop by-products and its residues. Materials from renewable resources are being sought to replace not only the reinforcement element but also the matrix phase of composite materials, thereby alleviating some of the sustainability issues associated with using synthetics in composites. The widespread use of agricultural crops in construction and the building industry would greatly reduce the impact of artificial construction material use, since FRPs are extensively used worldwide in various civil and mechanical engineering divisions. These factorial considerations combine to provide a substantial environmental benefit to the use of crop-based materials in the making of FRPs. Natural fibres are a good substitution as reinforcement for composite products in place of the customary synthetic fibres such as E glass and they are being researched extensively for their suitable applications [13–17]. It is estimated that there are about 2.3 million tonnes of glass fibres devoted to various applications around the globe so there are a number of opportunities for natural fibres to be used in place of existing glass fibres. Natural fibres have several advantages over glass fibre such as low density, low cost, high toughness, acceptable specific strength properties, good thermal properties, low embodied energy, reduced tool wear, and reduced irritation to the skin and respiratory system, and they also have a low energy requirement for processing and they are also biodegradable or recyclable depending on the selected matrix [18–20]. Further market penetration of natural fibre composite will occur only when their production can be rendered cost-effective and competitive to the present injection-molded thermoplastics used in many branches of science and engineering. Also, plant fibres are hydrophilic in nature due to attraction/interaction between the hydroxyl groups of fibre components and water molecules. The hydrophilic nature of plant fibres often results in poor compatibility with hydrophobic polymer matrices. Therefore, it becomes necessary to modify the surface of plant fibres for aiding in better adhesion between fibre and matrix. In this study, we have carried out and compared various treatment methods such as alkalization, benzoylation, and thermal treatment for surface modification and its corresponding effect on the properties of woven jute fibre reinforced polymer composites along with three durability studies, which are effect of normal water on woven jute FRP, effect of thermal aging on woven jute FRP, and fire flow test on woven jute FRP, were all carried out and analysed. The applications of modified woven jute fibre reinforced polymer composite in improving the flexural capacity of reinforced concrete beams and its suitability was evaluated as a new alternate reinforced polymer composite material used for structural strengthening. The type of concrete failure aided by strengthening the reinforced concrete with woven jute FRP composite was analysed pertaining to failure modes, ductility improvement, load-deflection behaviour, ultimate flexural strength, first crack load, and so forth.

2. Review of Plant Fibres

Natural fibres, often referred to as vegetable fibres, are extracted from plants and are classified into three categories, depending on the part of the plant they are extracted from, fruit fibres such as oil palm fibres, bast fibres such as jute fibres, and leaf fibres such as sisal fibres. Nowadays, there is a demand for these natural fibres to be used as reinforcement in polymer matrices. In recent years, there has been increasing interest in the replacement of fibreglass in reinforced plastic composites by natural fibres such as kenaf, oil palm, ramie, sisal, coir, and jute. Jute fibres are bast fibres, and are one of the strongest bast fibres, and it withstands rotting very easily. Jute is the most common agricultural fibre. The fibres of jute are nonabrasive, exhibit moderately higher mechanical properties, and are abundantly available exclusively in Bangladesh, India, Thailand, and also in some parts of Latin America. Researchers have shown that suitable pretreatments of jute yarn can lead to an improvement in its mechanical properties and that jute fibre composites have shown immense potential in terms of its mechanical characteristics [21–30]. The research concerning kenaf plastic composite is also growing tremendously along with the industry's and government's high demand for producing nonpetroleum-based materials. Several treatments have been proposed and used to improve interlaminar bonding of kenaf fibre composites. The fibre

has been mainly used in rope, twine, coarse cloth, and paper. However, nowadays, there is demand for this fibre to be used as a reinforcement for polymers. Kenaf fibres exhibit low density, nonabrasiveness during processing, high specific mechanical properties, biodegradability, and so forth. Recently, kenaf is being used as a raw material alternative to wood in pulp and paper industries for avoiding destruction of forests, and also it is used as nonwoven mats in the automotive industries, textiles, fibreboard and is also extensively being employed as fibre reinforcement to composites, since it shows promise [31–36]. Sisal too is a highly resistant and rigid natural fibre, mainly used in applications ranging from manufacturing of ropes and yarns for ropes and carpets to different textiles and handicrafts. Sisal fibres are majorly cultivated in Tanzania, Madagascar, Brazil, India, and so forth. They are extracted from the sisal plant leaves in the form of long fibre bundles. From a 100 kg of sisal leaves about 3.5 kg extractable fibre is obtained. These fibres have been used as a reinforcement in polymer composites and were characterized mechanically by various researchers. The sisal fibre composites have shown high elastic modulus and tensile strength which could be further improved by surface modifications [37–41]. A lot of research works have been conducted on alternative new fibres such as oil palm fruit bunch fibres. Oil palm biomass is a natural waste product, and hence, available at a minimal cost. Malaysia is one of the leading producers of palm oil. Lignocellulosic fibres can be extracted from the trunk, frond, fruit mesocarp, and empty fruit bunches of oil palm trees. Empty fruit bunches are the fibrous mass left behind after separating the fruits from sterilized fresh fruit bunches. Fibre modifications and coupling agents could be considered for the optimization of the interface, and for the improvement of their properties [42–46]. Fibres of ramie too have shown very high tensile strength and the tensile strength, of ramie is approximately equal to that of glass fibre. Hence, ramie fibre composites have been extensively researched upon for their strong mechanical properties with added environmental benefits. The effect of different ramie fibre surface-treatment methods including silane treated, and alkali treated on the mechanical properties and thermal properties of ramie fibre composites are also being researched upon, for additional strength improvements [47, 48]. Even coir fibre is an important lignocellulosic fibre obtained from coconut trees, is a very cheap and ecofriendly material which is friendly to the environment, and grows extensively in tropical countries. Coir fibres have many advantages like low density, lower cost, availability, higher lignin content, low elastic modulus, and high elongation at break. Coir fibres too are being considered as a reinforcement in polymer composites by various researchers, since their mechanical properties can be improved by various chemical and physical treatment processes and because of them being natural, resulting in several environmental benefits [49–54]. Although various positive and enhanced mechanical characterizations have been underway and yielded positive results with natural fibre composites, also pertaining to their use in various crop industry, textile engineering, mechanical engineering, agricultural engineering, and so forth, very scare research has been devoted to the use of natural fibres as reinforcements in composites, to be used as a strengthening material for structural strengthening. In order to evaluate the effectiveness of FRP materials which uses natural fibres as their reinforcements, to be used as a strengthening material, it might be necessary to investigate the mechanical issues of these FRPs as well as its effect on the various strength parameters of concrete structures simultaneously. This study investigates the mechanical property of the jute fibre FRP with suitable pretreatments using alkali treatment, which is a very commonly established treatment method, followed by benzyl chloride treatment, and lastly heat treatment, which has shown promise in case of the treatment of woven fabrics or yarns, followed by evaluating the effectiveness of flexural strengthening provided by woven jute FRP on the reinforced concrete beams.

3. Pretreatment and Characterization of Jute FRP Composite

3.1. Materials. The woven jute was collected from Extra Weave Private Ltd, Cherthala, Kerala, India. All other chemicals used for the fabrication of the natural woven jute FRP composite for its mechanical characterisations and structural strengthening, such as MBrace saturant, which consists of Part A epoxy resin and Part B hardener, were also collected and utilized. Strengthening of the RC beams with FRP composite wrapping using natural jute FRP composite was carried out with the help of chemicals such as concresive 2200 and MBrace primer in conjunction with the MBrace saturant (epoxy-rein-hardener system) were all obtained suitably for the said purpose.

3.2. Pretreatment of Jute Fibres. The chemical treatment of fibre is aimed at improving the adhesion between the fibre surface and the polymer matrix by modifying the fibre surface and the fibre strength. It also reduces the water absorption capacity of the fibre and helps in improving the mechanical properties. Following are the different pretreatments carried out. The woven jute mats were cut into the size required for flexural strength test as per ISO 14125:1998 and tensile strength test as per ISO 527-4:1997(E), and then, the various pretreatments were carried out. Some samples were left untreated as controlled samples for comparison study purpose.

3.2.1. Alkali Treatment. Alkaline treatment is one of the most commonly used chemical treatment procedures, for treating natural fibres when used as reinforcements in thermoplastics and thermosets. The important modification done by alkaline treatment is the disruption of hydrogen bonding in the network structure, thereby increasing surface roughness. This treatment removes a certain amount of lignin, wax, and oils covering the external surface of the fibre cell wall. Addition of aqueous sodium hydroxide (NaOH) to natural fibre promotes the ionization of the hydroxyl group to the alkoxide. Thus, alkaline processing directly influences the cellulosic fibril, the degree of polymerization, and the extraction of lignin and hemicellulosic compounds. It is reported that alkaline treatment has two effects on the fibre: it increases surface

(a) (b)

Figure 1: (a) Tensile testing; (b) tensile fracture samples of woven jute FRP.

roughness resulting in better mechanical interlocking and it increases the amount of cellulose exposed on the fibre surface, thus increasing the number of possible reaction sites. Consequently, alkaline treatment has a lasting effect on the mechanical behaviour of natural fibre, especially on fibre strength and stiffness. Woven jute fibre mats in deemed sizes were immersed in 4% NaOH solution at room temperature. Then, they were removed from the NaOH solution and then washed several times with fresh water to remove any NaOH sticking to the surface, followed by neutralisation with dilute acetic acid. Finally, these woven jute fibre mats were washed again with distilled water, ensuring that a final pH-7 was maintained. The fibre mats were then dried at room temperature for 48 hours followed by oven drying at 50°C for 24 hours.

3.2.2. Bezoylation Treatment. Benzoylation is an important transformation in organic synthesis. Benzyl chloride is most often used in fibre treatment. Benzyl chloride includes benzyl ($C_6H_5C{=}O$) which is attributed to the decreased hydrophilic nature of the treated fibre and improved interaction with the hydrophobic polymer matrix. Woven jute fibre mats in deemed sizes were immersed in 10% NaOH solution agitated with benzyl chloride. This mixture was kept for 15 minutes. After that, the fibre mats were removed from the mixture of NaOH and benzyl chloride and washed thoroughly with normal water. Then, these wet fibre mats were dried thoroughly using filter paper (white paper). Then, they were soaked in ethanol for 1 hour to remove any benzyl chloride sticking to their surfaces. Finally, the fibre mats were washed thoroughly with water and then dried in the oven at 40°C for 48 hours.

3.2.3. Heat Treatment. The mechanical treatment in the form of heat treatment was carried out in the following manner. Woven jute fibre mats in deemed sizes were placed into the oven at 50°C for 48 hours. After that, these samples were kept in an air tight chamber so that atmospheric moisture could not be absorbed by these samples. Basically, the raw fibres when exposed to atmosphere absorb moisture, and this moisture which gets accumulated in the fibres requires to be eliminated. This elimination of the moisture from the fibres can be attained by the process of heat treatment. Heat-treated composites of natural textile or fabrics have higher strength than untreated composites of natural jute fibre textiles.

3.3. Fabrication of Composites. A plastic bit mould with suitable dimensions was used for casting the woven jute composite sheets. The usual hand lay-up technique was used for preparation of the samples. A calculated amount of epoxy resin and hardener ratio of 10 : 4 by weight was thoroughly mixed with gentle stirring to minimize air entrapment. For quick and easy removal of composite sheets, a mould releasing agent was used, which was silicone grease. Electrical insulating paper was put underneath the plastic bit mould, and silicone grease was applied at the inner surface of the mould. After keeping the mould on the insulating sheet, a thin layer (≈2 mm thickness) of mixture of epoxy and hardener was poured. Then the woven jute fibre mats (both pretreated and untreated) were separately distributed on the mixture on different moulds. The remaining mixture was then poured into the mould on top of the fabric mats. Care was taken to avoid formation of air bubbles. Pressure was then applied from above to the mould, and with this pressure still on top of the composite sheet, it was allowed to cure at room temperature for 48 hrs. After 48 hrs, the samples were taken out from the mould and kept in an air tight container for further experimentation.

3.4. Mechanical Testing. Two mechanical tests were performed for all the samples of woven jute fibre composites, the two tests were tensile strength test, and flexural strength test. All treated FRP composites were subjected to the above mentioned two tests. During the tensile test, an uniaxial load was applied through both the ends of the specimen, using suitable jaws as an attachment to the UTM. The tensile test was performed in the universal testing machine (UTM) which was HEICO digital universal testing machine, and results were obtained digitally with the digital data acquisition system, which aided us in calculating the tensile strength of composite samples. The tensile strength test for jute FRP composites was done in accordance to ISO 527-4:1997(E), as jute falls under the category of Type-2 materials. All the results were taken as an average value of 5 samples each. Figure 1 shows the woven jute FRP composite under tensile load conditions and the tensile fractures in the composite samples. Jute FRP composites displayed both diagonal and straight types of fracture (fracture exactly perpendicular to the direction of the woven jute fabric). All these failure modes are accepted modes of tensile fracture in accordance to ISO 527-4:1997(E) and ISO 527-5:1997(E). The flexural strength of a composite is a 3-point bend test, which generally promotes failure by interlaminar shear. This test was conducted as per ISO 14125:1998 standard using

Table 1: Tensile strength property of pretreated and untreated (controlled) woven jute FRP composites.

Mechanical property	Alkali treated jute fabric FRP	Benzoylated treated jute fabric FRP	Untreated jute fabric FRP	Thermally/heat treated jute fabric FRP
Tensile strength (MPa)	83.836	101.534	148.603	189.479
Tensile modulus (MPa)	15000	13500	16000	32500
Flexural strength (MPa)	158.631	97.572	183.932	208.705
Flexural modulus (MPa)	2750	2500	4250	4500

(a) (b)

Figure 2: (a) Flexural testing; (b) flexural fracture of woven jute FRP.

a load cell of high sensitivity. The loading arrangement is shown in Figure 2. Since jute belongs to Class II Type material, hence, all the restrictions of the specimen dimensions for flexural testing were followed, as per the code ISO 14125:1998. After the flexural failure occurred, all the specimens of the FRP composites showed a single line fracture (perpendicular to the plane of the composite direction). Also both the tensile modulus of elasticity and the flexural modulus were found out for all the samples of woven jute FRP composites subjected to different pretreatments were also obtained. The modulus of elasticity, which is equal to the Young's modulus, is a material property that describes its stiffness and is therefore one of the most important properties of solid materials. Mechanical deformation puts energy into a material. This energy is stored elastically or dissipated plastically. The way a material stores this energy is summarized in the stress-strain curves. Stress is defined as force per unit area and strain as elongation or contraction per unit length. When a material deforms elastically, the amount of deformation likewise depends on the size of the material, but the strain for a given stress is always the same, and the two are related by Hooke's Law (stress is directly proportional to strain). Moduli of elasticity, both tensile and flexural modulus were obtained since these parameters play a vital role in evaluating the mechanical characteristics of a material. The tensile strength, tensile modulus (modulus of elasticity), flexural strength, and flexural modulus are presented in Table 1, and a graphical comparison of the tensile and flexural behavior of woven jute FRP composites, subjected to different pretreatments and no treatment (i.e., controlled samples) is presented in Figure 3.

4. Durability Study of Woven Jute FRP Composite

While most of us have general sense of what the term "durability" means, is not easily defined in the context of infrastructure materials, and numerous definitions have been proposed in the literature. In the current educational module durability, is defined on the basis of a definition offered by Karbhari et al. [55] as the ability of an FRP element "to resist cracking, oxidation, chemical degradation, delamitation, wear, and/or the effects of foreign object damage for a specified period of time, under the appropriate load conditions, under specified environmental condition." The available data on the durability of FRP materials is somewhat limited and can thus appear contradictory in some cases. This is due to the many different forms of FRP materials and fabrication processes currently used. Furthermore, FRPs used in civil engineering applications are substantially different from those used in the aerospace industry, and hence their durability cannot be assumed to be the same. All engineering materials are subject to mechanical and physical deterioration with time, load, and exposure to various harmful environments. When FRPs are used as reinforcement or are used for the strengthening of reinforced concrete structures, then they can be expected to be exposed to a variety of potentially harmful physical and chemical environments and can undergo potential damage if used improperly in a number of harmful environments. Here, durability of woven jute FRP composite was evaluated under three most common environmental conditions of civil infrastructure.

4.1. Effect of Normal Water. The mechanical properties of thermoset resin matrix composite materials are affected when exposed to wet environments. The absorbed water causes matrix plasticization and or interface degradation. The effect of water environment on moisture (H_2O) absorption characteristics of woven jute epoxy composite material has been investigated by the measurement and analysis of percentage moisture content, thickness swelling, and effect of water on the tensile strength property of woven jute FRP composite. Firstly, the composites were weighed and their thicknesses were measured. Normal water was then collected and heated (till bubbles started appearing) to 100°C along

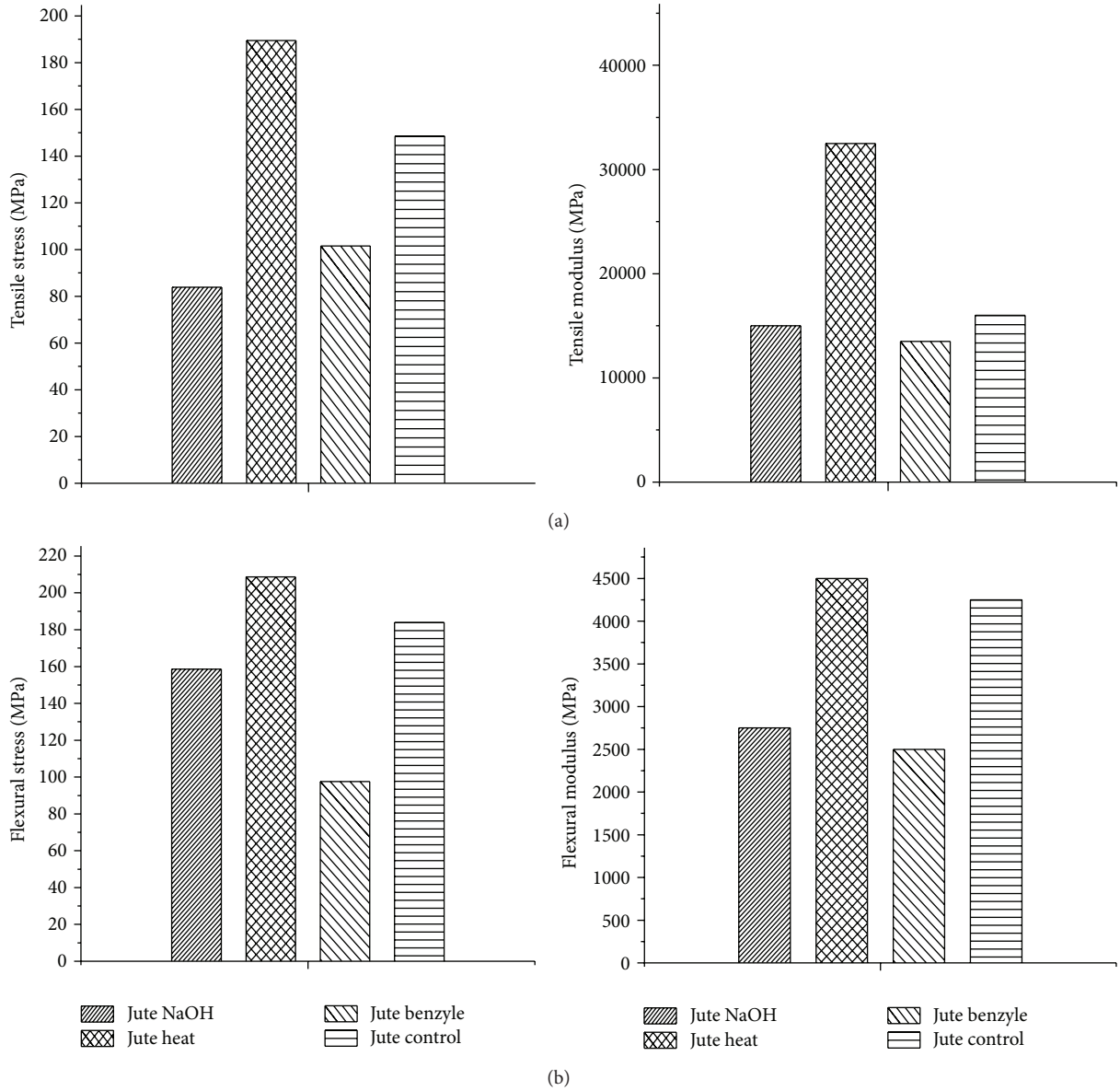

Figure 3: (a) Tensile behaviour of jute FRP composite, woven jute being subjected to different pretreatments; (b) flexural behaviour of jute FRP composite, woven jute being subjected to different pretreatments.

with the composites for 30 min, then the composites were removed from the hot water and wiped with cotton and then weighed again and their thicknesses were measured. The relative mass change of the epoxy in the specimens under study was expressed as a percentage obtained using the expression: Moisture content = (weight of soaked specimen − weight of dry specimen)/weight of dry specimen. Thickness swelling index was also measured by measuring the thickness of the composites before and after boiling. Lastly, tensile strength tests were carried out on these composite samples. It was observed that the moisture content percent was 6.6% and thickness swelling was 8.9%, but the tensile strength increased from 189.48 MPa under dry conditions to 213.42 MPa under wet conditions. The hygrothermal effects on the woven jute FRP could be viewed as a result of two mechanisms. Firstly, at the macroscopic level, the expansion of the matrix due to absorption of water may cause tensile stresses in the fibres and compressive stresses in the matrix which is similar to differential thermal expansion. Secondly, at the molecular level, the diffusing molecules of water may strain or rupture the intermolecular bond in the matrix and at the interface.

4.2. Effect of Thermal Aging. Thermal aging behaviour of composites is of special interest because of their expanding use for structural applications where increased temperatures is a common environmental condition. There are significant chemical and structural changes in epoxy networks which take place during thermal aging. Delamination and microcracking are some of the most frequently observed damaging

phenomena that may develop in polymer composites exposed to cryogenic temperatures (low temperature conditions). It is important to understand the aging mechanism of polymer composites for their use in thermal environments. The mechanical behaviour of composites depends on the ability of interface to transfer stress from the matrix to the reinforcement fibre. Two batches of samples were fabricated for this test. The first batch of samples was kept in temperature of +75°C (in oven) for 10 hours. And the second batch of samples was similarly exposed to ultra-low deep freezing conditions at −75°C temperature, in the freezer for 6 hours. These were followed by tensile strength testing for both the batches of the samples immediately. It was observed that the tensile strength of woven jute FRP composite increased from 189.48 MPa under unexposed conditions to 197.51 MPa under high temperature, that is, +75°C conditions, and came down to 168.11 MPa under low temperature, that is, −75°C conditions. The most common damage modes in thermal aging are matrix cracking, delamination growth, and fibre fracture. Cryogenic exposure introduces matrix cracking and/or interfacial debonding. During cryogenic conditioning the fibre/matrix adhesion is low. So the first form of damage in laminates is commonly matrix microcracks and interlaminar cracks at such low temperature conditions. This is one of the reasons for the decrease in the tensile strength of composites, when subjected to very low temperatures. Thermal conditioning at higher temperatures imparts better adhesion, and thus an improved tensile strength values are observed, since fibre cross linking is highly probable during thermal conditioning when the composites are exposed to higher temperatures, hence, it increases the tensile strength of the composites.

4.3. Fire Flow Test. From the civil engineering point of view, we are looking towards implementing the FRP composite in old structures or deficient structures as a retrofitting or strengthening material. A fire flow study of any material is very important for the constructional performance, upon studying we can easily know that if any fire-related accident happens, how fast the fire can flow with respect to time considering the building material and how we can reduce the flow rate of fire and what will be the effect in the environment when those particular materials are burnt. This test was performed in accordance to ASTM D635 standard, and the burning rate was measured. It was observed that woven jute FRP composite had a burning rate of 8.1 mm/min.

5. Flexural Strengthening of RCC Beams with Woven Jute FRP Composite

5.1. RCC Beams Specimens. Ordinary Portland cement of 53 grade, conforming to IS: 12269-1987, has been used. Locally available clean river sand have been used in this work. The maximum size of coarse aggregate considered was 12 mm. The coarse aggregate used for the casting of RCC beams passed through 12 mm IS sieve. As per Indian standard specifications, the mix proportion of the concrete was carried out, in accordance to IS 10262-2009, in order to achieve the desired compressive strength of 20 N/mm^2. In accordance, the mix proportion by weight of cement: fine aggregate: coarse aggregate was found to be 1 : 2.07 : 1.87. The designed water cement ratio was 0.5. Three numbers of cubes were also cast using the stated mix proportion and water cement ratio, and the average compressive strength for 28 days was 22.309 N/mm^2. Here, Fe 415 HYSD bars of 8 mm diameter, having characteristic strength of 415 N/mm^2, were used. Three samples of bars were placed in the universal testing machine one after another and were tested for their yield strength. It was found that the bars had average yield strength of 415 N/mm^2. The mentioned bars were both used for the longitudinal reinforcement as well as stirrups. The experimental program contained three beam groups. All the three groups of beams were utilized for the study of the effect of flexural strengthening. All the beams in groups A, B, and C had the same reinforcement detailing, although the beam length for design was 1.3 m, it was cast as 1.4 m, for providing 50 mm clearance from both the sides at the supports and had a cross section of 140 mm width and 200 mm depth. The RCC beam design was carried out as per IS-456: 2000. The entire reinforcement details, which were followed for all the three groups of beams, are shown in Figure 4. All the beams were designed such that they are strong in shear, so that flexural failure takes place before shear failure, so that the flexural strengthening effect could be evaluated.

5.2. Strengthening Scheme. The beams in group A were designed as controlled specimen (2 number of models, Con1 and Con2), where no FRP application was carried out. The beams in group B were designed to investigate the effect of full wrapping technique 90° (3-sided U wrap) for flexural strengthening provided by using woven jute FRP (2 number of models, JF1 and JF2). The beams in group C were designed to investigate the effect of strip wrapping technique 90° (3-sided U wrap) where 50% of the total area was used for strengthening, that is, 62 mm strips were placed at 124 mm C/C throughout the length of the beam and at a clear gap of 49 mm at the support ends, for flexural strengthening provided by using woven jute FRP (2 number of models, JF3 and JF4); a summary of the test beams are shown in Table 2. The beams were prepared by grinding 3 side surfaces with the help of a grinding machine, this was done so as to roughen the three sides of the beam where FRP application would be carried out, and roughening the beam surface ensures good boding of the composite material. After grinding, all the three side surfaces of the beams were cleaned with an air nozzle and finally were wiped to remove any dust or loose particles. Small surface defects in the concrete beam were repaired and made good using concresive 2200. Then, a coat of MBrace primer was applied on all the three sides of the beams in group B and C. MBrace primer is a low viscosity, 100% solids polyamine cured epoxy. It is the first applied component of the MBrace system, and it is used to penetrate the pore structure of cementitous substrates and to provide a high bond base coat for the MBrace system. The primer coat was allowed to air cure for 8 hours. Next, resin Part A and hardener Part B of the two component MBrace saturant were mechanically premixed as per the guidelines of the manufacturer for

Table 2: Summary of test beams.

Beam group	Wrapping configuration	Strengthening material	Beam designation	Type of strengthening	Strengthening scheme
Group A	Nil 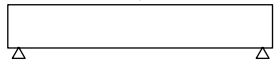	Nil	Control specimen Con1, Con2	No strengthening	Nil
Group B	Full wrapping 90°, single layer 	Jute FRP	JF1, JF2	Flexural strengthening throughout using jute FRP	U-Wrap, three-sided wrap
Group C	Strip wrapping 90°, single layer 62 mm strips at 124 mm C/C (at a clear gap of 62 mm) so as to achieve 50% of total area strengthening, with end clear gaps of 49 mm. 	Jute FRP	JF3, JF4	Flexural strengthening throughout using jute FRP	U-Wrap, three-sided wrap

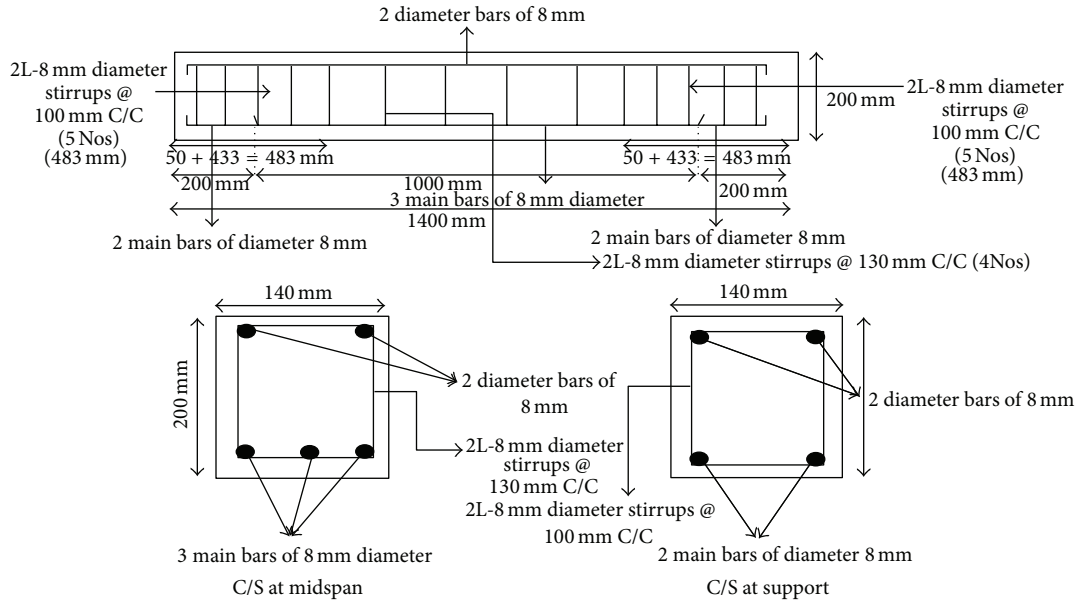

Figure 4: Reinforcement detailing of RCC beams (all sets, group A, B, and C).

3 minutes or until homogeneousness. The property of the MBrace saturant as provided by the manufacturer is given in Table 3. The ratio of mixing of resin and hardener was followed as per the manufacturer, which stood to be 3 : 1. Then the neatly measured and cut pieces of woven jute fibres were correspondingly applied on the respected beams JF1, JF2, JF3, and JF4. The woven jute fibres were placed on top of epoxy resin coating immediately on the respective beams, and the resin was squeezed through the roving of the fabric with plastic laminating roller. It was made sure that all the woven jute fibre reinforcements are properly impregnated in the resin hardener mix, and lastly one more coat of epoxy-hardener mix was applied on top of the woven jute fibres on all the respective beams, as a finishing layer. Air bubbles entrapped at the epoxy/concrete or epoxy/fibre interface were eliminated. All the strengthened concrete beams were cured for at least two weeks at room temperature before the beams were tested. The entire strengthening process is demonstrated in Figure 5.

Table 3: Typical properties of MBrace Saturant.

Mechanical property	MBrace Saturant
Description	2 parts; Part A: epoxy and Part B: hardener
Density	1.06 kg/Lt (Mixed density)
Colour	Blue
Bond strength	>2.5 N/mm^2 (Failure in concrete)

5.3. Test Setup. A third point loading system was adopted for the beam tests. At the end of each load increment, deflection, ultimate load, type of failure, and so forth were carefully observed and recorded. The experimental set-up under

Figure 5: (a) Surface preparation of beams by grinding; (b) primer application on beam surface; (c) application of epoxy-hardener mix on the beam; (d) bonding of woven jute; (e) bonding of woven jute in strips; (f) final coating of epoxy-hardener mix on the bonded fabric.

the third point loading system is shown in Figure 6. All the three sets of beams under group A, B, and C were tested to find out their ultimate flexural strengths, and the deflection at the centre were noted.

5.4. Results and Discussions. The ultimate load carrying capacity, that is, the ultimate flexural strength of all the beams along with the nature of failure and deflections, are given in Table 4. The flexural fractures and cracks of all the beam specimens are as demonstrated in various subparts of Figure 7. Load deflection curves for strengthened beams along with control specimens are as shown in Figure 8, and the comparisons of the ultimate flexural strength of all the beams along with the comparison of the first crack loads are represented in Figure 9. The various failure modes along with the load deflection behavior and the ultimate flexural strength of the controlled beams and the strengthened beams are discussed below.

5.4.1. Failure Modes and Flexural Strength Study of Controlled Beams. The first set of beam, that is, group A and Con1 and Con2, failed in flexure which proved that the beams were strong in shear, and henceforth flexural failure took place before shear failure. Major vertical cracks developed in the midspan that is, in the pure flexure zone, these cracks firstly developed at the lower face, that is, at the bottom side of the beam, and extended from the bottom side towards the top face of the beam. Both the beams Con1 and Con2 failed in similar manner, and Figure 7(a) depicts the clear representation of the failure of group A beams. The average ultimate flexural strength of group A beams was 80 KN.

5.4.2. Failure Modes and Flexural Strength Study of Fully U Wrapped Beams. In the second set of beams in group B, in which the beams were strengthened by fully U wrapped woven jute FRP, JF1, and JF2, it was seen that both beams failed in flexure and their flexural strength was much higher than that of Group A beams. When load was applied on JF1 and JF2, firstly the matrix started cracking, then on further increment of load, the jute fibres in jute FRP started to crack, then again on further load increment the cracks in jute FRP started to widen, then the RCC beam showed vertical crack in the flexure zone, and then this crack started to slowly move from the bottom side of the beam to the top side. Both the failure modes depicted in JF1 and JF2 were very ductile in nature, and the beam carried huge deflection. There was no debonding of jute FRP at all from the beam face in any direction even at very high load, and hence cracks were visualized only on the woven jute FRO and not on the RCC beam. Only a single crack appeared in JF1 on the woven jute FRP, and this crack started to widen with the increase in the load, without the development of any other cracks. The widening of this crack showed and exposed the crack in the RCC beam, at the same location. In the other beam JF2, two cracks appeared on the woven jute FRP which started to widen with the increase in the load, without the development of any other cracks, and the widening of the two cracks exposed the cracks in the RCC beam at the same locations. All the cracks observed in both the beams JF1 and JF2 were at the beam flexure zone, and the ultimate flexural load was reached by further widening of these cracks, without the generation of any other alternate cracks. The average ultimate strength of group B beams JF1 and JF2 was 130 KN. Both the beams JF1 and JF2 failed in similar manner. Figure 7(b) depicts the clear representation of the failure mode of JF1, and Figure 7(c) depicts that of JF2.

5.4.3. Failure Modes and Flexural Strength Study of Partially U Wrapped Beams. The third set of beams in group C, in which the beams were strengthened by strips, that is, U wrapped woven jute FRP in strips, JF3 and JF4, and all strip wrapped strengthened beams were tested to find out their ultimate flexural strength. It was seen that the beams JF3 and JF4 showed higher ultimate load carrying capacity than that of group A beams, but lower than that of group B beams. In the group C beams, it was observed that cracks first developed

Table 4: Summary of test results.

Group designation	Beam designation	Failure of FRP	Deflection at midspan (mm)	Average deflection at midspan (mm)	Comments on deflection	Pultimate, (KN)	Pultimate, (KN) average	Strengthening effect (%)
Group A	Con1 Con2	—	11.271 11.581	11.426	—	78 82	80	—
Group B	JF1 JF2	Yes	23.882 23.540	23.211	Results in huge deflection, hence gives sufficient warning.	126 134	130	62.5%
Group C	JF3 JF4	No	17.021 18.705	17.863	Deflections are lower than fully wrapped beams, since failure occurs at lower loads as compared to fully wrapped beams.	97 103	100	25%

(a) (b)

Figure 6: (a) Two pint loading system on a 50 ton loading frame; (b) loading on fully wrapped beam with woven jute FRP.

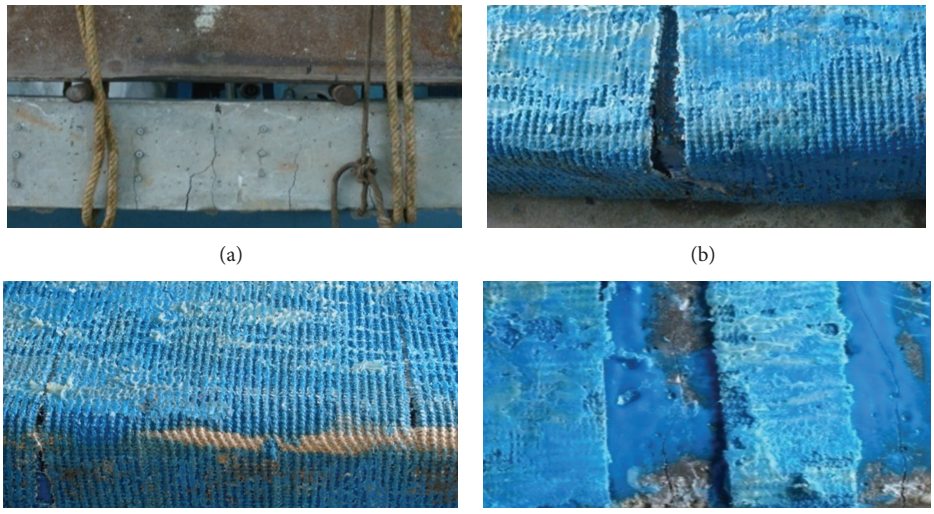

(a) (b)

(c) (d)

Figure 7: (a) Control beams (group A, Con1) under load; (b) formation of flexure crack in the beam JF1, under load; (c) formation of flexure crack in the beam JF2, under load; (d) formation of flexure crack in the beam JF3, under load.

in the RCC beams, that is, on the concrete surface only, and not on the woven jute FRP composite; this indicated that the presence of bonded woven jute FRP on RCC beams imparted additional strength to the beams, and thereby enhanced their flexural strength as compared to controlled beams. When load was applied on JF3 and JF4, then major vertical cracks developed in the mid span that is, in the pure flexure zone, and these cracks developed only in the beam area, and a single flexural crack did not develop on the FRP nor did the FRP undergo rupture or debonding, these cracks on the beam firstly developed at the lower face, that is, beam bottom face, and extended from the bottom side towards the top face of the beam. The strip wrapping technique of FRP strengthening increased the ultimate load carrying capacity up to a point which lied between the load carrying capacity increased by that of full wrapping technique and the unstrengthened, that is, controlled beams. The failure modes of beams JF3 is depicted in Figure 7(d), which clearly shows the flexural cracks in all the beams. The average ultimate strength of group C beams JF3 and JF4 was 100 KN.

6. Conclusions

The following conclusions can be drawn from the study.

(1) The woven jute FRP composite which was mechanically subjected to heat has shown highest tensile strength of 189.479 N/mm^2 and tensile modulus of 32500 N/mm^2, which is the highest tensile strength value, obtained from all the pretreatment procedures used for pretreating the woven jute, and is also higher as compared to controlled samples of woven jute FRP, where no treatment was carried out.

(2) Similarly, the woven jute FRP composite which was mechanically subjected to heat has shown the highest flexural strength of 208.705 N/mm^2 and flexural modulus of 4500 N/mm^2, which is the highest flexural strength value, obtained from all the pretreatment procedures used for pretreating the woven jute, and is also higher as compared to controlled samples of woven jute FRP, where no treatment was carried out.

(3) It was observed that the composites of woven jute FRP, which was untreated or control specimen along with the heat treated woven jute FRP composite, displayed highest tensile and flexural strength, that is, superior mechanical properties, as compared to both the chemically treated, that is, alkali treated or benzylated woven jute FRP composite samples. The reason for this lies in the fact that, we are hereby using woven yarns of jute (not loose jute fibres), chemical treatment results in, partial unwinding of yarns (as hemicellulose dissolves off) and hence the alignment of the fibres gets antagonized. This results in, lowering of strength of woven or textile composites, when subjected to chemical treatment. Another reason is that as woven jute

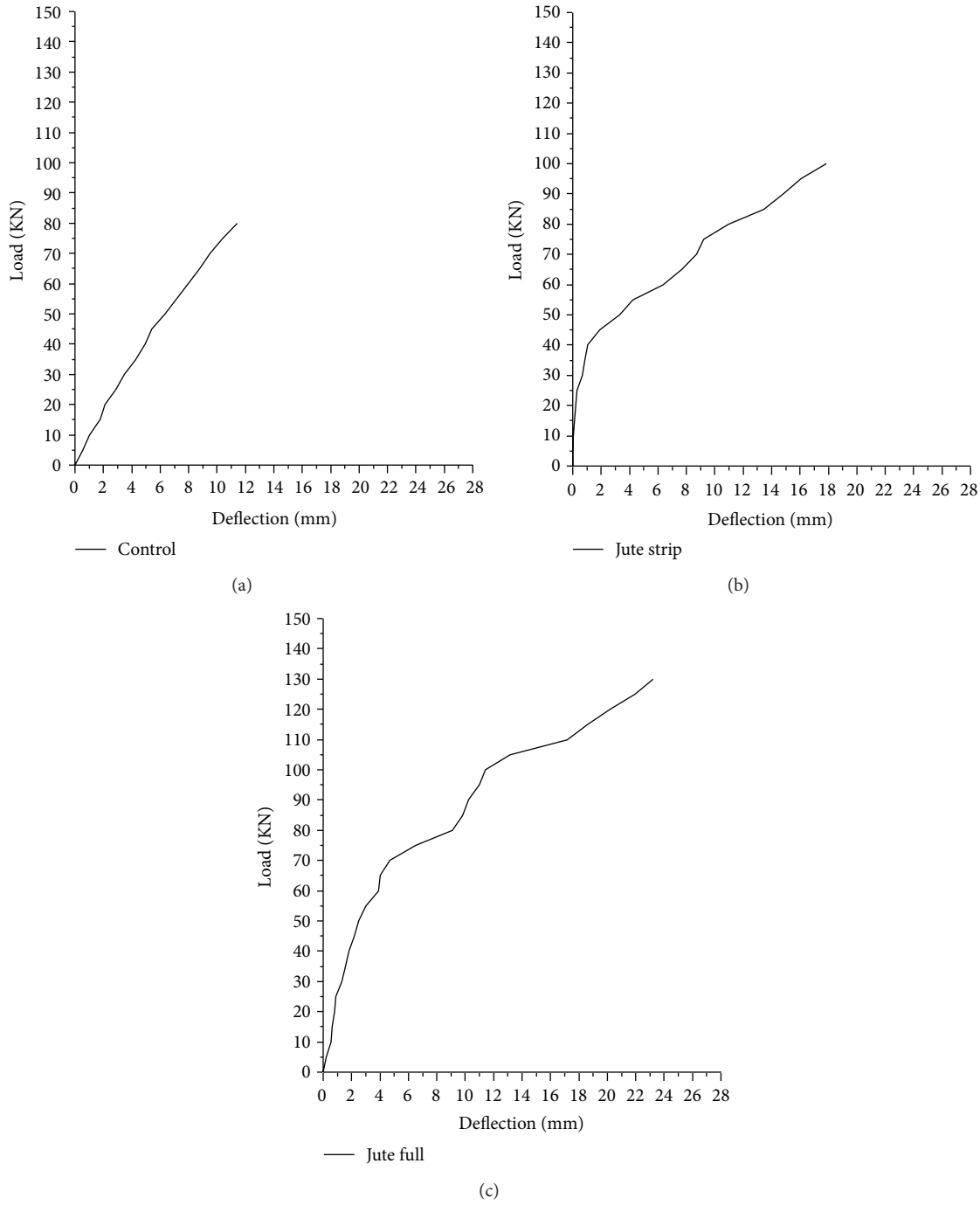

Figure 8: Load versus midspan deflection of (a) Control; (b) woven jute FRP strip wrapped beams; (c) woven jute FRP fully wrapped beams.

is composed of thick strands and knots of the fibres, the alkali and benzyl chloride agents do not penetrate the fabric or textile uniformly, and therefore the interfacial properties between the woven jute and the matrix does get improved enough. The lower strength properties of the composites containing alkali treated as well as benzylated woven jute fibres because of the result of nonuniform penetration of chemicals within the thick strands of the fabric or textile. It can be seen that the highest values are exhibited by thermally treated composites. This could be attributed to the fact that upon continuous heat treatment, the crystallinity of cellulose increases due to the rearrangement of molecular structure at elevated temperatures. The thermal treatment also resulted in moisture loss of the woven jute, thereby enhancing the extent of bonding between woven jute and the matrix.

(4) It can also be concluded that the heat treatment process which aids in the demoisturisation of fibres is a better treatment method as compared to any other chemical treatment method for improving mechanical properties of natural fibre woven or textile composites. Thermally treated

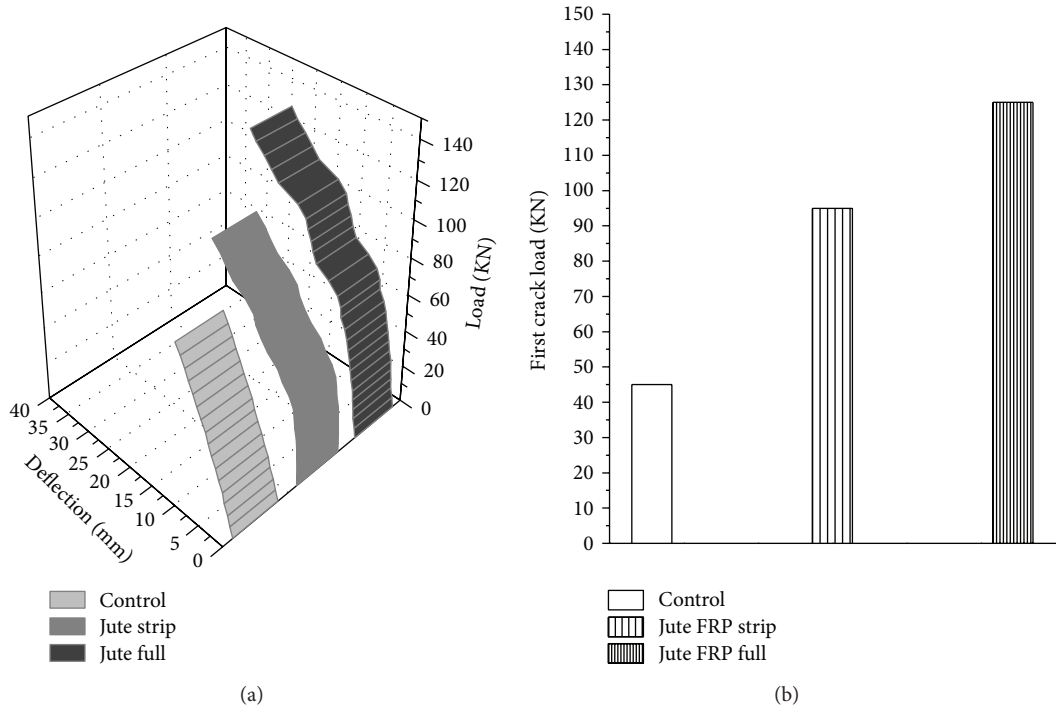

Figure 9: (a) Comparison of ultimate load carrying capacity of all beams; (b) comparison of first crack load of all beams.

composites exhibited superior mechanical properties, both in terms of tensile strength and flexural strength because of increased crystallinity.

(5) From the durability study based on the effect of normal water on woven jute FRP, it could be concluded that woven jute FRP composites behaved similarly to artificial FRP composites of glass and carbon, that is, ultimate tensile strength of wet samples were higher than that for dry samples. This could be attributed to the fact that high amounts of water causes swelling of the fibres, which fills the gaps between the fibre and the polymer-matrix and eventually leads to an increase in the mechanical properties of the fibre composites, but the percentage of moisture absorption and thickness swelling of woven jute FRP composites were slightly on the higher side as compared to artificial FRP composites.

(6) From the durability study based on the effect of thermal aging on woven jute FRP, it could be concluded that woven jute FRP composites behaved similarly to artificial FRP composites of glass and carbon, that is, ultimate tensile strength under cryogenic exposure was lower, and ultimate tensile strength under higher temperature conditioning was higher.

(7) The work being done in this study is important to the composites industry because it is a beginning of systematic research into how the fibre type and also the content affect the overall fire performance of the composites. The burning rate of jute FRP was substantially lower than the burning rate of other artificial FRP composites.

(8) The application of woven jute FRP sheets showed a better performance in increasing the ultimate flexural strength capacity of RC beams as compared to the controlled RC beams. Maximum ultimate load of 126 KN and 134 KN was carried, respectively, by the beams JF1 and JF2, when full U wrapping technique was used, whereas the controlled RCC beams failed at an average ultimate load of 80 KN. Thus, we can conclude that flexural strengthening of RCC beams can be achieved by the use of woven jute FRP composites.

(9) In the beams, JF1 and JF2, the strengthening effect was very noteworthy with one layer itself, providing an increase in the flexural strength by 62.5%, and woven jute FRP bonding also promoted ductile failure without any concrete crushing or FRP rupture or any debonding of FRP, even at very high loads. Hence with increasing the number of layers of jute FRP, a more significant strength improvement could be attained in the flexural strength.

(10) Increase in the ultimate flexural strength of beams by 25%, with woven jute FRP in strips, was observed for beams belonging to group C, where the strip wrapping technique was followed. The presence of strips delayed the first crack formation at locations where FRP was bonded to the beams. By the use of natural jute FRP in the strengthened beams, the initial cracks were formed at higher loads than their respective control beams. This showed that the use of natural woven FRP is very effective in the case of flexural strengthening of structures.

(11) The ultimate strength of beams could be increased by the use of natural woven jute FRP, being bonded to the beam in full length or being bonded in strips. The ultimate flexural loads of beams strengthened with U full wrapping were greater than the beams strengthened by bonding using strip wrapping. Increase in strength depends on the width of the strip that was bonded to the beam.

(12) The load deflection behavior was better for beams strengthened with woven jute FRP compared to the controlled beams. Woven jute FRP strengthened beams in full length depicted typical ductile failure and carried large deflections before undergoing failure and totally avoided any mode of catastrophic failure of beams.

(13) Natural woven fibres of jute FRP have great potential in increasing the load carrying capacity of RCC beams, and also enhanced the material efficiency. Hence, the woven jute FRP can be regarded as a suitable strengthening material for flexural strengthening of concrete structures particularly, and as a good alternative methodology among the fabric reinforcement in FRP considering economic and environmental aspects of FRP products.

Acknowledgments

The authors acknowledge the support extended to the work by various undergraduate and postgraduate students working under the guidance of the authors and also laboratory supporting staff members and the laboratory assistants.

References

[1] K.-T. Lau and L.-M. Zhou, "Mechanical performance of composite-strengthened concrete structures," *Composites B*, vol. 32, no. 1, pp. 21–31, 2001.

[2] S. A. Sheikh, "Performance of concrete structures retrofitted with fibre reinforced polymers," *Engineering Structures*, vol. 24, no. 7, pp. 869–879, 2002.

[3] F. Ceroni, "Experimental performances of RC beams strengthened with FRP materials," *Construction and Building Materials*, vol. 24, no. 9, pp. 1547–1559, 2010.

[4] J. Dong, Q. Wang, and Z. Guan, "Structural behaviour of RC beams with external flexural and flexural-shear strengthening by FRP sheets," *Composites B*, vol. 44, no. 1, pp. 604–612, 2013.

[5] R. Al-Amery and R. Al-Mahaidi, "Coupled flexural-shear retrofitting of RC beams using CFRP straps," *Composite Structures*, vol. 75, no. 1–4, pp. 457–464, 2006.

[6] J. A. O. Barros, S. J. E. Dias, and J. L. T. Lima, "Efficacy of CFRP-based techniques for the flexural and shear strengthening of concrete beams," *Cement & Concrete Composites*, vol. 29, no. 3, pp. 203–217, 2007.

[7] A. A. El-Ghandour, "Experimental and analytical investigation of CFRP flexural and shear strengthening efficiencies of RC beams," *Construction and Building Materials*, vol. 25, no. 3, pp. 1419–1429, 2011.

[8] M. R. Esfahani, M. R. Kianoush, and A. R. Tajari, "Flexural behaviour of reinforced concrete beams strengthened by CFRP sheets," *Engineering Structures*, vol. 29, no. 10, pp. 2428–2444, 2007.

[9] S. Hashemi and R. Al-Mahaidi, "Flexural performance of CFRP textile-retrofitted RC beams using cement-based adhesives at high temperature," *Construction and Building Materials*, vol. 28, no. 1, pp. 791–797, 2012.

[10] J. R. Correia, F. A. Branco, and J. G. Ferreira, "Flexural behaviour of GFRP-concrete hybrid beams with interconnection slip," *Composite Structures*, vol. 77, no. 1, pp. 66–78, 2007.

[11] T. H. Almusallam, "Load-deflection behavior of RC beams strengthened with GFRP sheets subjected to different environmental conditions," *Cement and Concrete Composites*, vol. 28, no. 10, pp. 879–889, 2006.

[12] J. R. Correia, L. Valarinho, and F. A. Branco, "Post-cracking strength and ductility of glass-GFRP composite beams," *Composite Structures*, vol. 93, no. 9, pp. 2299–2309, 2011.

[13] S. V. Joshi, L. T. Drzal, A. K. Mohanty, and S. Arora, "Are natural fiber composites environmentally superior to glass fiber reinforced composites?" *Composites A*, vol. 35, no. 3, pp. 371–376, 2004.

[14] J. Summerscales, N. Dissanayake, A. Virk, and W. Hall, "A review of bast fibres and their composites. Part 2—composites," *Composites A*, vol. 41, no. 10, pp. 1336–1344, 2010.

[15] V. K. Mathur, "Composite materials from local resources," *Construction and Building Materials*, vol. 20, no. 7, pp. 470–477, 2006.

[16] A. C. Milanese, M. O. H. Cioffi, and H. J. C. Voorwald, "Mechanical behavior of natural fibre composites," *Procedia Engineering*, vol. 10, pp. 2022–2027, 2011.

[17] G. Koronis, A. Silva, and M. Fontul, "Green composites: a review of adequate materials for automotive applications," *Composites B*, vol. 44, no. 1, pp. 120–127, 2013.

[18] A. K. Bledzki and J. Gassan, "Composites reinforced with cellulose based fibres," *Progress in Polymer Science*, vol. 24, no. 2, pp. 221–274, 1999.

[19] K. G. Satyanarayana, G. G. C. Arizaga, and F. Wypych, "Biodegradable composites based on lignocellulosic fibers—an overview," *Progress in Polymer Science*, vol. 34, no. 9, pp. 982–1021, 2009.

[20] M. Q. Zhang, M. Z. Rong, and X. Lu, "Fully biodegradable natural fiber composites from renewable resources: all-plant fiber composites," *Composites Science and Technology*, vol. 65, no. 15-16, pp. 2514–2525, 2005.

[21] T. Munikenche Gowda, A. C. B. Naidu, and R. Chhaya, "Some mechanical properties of untreated jute fabric-reinforced polyester composites," *Composites A*, vol. 30, no. 3, pp. 277–284, 1999.

[22] J. Gassan and A. K. Bledzki, "Possibilities for improving the mechanical properties of jute/epoxy composites by alkali treatment of fibres," *Composites Science and Technology*, vol. 59, no. 9, pp. 1303–1309, 1999.

[23] J. Gassan and A. K. Bledzki, "Alkali treatment of jute fibers: relationship between structure and mechanical properties," *Journal of Applied Polymer Science*, vol. 71, no. 4, pp. 623–629, 1999.

[24] A. Stocchi, B. Lauke, A. Vázquez, and C. Bernal, "A novel fiber treatment applied to woven jute fabric/vinylester laminates," *Composites A*, vol. 38, no. 5, pp. 1337–1343, 2007.

[25] W.-M. Wang, Z.-S. Cai, and J.-Y. Yu, "Study on the chemical modification process of jute fiber," *Journal of Engineered Fibers and Fabrics*, vol. 3, no. 2, pp. 1–11, 2010.

[26] X. Y. Liu and G. C. Dai, "Surface modification and micromechanical properties of jute fiber mat reinforced polypropylene composites," *Express Polymer Letters*, vol. 1, no. 5, pp. 299–307, 2007.

[27] C.-H. Chen, C.-Y. Chen, Y.-W. Lo, C.-F. Mao, and W.-T. Liao, "Characterization of alkali-treated jute fibers for physical and mechanical properties," *Journal of Applied Polymer Science*, vol. 80, no. 7, pp. 1013–1020, 2001.

[28] M. Jawaid, H. P. S. Abdul Khalil, and A. Abu Bakar, "Woven hybrid composites: tensile and flexural properties of oil palm-woven jute fibres based epoxy composites," *Materials Science and Engineering A*, vol. 528, no. 15, pp. 5190–5195, 2011.

[29] K. S. Ahmed and S. Vijayarangan, "Tensile, flexural and interlaminar shear properties of woven jute and jute-glass fabric reinforced polyester composites," *Journal of Materials Processing Technology*, vol. 207, no. 1–3, pp. 330–335, 2008.

[30] P. Sudhakara, D. Jagadeesh, Y. Wang et al., "Fabrication of *Borassus* fruit lignocellulose fibre/PP composites and comparison with jute, sisal and coir fibres," *Carbohydrate Polymers*, vol. 98, no. 1, pp. 1002–1010, 2013.

[31] M. S. Meon, M. F. Othman, H. Husain, M. F. Remeli, and M. S. M. Syawal, "Improving tensile properties of kenaf fibres treated with Sodium hydroxide," *Procedia Engineering*, vol. 41, pp. 1587–1592, 2012.

[32] O. M. L. Asumani, R. G. Reid, and R. Paskaramoorthy, "The effects of alkali-silane treatment on the tensile and flexural properties of short fibre non-woven kenaf reinforced polypropylene composites," *Composites A*, vol. 43, no. 9, pp. 1431–1440, 2012.

[33] S. Ochi, "Mechanical properties of kenaf fibers and kenaf/PLA composites," *Mechanics of Materials*, vol. 40, no. 4-5, pp. 446–452, 2008.

[34] S. Shibata, Y. Cao, and I. Fukumoto, "Lightweight laminate composites made from kenaf and polypropylene fibres," *Polymer Testing*, vol. 25, no. 2, pp. 142–148, 2006.

[35] B. F. Yousif, A. Shalwan, C. W. Chin, and K. C. Ming, "Flexural properties of treated and untreated kenaf/epoxy composites," *Materials and Design*, vol. 40, pp. 378–385, 2012.

[36] H. Deka, M. Misra, and A. Mohanty, "Renewable resource based "all green composites" from kenaf biofiber and poly(furfuryl alcohol) bioresin," *Industrial Crops and Products*, vol. 41, pp. 94–101, 2012.

[37] M. Ramesh, K. Palanikumar, and K. H. Reddy, "Comparative evaluation on properties of hybrid glass fiber-sisal/jute reinforced epoxy composites," *Procedia Engineering*, vol. 51, pp. 745–750, 2013.

[38] M. Ramesh, K. Palanikumar, and K. H. Reddy, "Comparative evaluation on properties of hybrid glass fiber-sisal/jute reinforced epoxy composites," in *Proceedings of the 3rd Nirma University International Conference on Chemical, Civil and Mechanical Engineering Tracks (NUiCONE '12)*, Nirma University, Ahmedabad, India, December 2012.

[39] K. Mylsamy and I. Rajendran, "The mechanical properties, deformation and thermomechanical properties of alkali treated and untreated Agave continuous fibre reinforced epoxy composites," *Materials and Design*, vol. 32, no. 5, pp. 3076–3084, 2011.

[40] F. D. A. Silva, R. D. T. Filho, J. D. A. M. Filho, and E. D. M. R. Fairbairn, "Physical and mechanical properties of durable sisal fiber-cement composites," *Construction and Building Materials*, vol. 24, no. 5, pp. 777–785, 2010.

[41] M. Ramesh, K. Palanikumar, and K. H. Reddy, "Mechanical property evaluation of sisal-jute-glass fiber reinforced polyester composites," *Composites B*, no. 48, pp. 1–9, 2013.

[42] A. Kalam, B. B. Sahari, Y. A. Khalid, and S. V. Wong, "Fatigue behaviour of oil palm fruit bunch fibre/epoxy and carbon fibre/epoxy composites," *Composite Structures*, vol. 71, no. 1, pp. 34–44, 2005.

[43] A. A. Mamun, H.-P. Heim, D. H. Beg, T. S. Kim, and S. H. Ahmad, "PLA and PP composites with enzyme modified oil palm fibre: a comparative study," *Composites A*, vol. 53, pp. 160–167, 2013.

[44] M. M. Haque, M. Hasan, M. S. Islam, and M. E. Ali, "Physico-mechanical properties of chemically treated palm and coir fiber reinforced polypropylene composites," *Bioresource Technology*, vol. 100, no. 20, pp. 4903–4906, 2009.

[45] M. Jawaid, H. P. S. Abdul Khalil, A. Hassan, R. Dungani, and A. Hadiyane, "Effect of jute fibre loading on tensile and dynamic mechanical properties of oil palm epoxy composites," *Composites B*, vol. 45, no. 1, pp. 619–624, 2013.

[46] A. Alawar, A. M. Hamed, and K. Al-Kaabi, "Characterization of treated date palm tree fiber as composite reinforcement," *Composites B*, vol. 40, no. 7, pp. 601–606, 2009.

[47] T. Yu, J. Ren, S. Li, H. Yuan, and Y. Li, "Effect of fiber surface-treatments on the properties of poly(lactic acid)/ramie composites," *Composites A*, vol. 41, no. 4, pp. 499–505, 2010.

[48] C. Z. P. Júnior, L. H. de Carvalho, V. M. Fonseca, S. N. Monteiro, and J. R. M. d'Almeida, "Analysis of the tensile strength of polyester/hybrid ramie-cotton fabric composites," *Polymer Testing*, vol. 23, no. 2, pp. 131–135, 2004.

[49] S. Harish, D. P. Michael, A. Bensely, D. M. Lal, and A. Rajadurai, "Mechanical property evaluation of natural fiber coir composite," *Materials Characterization*, vol. 60, no. 1, pp. 44–49, 2009.

[50] N. Defoirdt, S. Biswas, L. D. Vriese et al., "Assessment of the tensile properties of coir, bamboo and jute fibre," *Composites A*, vol. 41, no. 5, pp. 588–595, 2010.

[51] F. I. Romli, A. N. Alias, A. S. M. Rafie, and D. L. A. Abdul Majid, "Factorial study on the tensile strength of a coir fibre-reinforced epoxy composite," *AASRI Procedia*, vol. 3, pp. 242–247, 2012.

[52] C. Asasutjarit, S. Charoenvai, J. Hirunlabh, and J. Khedari, "Materials and mechanical properties of pretreated coir-based green composites," *Composites B*, vol. 40, no. 7, pp. 633–637, 2009.

[53] N. G. Jústiz-Smith, G. J. Virgo, and V. E. Buchanan, "Potential of Jamaican banana, coconut coir and bagasse fibres as composite materials," *Materials Characterization*, vol. 59, no. 9, pp. 1273–1278, 2008.

[54] M. M. Rahman and M. A. Khan, "Surface treatment of coir (*Cocos nucifera*) fibers and its influence on the fibers' physico-mechanical properties," *Composites Science and Technology*, vol. 67, no. 11-12, pp. 2369–2376, 2007.

[55] V. M. Karbhari, J. W. Chin, D. Hunston et al., "Durability gap analysis for fiber-reinforced polymer composites in civil engineering," *Journal of Composites for Construction*, vol. 7, no. 3, pp. 238–247, 2003.

Hindawi Publishing Corporation
Advances in Materials Science and Engineering
Volume 2013, Article ID 167105, 14 pages
http://dx.doi.org/10.1155/2013/167105

Research Article

Efficacy of Thermally Conditioned Sisal FRP Composite on the Shear Characteristics of Reinforced Concrete Beams

Tara Sen[1] and H. N. Jagannatha Reddy[2]

[1] *Department of Civil Engineering, National Institute of Technology, Agartala, Barjala, Tripura (West), Jirania 799055, India*
[2] *Department of Civil Engineering, Bangalore Institute of Technology, K. R. Road, V. V. Puram, Bangalore 560004, India*

Correspondence should be addressed to Tara Sen; tarasen20@gmail.com

Received 30 May 2013; Revised 8 August 2013; Accepted 28 August 2013

Academic Editor: Hazizan Md Akil

The development of commercially viable composites based on natural resources for a wide range of applications is on the rise. Efforts include new methods of production and the utilization of natural reinforcements to make biodegradable composites with lignocellulosic fibers, for various engineering applications. In this work, thermal conditioning of woven sisal fibre was carried out, followed by the development of woven sisal fibre reinforced polymer composite system, and its tensile and flexural behaviour was characterized. It was observed that thermal conditioning improved the tensile strength and the flexural strength of the woven sisal fibre composites, which were observed to bear superior values than those in the untreated ones. Then, the efficacy of woven sisal fibre reinforced polymer composite for shear strengthening of reinforced concrete beams was evaluated using two types of techniques: full and strip wrapping techniques. Detailed analysis of the load deflection behaviour and fracture study of reinforced concrete beams strengthened with woven sisal under shearing load were carried out, and it was concluded that woven sisal FRP strengthened beams, underwent very ductile nature of failure, without any delamination or debonding of sisal FRP, and also increased the shear strength and the first crack load of the reinforced concrete beams.

1. Introduction

The recent developments in the application of advanced composites in the construction industry for concrete strengthening are increasing on the basis of specific requirements, national needs, and industry participation. The need for efficient strengthening techniques of existing concrete structures has resulted in research and development of composite strengthening systems. For years, civil engineers have been in search for alternatives to steels and alloys to combat the high costs of repair and maintenance of structures damaged by corrosion and heavy use. Since the 1940s, composite materials, formed by the combination of two or more distinct materials in a microscopic scale, have gained increasing popularity in the engineering field. Fiber Reinforced Polymer (FRP) is a relatively new class of composite material manufactured from fibers and resins and has proven efficient and economical for the development and repair of new and deteriorating structures in civil engineering. The mechanical properties of FRPs make them ideal for widespread applications in construction worldwide. Strengthening of reinforced concrete (RC) structures is frequently required due to inadequate maintenance, excessive loading, change in use or in code of practice, and/or exposure to adverse environmental conditions. The use of FRP composites as a replacement to steel reinforcement has proved to be a promising solution to this problem [1–5]. FRP composites possess some outstanding properties such as resistance to corrosion, good fatigue and damping resistance, high strength to weight ratio, and electromagnetic transparency. FRP has found an increasing number of applications in construction either as internal or as external reinforcement for concrete structures [6–13]. It is well known that FRP possesses a major advantage over conventional steel in reinforcing concrete structures. The fibers, typically composed of carbon or glass, provide the strength and stiffness. The matrix, commonly

made of polyester, epoxy, or nylon, binds and protects the fibers from damage and transfers the stresses between fibers. Various researches on different reinforcements in the form of fibers, which can be suitably used for processing of FRP, are underway. One such newly developed reinforcement is the use of natural fibers in the processing of FRP [14–17]. Similarly, common matrix materials include epoxy, phenolic, polyester, polyurethane, polyetheretherketone (PEEK), and vinyl ester. Among these resin materials, PEEK is most widely used. Epoxy, which has higher adhesion and less shrinkage than PEEK, comes in second for its high cost.

In the last decade, there has been a fast development in the area of composites reinforced with vegetable fibers for processing of FRP. The cellulosic fibers have a lot of important features such as low cost, low density, specific resistance, biological degradability, CO_2 neutrality, renewability, good mechanical properties, nontoxicity and can be easily modified by a chemical agent. Sisal (Agave sisalana), is a good example of such fibers. It was planted in India in the earliest of the civilization, and in those days it was used for making ropes. Nowadays, Sisal is mainly cultivated in Madhya Pradesh, Tamil Nadu, Kerela, Orissa, and also in Goa. India is also becoming one of the largest producers of natural fiber like sisal after Brazil and Africa. The sisal fibers, as well as most of the other lignocellulosic fibers are constituted of cellulose (65.8%), hemicellulose (12%), lignin (9.9%), pectin (0.8%), wax (0.3%), and water soluble compounds. Cellulose, which awards the mechanical properties of the complete natural fiber, is ordered in microfibrils enclosed by the other two main components: hemicellulose and lignin. Lignin is an aromatic biopolymer, an integral cell wall constituent of all vascular plants and hemicelluloses are a large group of polysaccharides found in the primary and secondary cell walls of the plants. These three mentioned components are responsible for the physical properties of the fibers. These natural fibers can be effectively used in the manufacture of fiber reinforced polymer composites because they possess attractive physical and mechanical properties [18–21]. They impart the composite high specific stiffness and strength, a desirable fiber aspect ratio, biodegradability, they are readily available from natural sources, and more importantly they have a low cost per unit volume basis [22–25]. Unlike the traditional engineering fibers, for example, glass and carbon fibers, along with mineral fillers, these lignocellulosic fibers are able to impart the composite certain benefits such as low density; less machine wear than that produced by mineral reinforcements; no health hazards; a high degree of flexibility [26–29]. One difficulty that has prevented a more extended utilization of the sisal fiber is their lack in providing good adhesion to most polymeric matrices. The hydrophilic nature of natural fibers adversely affects adhesion to a hydrophobic matrix and as a result, it may cause a loss of strength. To prevent this, the fiber surface has to be modified in order to promote adhesion. Several methods to modify the natural fiber surface have been proposed: the graft copolymerization of monomers onto the fiber surface, the use of maleic anhydride copolymers, alkyl succinic anhydride, stearic acid, and so forth. It has also been reported that the use of coupling agents such as silanes, titanates, zirconates, triazine compounds, and so forth also improve fiber-matrix adhesion and also the fiber-matrix interaction. But all these modification methods are mainly for short fiber composites, and none of these methods have given satisfactory results for the textile or woven fiber composites. The woven fiber composites behave in a completely different manner from short fiber composites. Any sort of chemical modification of woven or textile composites has resulted in lowering of tensile strength and flexural strength [30–34]. The major contribution to strength in textile composites is the alignment of yarns in warp and weft direction. Chemical treatment results in the partial unwinding of yarns (as hemicellulose dissolves off) and hence the alignment gets antagonized. This results in lowering of strength of the woven composites. Another reason is that as woven fibers are composed of thick strands and knots, the chemical agents cannot penetrate into the fabric and therefore the interfacial properties between the woven fibers and the matrix does not get enhanced. There has been recent, huge development and research on textile structural composites, and they are finding use in various high performance applications. Thermal conditioning, which in simple words can be said as heat treatment, provides an improvisation in the mechanical properties of woven fabric or textile composites in an effective manner. Physical method of thermal treatments, of woven yarn, does not make changes on the structural composition but modify the surface properties, this influences good mechanical bonding with the matrix and ensures enhanced composite properties [30–34].

2. Materials and Methodology for Composite Characterization

2.1. Materials. The sisal fabric with natural rubber backing was collected from Extra Weave Private Ltd., Cherthala, Kerala, India. The natural fibers of sisal could be used to reinforce both thermosetting and thermoplastic matrices. Thermosetting resins, such as epoxy, polyester, polyurethane, and phenolic are commonly used today in natural fiber composites, in which composites require high performance applications. They provide sufficient mechanical properties, in particular, stiffness and strength, at acceptably low price levels. Here, we have used MBrace saturant resin, which consisted of two parts, part A and part B. Part A was the epoxy resin which belonged to the group of bisphenol A. Part B was hardener which belonged to the group of polyamine, chemically belonging to the epoxide family. Both part A epoxy resin and part B hardener was used as the matrix material together, in combination. The epoxy resin and the hardener were both obtained from BASF Construction Chemicals Chandivali, Andheri East, Mumbai, India. MBrace saturant resin was easy to apply, 100% solid material that permitted adhesion of a lightweight sheet, within the MBrace composite strengthening system. The resin produced a high performance composite system to be used for external structural repair or upgrade application. All other chemicals used for the fabrication and for the concrete strengthening purpose, such as concresive 2200 and MBrace primer, were all obtained from BASF Construction Chemicals Chandivali,

Andheri East, Mumbai, India. MBrace primer was a low viscosity, 100% solid, polyamine cured epoxy. The primer was the first applied component of the MBrace system, it was used so as to penetrate the pore structure of cementitious substrates in order to provide a high bond base coat for the MBrace System.

2.2. Thermal Conditioning and Fabrication of Woven Sisal FRP Composites. The process of thermal conditioning could be achieved by either using convection currents or by using microwave radiation. Here, it was achieved by using thermostatically controlled oven, which uses convection currents for thermal conditioning, rather than using microwave radiation. There have been several disadvantages of using microwave radiation for thermal conditioning of natural fibers. It was to be kept in mind that the application of these woven sisal fibers in the form of woven fiber FRP composite was sought for in structural elements, in an effective manner, hence, we would be dealing with large quantities of such materials for real life use, if so established. Hence, this ruled out microwave radiation conditioning of the fibers, as it would lead to huge energy consumption as well would generate huge production costs. And since we were looking for cheap, biodegradable, sustainable material, with low production cost, but also with improved properties, which could be suitably compared with glass FRP composite, so that the utilization of natural FRP could be visualized worldwide, hence, cheaper treatments methods were sought for. Microwave radiation treatment is for low-flow capacity R and D applications and this makes them suitable for small-scale installations only. Convection heating is for fast product expansion and production, such as thermal treatment of lignocellulosic fibers for large scale natural FRP production. The main difference between conventional heating and microwave heating was the heating mechanism. While conventional techniques heated a surface, the microwaves heated the whole volume of the treated object. During the conventional heating, the heat was generated outside the treated product and conveyed by conduction or convection. Hence, the surface would get heated at first and afterwards the heat flowed towards the inside, which always remained colder than the outer surface. In this method of conventional heating, since heat was transferred molecule by molecule from the outside to the inside, hence, this process displayed the disadvantage of overheating the outer surface of the material; but it was quite clear that the advantages of convection heating outweighed the disadvantages and most of the shortcomings, as a measure for the treatment of natural woven fibers. Figure 1 gives the pictorial representation of the thermostatically controlled oven for convection heating and the mechanism of convection heating. The mechanical treatment in the form of thermal conditioning was carried out in the following manner: sisal fabric mats were cut into the size as required for flexural strength test as per ISO 14125:1998 and tensile strength test as per ISO 527-4:1997(E). Some of the samples of these woven fiber mats were then placed into the thermo-statically controlled oven at 80°C for 48 hours. After 48 hours, it was removed from the oven, and used for composite fabrication. The rest of the samples were left as they are, for composite fabrication, that is, the rest of the samples were not subjected to thermal conditioning, in other words these were the samples which were untreated and is referred to here as control samples. Thereafter, all the samples, which consisted of both thermally conditioned woven sisal fiber mats and untreated or raw or control samples of woven sisal fiber mats, which were not subjected to thermal conditioning, were all used for fiber reinforced polymer composite fabrication, so that a comparative study to deduce effect of thermal conditioning could be carried out. For the composite fabrication, a plastic bit mould of suitable dimension was used for casting the fabric composite sheets. The usual hand lay-up technique was used for the preparation of the samples. A calculated amount of epoxy resin and hardener ratio of 10 : 4 by weight was thoroughly mixed with gentle stirring to minimize air entrapment. For quick and easy removal of composite sheets, a mould releasing agent was used. Electrical insulating paper was put underneath the plastic bit mould and mould release agent, that is, either poly vinyl alcohol or silicone grease was applied at the inner surface of the mould. After keeping the mould on the insulating sheet, a thin layer (≈2 mm thickness) of mixture of epoxy and hardener was poured. Then, the fabric mats were separately distributed on the mixture on different moulds. The remaining mixture was then poured into the mould on top of the fabric mats. Care was taken to avoid formation of air bubbles. Pressure was then applied from the top (on top of the electrical insulating paper, placed above the FRP), with the help of flat weights, so that no air bubbles remained in the epoxy-fiber reinforced polymer mix. It was ensured that no air bubbles remained in the FRP, and then the pressure was withdrawn. Any arbitrary pressure could be applied by using suitable flat iron weights (e.g., steel I beams or flats, etc.), so that the pressure gets uniformly distributed, and no air bubbles exist in the composite. It was allowed to cure at room temperature for 48 hrs. After 48 hrs the samples were taken out from the mould and kept in an air tight container for further experimentation.

2.3. Mechanical Testing of Woven Sisal FRP Composite. Two mechanical tests were performed for all the three samples of woven sisal fiber composites, the two tests include tensile strength test, and flexural strength test. All the samples of the thermally conditioned sisal fibers, which was fabricated into composites and also the untreated or raw woven sisal fibers, which was fabricated into composites, were both subjected to these mentioned two tests, so as to obtain a comparison in their mechanical properties in order to evaluate the effect of thermal conditioning. During the tensile test, a uniaxial load was applied through both the ends of the specimen, using suitable jaws as an attachment to the UTM. The tensile test was performed in the universal testing machine (UTM) which in this case was HEICO digital universal testing machine and results were obtained digitally with the digital data acquisition system, which aided us to calculate the tensile strength of composite samples. The tensile strength test for woven sisal FRP composites, were done in accordance to ISO 527-4:1997(E), as sisal falls under the category of Type-2 materials. Figure 2 shows the tensile

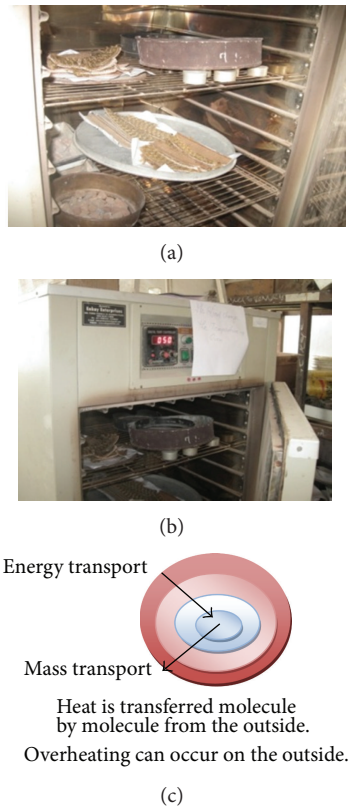

FIGURE 1: (a) samples in oven for thermal conditioning; (b) thermostatically controlled oven; (c) mechanism of convection heating.

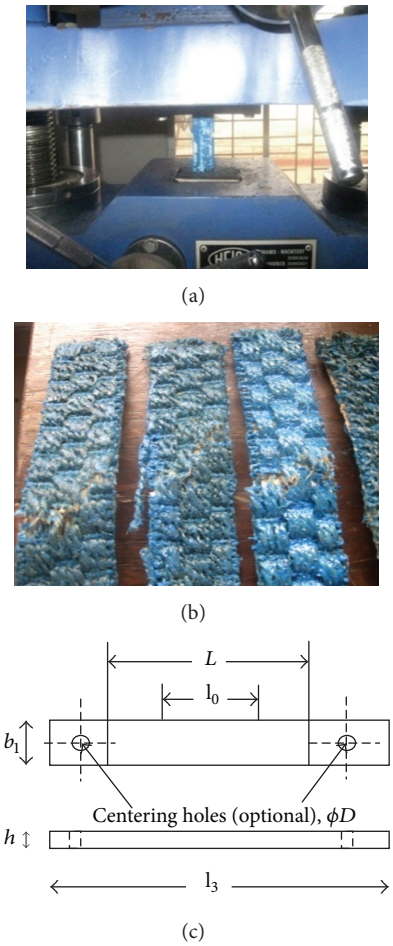

FIGURE 2: (a) Tensile testing; (b) tensile fracture samples of woven sisal FRP composite; (c) dimensions of the sample for tensile testing.

loading as well as the tensile fractures in the composite samples and also the sample dimensions for the tensile test. Sisal FRP composites displayed only diagonal type of fracture. The diagonal fracture failure mode is an accepted mode of tensile fracture in accordance to ISO 527-4:1997(E). The tensile testing of the composite was followed by flexural testing. The flexural strength of a composite is a 3-point bend test, which generally promotes failure by interlaminar shear. This test was conducted as per ISO 14125:1998 standard using a load cell of high sensitivity. The flexural loading arrangement as well as the flexural fracture is shown in Figure 3. Since sisal belonged to Class II type material, hence, all the restrictions of the specimen dimensions for flexural testing was followed for class II material, as per the code ISO 14125:1998. The flexural failure of all the specimens of the FRP composites showed a single line fracture (perpendicular to the plane of the composite direction). The tensile and the flexural strength test were carried out at a cross head speed of 1 mm/min, and this cross head speed was maintained throughout the testing. Table 1 gives the value of the flexural strength and tensile strength of woven sisal FRP composites and also describes the dimensions of various parameters used for tensile and flexural testing of the composite samples.

2.4. Effect of Thermal Conditioning on the Mechanical Properties of Woven Sisal Fibers. The effect of thermal conditioning or heat treatment, which was at elevated temperature, could be described as a threefold effect on the cellulosic fibers of sisal. Firstly, the modification of cellulosic structure by enhanced cross-linking, then secondly, increased amount of crystallinity in the fibers, and thirdly, by de-moisturization, which improved the adhesion between the fibers and the natural rubber backing of the fabric. High temperature in general accelerated as well as activated chemical reactions, in cellulosic materials, such as natural fibers of sisal, which consisted of 65.8% cellulose, it lead to the formation of radicals, which in turn directed to several other reactions. Also, at elevated temperatures, there was cross linking of cellulose, which reduced the swellability of the lignocellulosic fibers. This reaction was homogeneous with the temperature range of 70°C to 180°C. The natural fibers generally undergo degradation at about 200°C. Structural constituents of the fiber (cellulose, hemicelluloses, lignin, etc.) were sensitive to the different range of temperatures. It was seen that lignin started degrading at a temperature around 200°C and hemicelluloses and cellulosic constituents started degrading at higher temperatures. Hence, one must be careful enough to maintain the maximum temperature for thermal conditioning below 200°C, since vegetable fibers undergo degradation at higher temperatures above 200°C. In the presence of oxidation, cross-linking of cellulose was enhanced by formation of hemiacetal groups by the carbohydrate chains. Thermal

Table 1: Dimensions and mechanical properties of woven sisal FRP composite.

Type of woven sisal FRP composite	Parameters for flexural testing (All parameters in mm)				Parameters for tensile testing (All parameters in mm)				Tensile Strength (MPa)	Flexural Strength (MPa)
	C/C length between supports (L)	Total length (l)	Width (b)	Thickness (h)	Initial distance between grip (L)	Gauge length (L_0)	Overall length (L_3)	Thickness (h)		
Control or untreated woven sisal fibre FRP (prior to thermal conditioning)	64	164	15	3.98	115	50	150	3.98	205	311
Thermally conditioned treated woven sisal fibre FRP (after thermal conditioning)	64	164	15	3.98	115	50	150	3.98	223	350

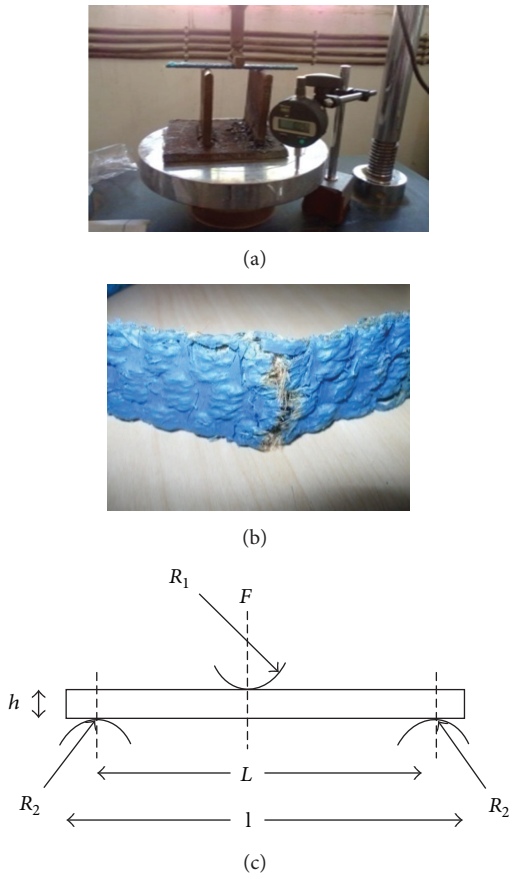

Figure 3: (a) Flexural testing (b) Flexural fracture of woven sisal FRP composite; (c) dimensions of the sample for flexural testing.

conditioning, basically a physical process, directed to the modification of the fiber surface morphology, rather than changing the fiber internal structure. Thermal conditioning also increased the crystallinity of the fibers, the crystallinity of the fibers could be attributed to the fact that upon consistent heat treatment at 80°C, for 48 hours, the crystallinity of cellulose increased due to the rearrangement of molecular structure at elevated temperatures, and it also resulted in moisture loss of the fabric, thereby, enhancing the extent of the bonding between fabric and the natural rubber backing of the fabric. As we know that de-moisturization plays a vital role in enhancing mechanical properties, hence, the overall mechanical properties of composites prepared with thermally conditioned woven sisal fibers in fabric form were better than the composites prepared with untreated or the control ones, that is, those fabricated composites which were tested for their mechanical properties without thermal conditioning.

3. Methodology for Shear Strengthening of Reinforced Concrete Beams

This chapter evaluates the applicability of the woven sisal FRP composite as a shear strengthening material for reinforced concrete beam members. In this study, the woven sisal FRP sheets were bonded on on the surface of the RCC (reinforced cement concrete) beam specimens and the strengthened specimens were tested under a two-point bending configuration for their ultimate shear strength.

3.1. Design of Reinforced Concrete Beams. The experimental program contained three beam groups. All the beams in groups A, B, and C had the same reinforcement detailing, although the beam length for design is 1.3 m, it is cast as 1.4 m for providing 50 mm clearance from both the sides at the supports. In accordance, the RCC beam design was carried out as per IS-456:2000. The entire reinforcement details, which were followed for all the three groups, have been shown in Figure 4. The beams were designed such that shear failure in the beam occurs before flexural failure. Hence, beams were strengthened in flexure, by providing additional flexural reinforcement, and it was also made sure that the beam design remains underreinforced, even after the provision of extra flexural reinforcement in the form of one main bar at the beam bottom. All the beams in groups B and C were utilized for evaluating the effect of shear strengthening provided by woven sisal fiber reinforced polymer composite, and beams in group A, which was not strengthened, were used for comparative shear strength study purpose. Casting of RCC beams was carried out with the reinforcing detailing as shown in Figure 4, using cement of 53 grade, clean river sand as fine aggregates, and 12 mm and down sized coarse aggregates, with the conjunction of clean water, using the mix proportion by weight of cement : fine aggregate : coarse aggregate as 1 : 2.07 : 1.87. along with a water cement ratio 0.5.

3.2. Strengthening of Reinforced Concrete Beams with Woven Sisal FRP. The beams in group A were designed as controlled specimen (ConS1, ConS2), where no FRP application was carried out, the beams in group B were designed to investigate the effect of full wrapping technique 90° (3 sided U wrap), for shear strengthening provided by using sisal FRP (SS1, SS2), and the beams in group C were designed to investigate the effect of strip wrapping technique 90° (3 sided U wrap) where 50% of the total area was used for strengthening, that is, 62 mm strips placed at 124 mm C/C at a clear gap of 49 mm at the ends, for shear strengthening provided by using sisal FRP (SS3, SS4), a summary of the test beams have been shown in Table 2. The beams were prepared by grinding 3 side surfaces with the help of a grinding machine, this was done so as to roughen the three sides of the beam where FRP application would be carried out, and for roughening the beam surface ensures good boding of the composite material. After grinding, all the three side surface of the beams were cleaned with an air nozzle, and finally wiped to remove any dust or loose particles. Small surface defects in concrete were repaired and made good using concresive 2200. Then, a coat of MBrace Primer was applied on all the three sides of the beams in group B and C. The primer coat was allowed to air cure for 8 hours. Next, Resin Part A and Hardener Part B of the two component MBrace saturant were mechanically premixed as per the guidelines of the BASF manufacturer for 3 minutes or until homogeneous. The property of the MBrace saturant as provided by the manufacturer is given in Table 3. The ratio of mixing of resin and hardener followed as per

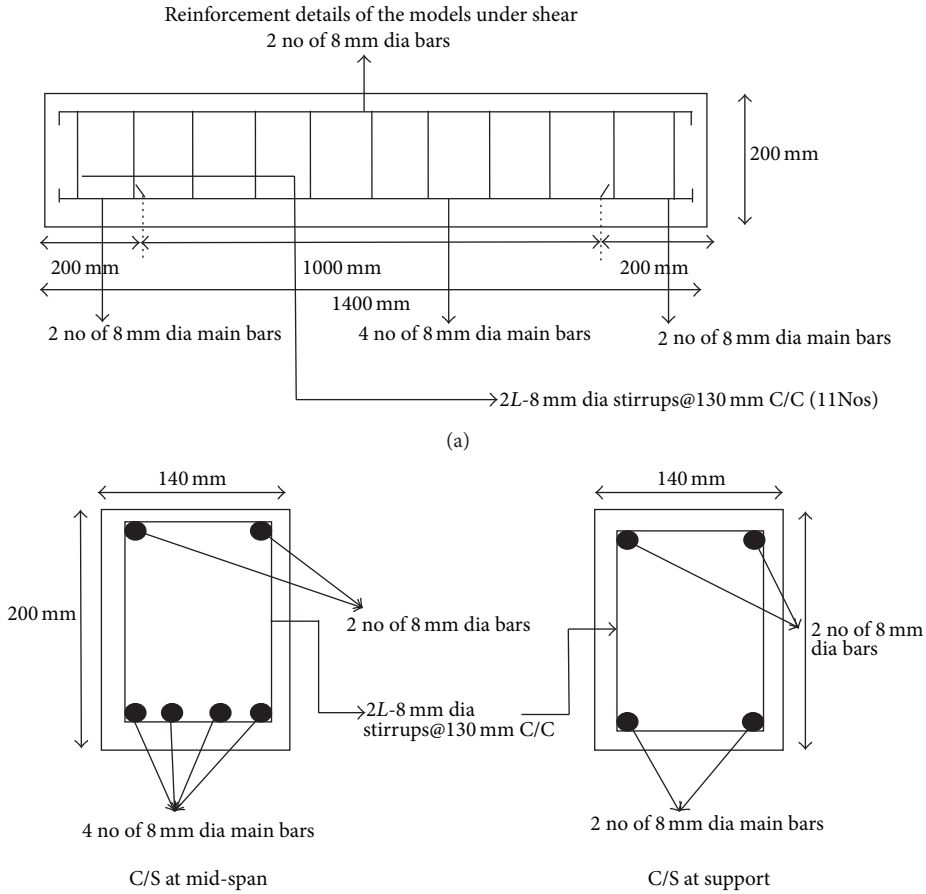

Figure 4: Reinforcement detailing of RCC beams (all sets, group A, B, and C).

Table 2: Summary of test beams.

Beam group	Wrapping configuration	Strengthening material	Beam designation	Type of strengthening	Strengthening scheme
Group A	Nil 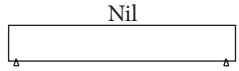	Nil	Control specimen ConS1, ConS2	No strengthening	Nil
Group B	Full wrapping 90°, single layer 	Sisal FRP	SS1, SS2	Shear strengthening throughout using woven sisal FRP	U-Wrap, three sided wrap
Group C	Strip wrapping 90°, single layer 62 mm strips at 124 mm C/C (at a clear gap of 62 mm) so as to achieve 50% of total area strengthening, with end clear gaps of 49 mm. 	Sisal FRP	SS3, SS4	Flexural strengthening in strips, throughout using woven sisal FRP	U-Wrap, three sided wrap

the manufacturer was 3 : 1. Then, the neatly measured and cut pieces of woven sisal fabric were applied on the beams SS1, SS2, SS3, and SS4. The composite fabric was placed on top of epoxy resin coating immediately on the respective beams and the resin was squeezed through the roving of the fabric with plastic laminating roller. It was made sure that all the fiber reinforcements are properly impregnated in the resin hardener mix. Air bubbles entrapped at the epoxy/concrete or epoxy/fabric interface were to be eliminated. All the strengthened concrete beams were cured for at least two

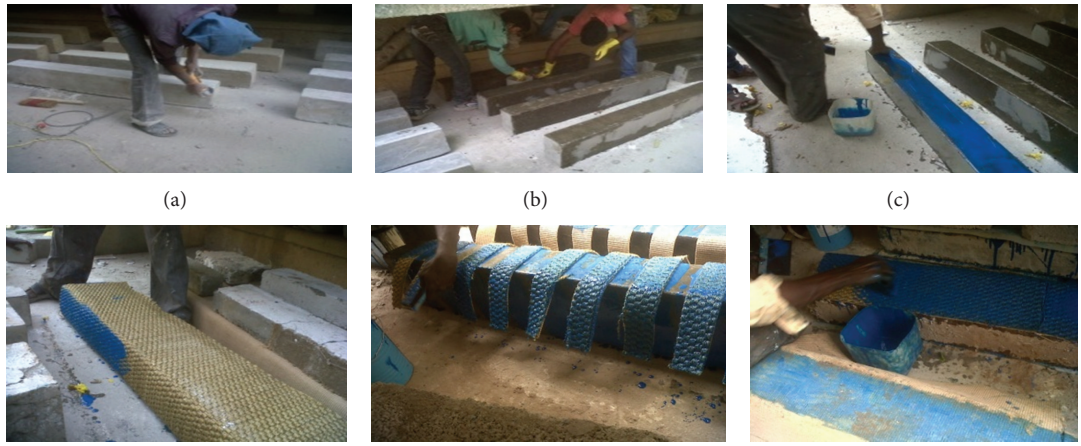

(a) (b) (c)

(d) (e) (f)

Figure 5: (a) surface preparation of beams by grinding; (b) primer application on beam surface; (c) application of epoxy hardener mix on the beam; (d) bonding of woven sisal (full wrap); (e) bonding of woven sisal (strip wrap); (f) final coating of epoxy hardener mix on the bonded fabric.

Table 3: Typical properties of MBrace saturant.

Mechanical property	MBrace saturant
Description	2 parts; Part A—Epoxy and Part B—Hardener
Density	1.06 kg/Lt (Mixed density)
Colour	Blue
Bond strength	>2.5 N/mm^2 (Failure in concrete)

weeks at room temperature before the beams were tested. The entire strengthening process that is surface preparation of beams and bonding of FRP has been demonstrated in Figure 5.

3.3. Experimentation. A two-point loading system was adopted for the tests. At the end of each load increment, deflection, ultimate load, type of failure, and so forth, were carefully observed and recorded. The experimental setup under the two-point loading system is as shown in the Figures 6(a) and 6(b). Deflection behavior under the load and at the centre of the beam and the ultimate shear strength of all the beams were noted.

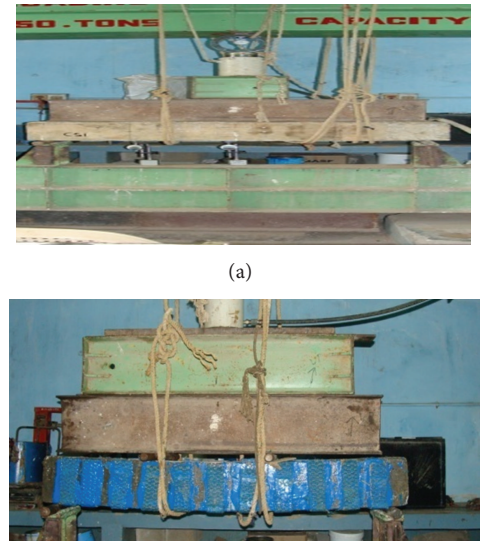

(a)

(b)

Figure 6: (a) two-point loading system on a 50 ton loading frame; (b) loading on strip wrapped beam with woven sisal FRP.

4. Results and Discussions

The mechanical characterizations of the woven sisal FRP composites in terms of tensile and flexural behavior are hereby presented in Figure 7. Figures 7(a) and 7(b) depict the comparative tensile and flexural behavior of the thermally treated and untreated or control woven sisal FRP composites. It was clearly observed that thermal treatment or conditioning improved the tensile as well as the flexural strength of woven sisal FRP composite in comparison to untreated or control woven sisal FRP composites. This thermally conditioned woven sisal was then used for strengthening of reinforced concrete beams in the form of thermally conditioned woven sisal FRP bonded to the reinforced concrete beams, and they were tested in order to evaluate their efficacy in improving the ultimate shear strength of reinforced concrete beams. Different types of modes of failure have been observed in the experiments of RCC beams strengthened in shear by sisal FRPs. All the three sets of beams in group A, B, and C were tested to find out their ultimate shear strength capacity. The ultimate load carrying capacity, that is, the ultimate shear strength of all the beams along with the nature of failure and deflections are given in Table 4. The fractured beam specimens belonging to various groups are as shown in Figure 8. Also, the load deflection curves for strengthened beams along with control specimens are as shown in Figure 9, and the comparison of the ultimate load carrying capacity and the first crack load are as shown in Figure 10. The three

Table 4: Experimental results of various beam groups.

Group designation	Beam designation	Failure of FRP	Deflection at midspan (mm)	Average deflection at midspan (mm)	Comments on deflection	Ultimate load (KN)	Ultimate load (KN) Average	Strengthening effect (%)
Group A	ConS1	—	8.201	8.643	—	88	90	—
	ConS2		9.085			92		
Group B	SS1	Yes	9.927	10.105	Results in higher deflection, hence, gives sufficient warning.	163	160	77.8%
	SS2		10.283			157		
Group C	SS3	No	6.825	6.656	Deflections are lower than fully wrapped beams.	117	120	33.4%
	SS4		6.487			123		

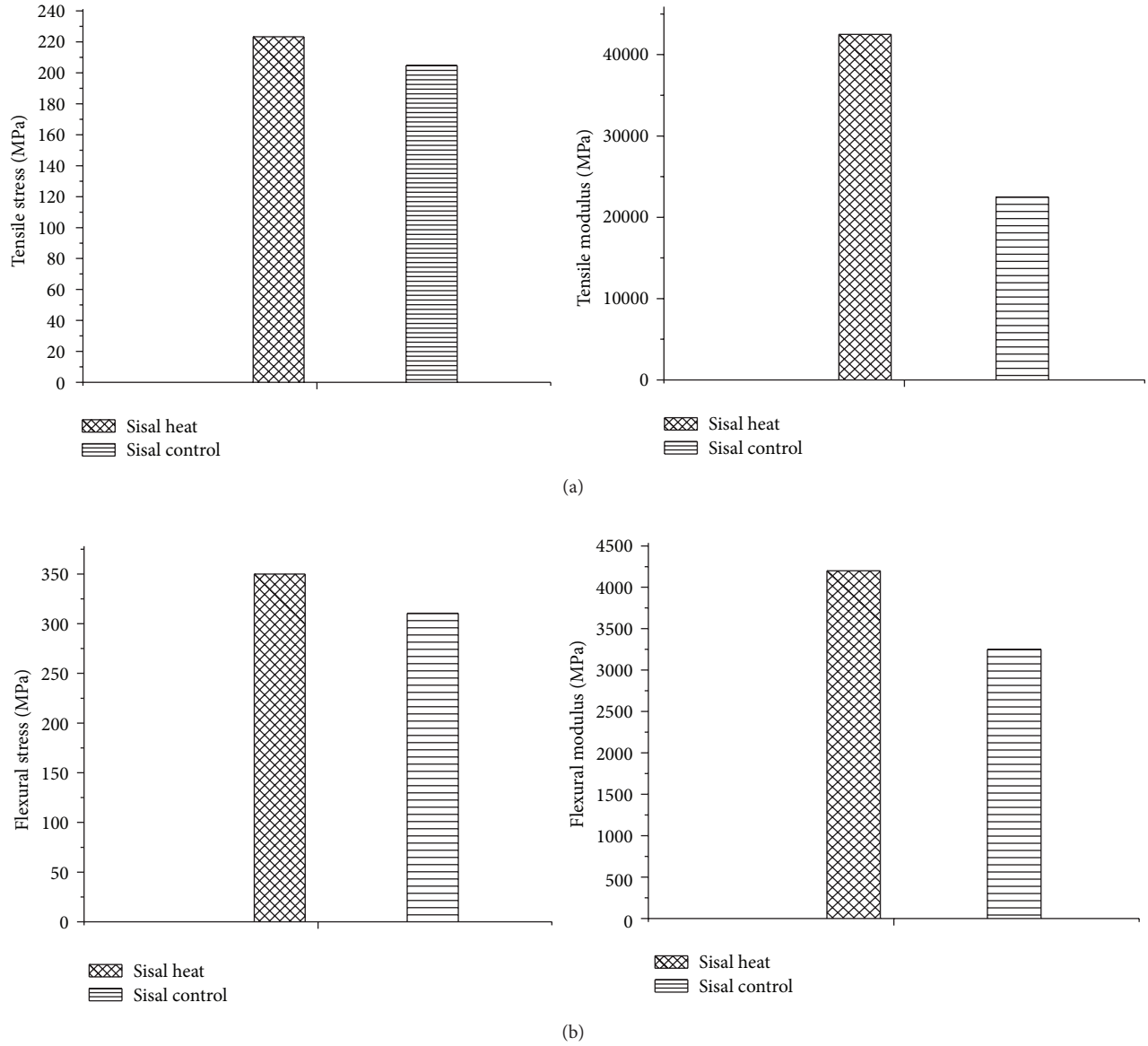

Figure 7: (a) Comparison of tensile behaviour of thermally conditioned and control woven sisal FRP composite, (b) Comparison of flexural behaviour of thermally conditioned and control woven sisal FRP composite.

sets of beams, that is, Groups A, B, and C were all tested for their ultimate shear strengths, in order to evaluate the shear capacity. The beams in Group A, ConS1, and ConS2 (2 number of sample models) were taken as the control beams. It was observed that the beams ConS1 and ConS2 had less load carrying capacity when compared to that of the fully strengthened beams as well as partially strengthened beams, that is, groups B and C beams, respectively. The second set of beams in Group B, which were strengthened by 90° fully wrapped FRP in single layer by woven sisal FRP, are the ones which displayed the highest shear strength, whereas the last set of beams in Group C, which were strengthened by 90° strip wrapped woven sisal FRP in single layer are the ones which has shown ultimate strength higher than the control specimens. The first set of beams that is group A, ConS1, and ConS2, failed in shear which proved that the beams were deficient in shear, and also that shear failure occurred before flexural failure. A large number of inclined cracks, which were 45° inclined to the horizontal reference of the beams developed from near the support region extending in 45° angles towards the load, that is, towards the upper face of the beam. So, it can be concluded that pure shear cracks developed at the lower face that is the bottom of the beam and extended from the bottom towards the top face of the beam at inclined 45° angles. Both the beams ConS1 and ConS2 failed in similar manner and Figure 8(a) depicts the clear representation of the failure of group A beams. The average shear strength of group A beams was 90 KN. In the second set of beams in group B, models SS1 and SS2 (2 number of sample models), it was seen that both these beams failed in the shear

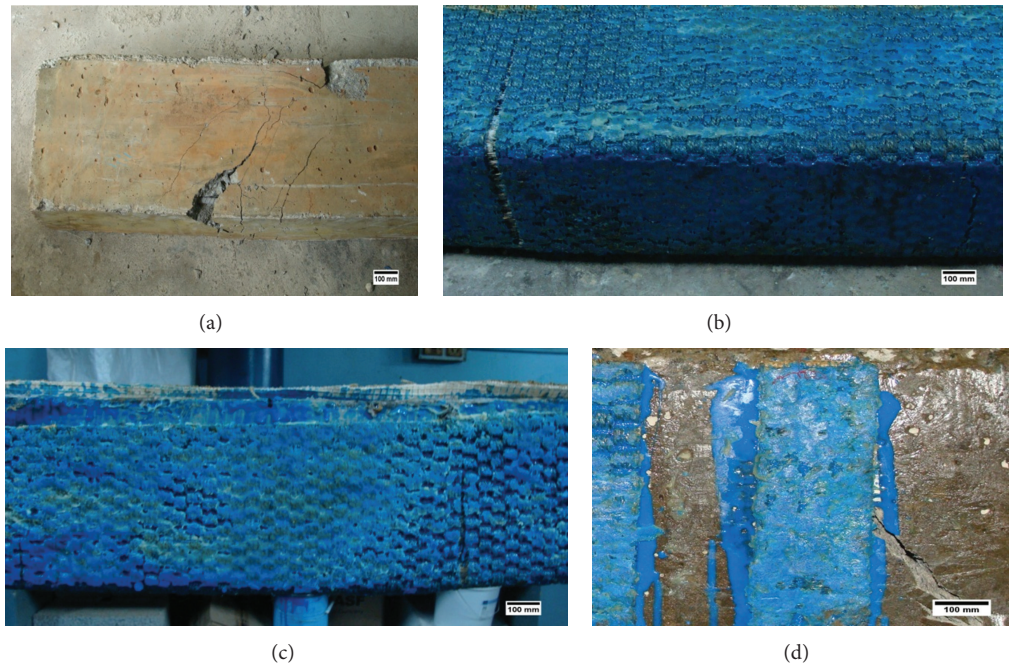

Figure 8: (a) fracture crack of beam ConS1; (b) fracture crack in the left and right shear zone of beam SS1; (c) fracture crack in the left and right shear zone of beam SS2; (d) fracture crack in the shear zone, and no crack in FRP, in beam SS3.

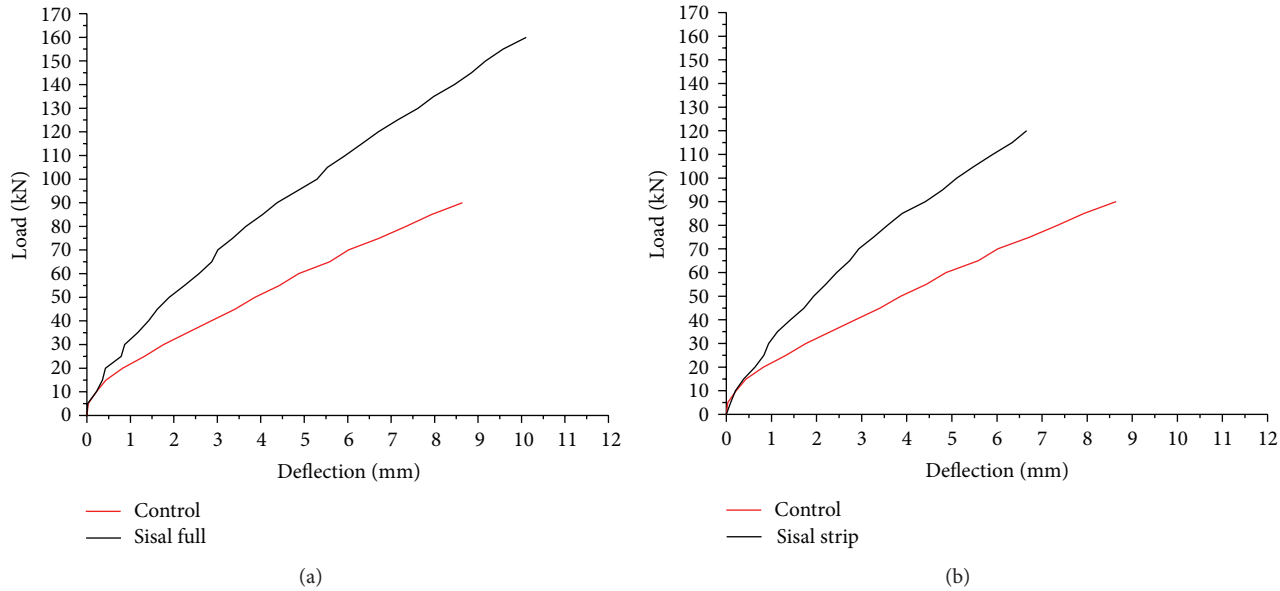

Figure 9: (a) load versus average midspan deflection of Groups A and B beams; (b) load versus average midspan deflection of Groups A and C beams.

regions, with the development of single crack in the woven sisal FRP, and their shear strength was much higher than that of Group A beams. When load was applied on SS1 and SS2, then firstly the matrix started cracking, then on further increment of load, the sisal fibers in sisal FRP started to crack, then again on further load increment the cracks in sisal FRP started to widen, with absolutely no de-bonding of FRP at all from any sides of the beam, the vertical crack was in the sisal FRP alone, in the shear zone, that is near the support and then this crack started slowly moving from the bottom face of the beam to the top face. Both of the failure modes depicted by SS1 and SS2 were very ductile in nature, with large deflections. Since, there was no de-bonding of sisal FRP, hence the cracks in the RCC beam itself could not be visualized. The ultimate load carrying capacity was reached by further widening of the single crack without generation of any other alternate cracks on the woven sisal FRP. Hence, in each beam, two numbers of cracks were observed at both the shear regions in beam.

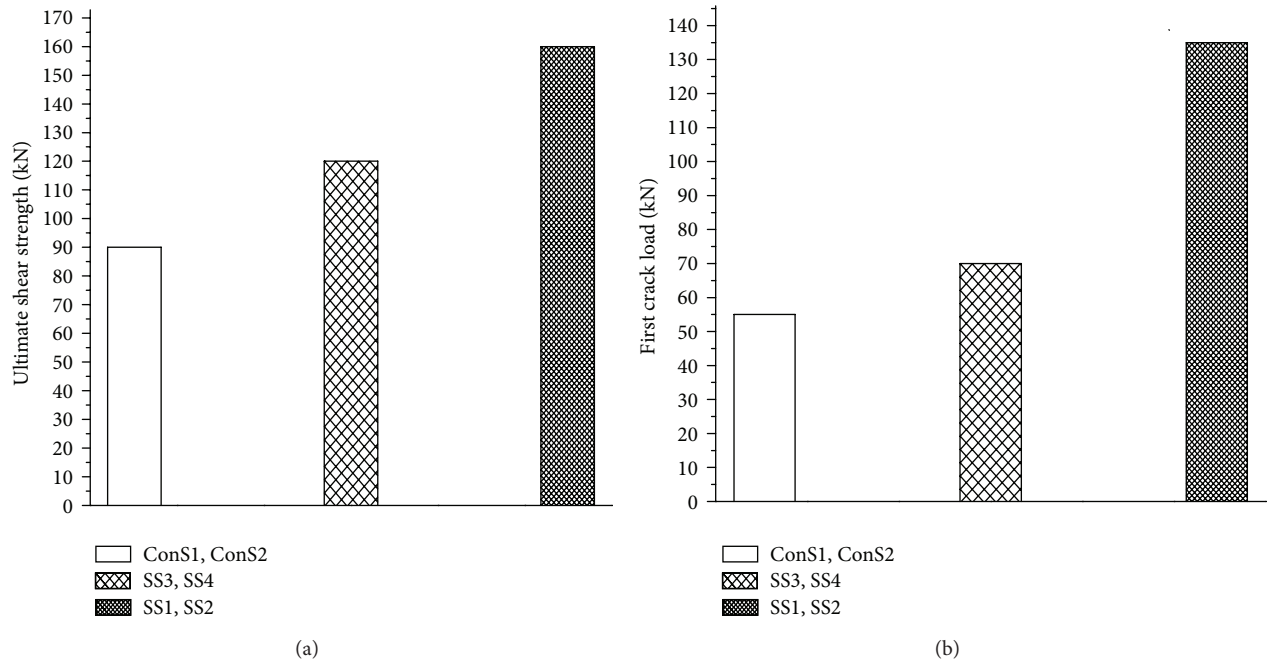

Figure 10: (a) comparison of ultimate shear strength of all beams; (b) comparison of first crack load of all beams.

The average ultimate strength of group B beams SS1 and SS2 was 160 KN. Both the beams SS1 and SS2 failed in similar manner and Figures 8(b) and 8(c) depicts the clear representation of the failure mode of these beams. A comparative load versus mid span (average) deflection behavior of group A and B beams is as shown in Figure 9(a). It is very evident that the load deflection behavior of group B beams is much superior, because these beams have higher ultimate load carrying capacity, and also their ultimate deflection of 10.105 mm is higher than group A beams, which has a ultimate deflection of 8.643 mm, because the ultimate load carrying capacity increases by 77.8% because of strengthening effect. In the third set of beams, that is group C, in which the beams were strengthened by strips of 62 mm placed at 124 mm C/C (at a clear gap of 62 mm, so as to achieve 50% area FRP strengthening, and leaving a clear edge length of 49 mm at the supports), it was seen that both the beams SS3, SS4, displayed that their ultimate load carrying capacity was higher than that of Group A beams, but lower than that of group B beams. It was observed for group C beams, that cracks first developed in the RCC beams and not on the sisal FRP, this indicated that the presence of bonded natural FRP on RCC beams, be it a woven natural FRP like woven sisal, imparts additional strength to the beams, and there by enhances their shear strength. When load was applied on SS3, SS4, then inclined cracks, which were 45° inclined to the horizontal reference of the beams developed near the support region extending in 45° angles from the supports towards the load that is, towards the upper face of the beam, but the interesting facet was that a single shear crack did not develop on the sisal FRP nor did the FRP undergo rupture of any nature or even de-bonding. On further increase in the load, large number of inclined cracks, described as above, developed, but again none of the cracks continued through the sisal FRP, this generation of shear cracks in the shear region and its increase in number and length only was restricted to the unbounded RCC beam area. The strip wrapping technique of FRP strengthening increased the ultimate load carrying capacity up to a point which lied between the load carrying capacity of fully wrapped beams and that of control beams. All the failure modes of group C beams are depicted in Figure 8(d), respectively, which clearly shows the shear cracks in all these beams. The average ultimate strength of group C beams SS3, SS4 was 120 KN. A comparative load versus mid span (average) deflection behavior of group A and C beams is as shown in Figure 9(b). It is very evident that the load deflection behavior of group C beams is much superior than group A beams, and lies somewhere in between group A and B beams. Beams in group C have higher ultimate load carrying capacity than group A beams, and their ultimate deflection 6.656 mm is lower than group A beams, which has an ultimate deflection of 8.643 mm, because there is only 33.4% increase in the load carrying capacity, whereas the effect of full wrapping increases the load carrying capacity by double the amount (77.8%).

5. Conclusions

(1) The performance of thermally conditioned woven sisal fiber reinforced polymer (FRP) composites was superior to the untreated or raw woven sisal fiber reinforced composites.

(2) The tensile test showed that thermally conditioned woven sisal FRP composite had higher tensile strength value of 223 N/mm^2 as compared untreated

or raw woven sisal fiber reinforced composites, which had a tensile strength value of 205 N/mm^2.

(3) The flexural test also showed that thermally conditioned woven sisal FRP composite had higher flexural strength value of 350 N/mm^2 as compared to untreated or raw woven sisal fiber reinforced composites, which had a flexural strength value of 311 N/mm^2.

(4) The treatment of thermal conditioning aided in enhancing the mechanical properties of woven sisal fiber reinforced polymer composites by the virtue of modification of cellulosic structure by enhanced cross-linking, increased amount of crystallinity in the fibers, and by de-moisturization, which improved the adhesion between the fibers and the natural rubber backing of the fabric.

(5) The study showed that the reinforcement of woven sisal fiber reinforced polymer composites created a new alternate material with properties that are generally with superior mechanical properties.

(6) When the thermally treated woven sisal fiber reinforced polymer composites were used for strengthening of reinforced concrete beams, then it resulted in significantly increasing the first crack load and the ultimate load carrying capacity of the strengthened beams, when strengthened using both full wrapping and strip wrapping techniques as compared to that of control beams, indicating the reinforcing effect of the woven sisal FRP composite. The maximum increase in the ultimate load carrying capacity by full wrapping technique was 77.8% and by strip wrapping technique was 33.4%. The presence of natural FRP bonded on the beam inhibited the development of the cracks, and delayed the formation of cracks.

(7) As the degree of strengthening increased, in view of full wrapping and strip wrapping, the load carrying capacity increased with an improvement in the load deflection behavior. Even at higher loads, the woven sisal FRP did not undergo any delamination or rupture and displayed ductile type of failure with huge deflections in the reinforced concrete beam at such high loads. Control beams failed at 90 KN, where as the beams strengthened by using thermally treated woven sisal FRP, by full wrapping technique failed at 160 KN and lastly the beams strengthened by using thermally treated woven sisal FRP, by strip wrapping technique failed at 120 KN, this depicted the effect of shear strengthening, provided by the use of natural woven sisal FRP, bonded to reinforced concrete beams.

(8) All strengthened beams failed by failure of inside steel, at their corresponding ultimate load and they were also marked by huge deflections in the beams. The presence of bonded sisal FRP totally avoided any catastrophic failure of reinforced concrete beams, by concrete crushing or by FRP delamination.

(9) The cracks at ultimate load of strengthened beams by strip wrapping, were more in number compared to cracks in the control beams, indicating clearly the composite action due to bonded woven sisal FRP composite. The cracks at ultimate load of strengthened beams by full wrapping technique, could not be visualized, since the woven sisal FRP remained bonded to the beam even at failure.

(10) The use of natural woven sisal FRP was very effective in the case of shear strengthening of reinforced concrete beams. The ultimate shear strength of all the strengthened beams increased with the increasing width of the FRP, as strip wrapping showed lesser load carrying capacity than full wrapping.

Acknowledgments

The authors acknowledge the support extended to the work by various undergraduate and postgraduate students working under the guidance of the authors and also the laboratory supporting staff members and the laboratory assistants.

References

[1] K.-T. Lau and L.-M. Zhou, "Mechanical performance of composite-strengthened concrete structures," *Composites B*, vol. 32, no. 1, pp. 21–31, 2001.

[2] S. A. Sheikh, "Performance of concrete structures retrofitted with fibre reinforced polymers," *Engineering Structures*, vol. 24, no. 7, pp. 869–879, 2002.

[3] R. Al-Amery and R. Al-Mahaidi, "Coupled flexural-shear retrofitting of RC beams using CFRP straps," *Composite Structures*, vol. 75, no. 1–4, pp. 457–464, 2006.

[4] F. Ceroni, "Experimental performances of RC beams strengthened with FRP materials," *Construction and Building Materials*, vol. 24, no. 9, pp. 1547–1559, 2010.

[5] J. Dong, Q. Wang, and Z. Guan, "Structural behaviour of RC beams with external flexural and flexural-shear strengthening by FRP sheets," *Composites B*, vol. 44, pp. 604–612, 2013.

[6] J. A. O. Barros, S. J. E. Dias, and J. L. T. Lima, "Efficacy of CFRP-based techniques for the flexural and shear strengthening of concrete beams," *Cement and Concrete Composites*, vol. 29, no. 3, pp. 203–217, 2007.

[7] A. A. El-Ghandour, "Experimental and analytical investigation of CFRP flexural and shear strengthening efficiencies of RC beams," *Construction and Building Materials*, vol. 25, no. 3, pp. 1419–1429, 2011.

[8] M. R. Esfahani, M. R. Kianoush, and A. R. Tajari, "Flexural behaviour of reinforced concrete beams strengthened by CFRP sheets," *Engineering Structures*, vol. 29, no. 10, pp. 2428–2444, 2007.

[9] R. Al-Rousan and M. Issa, "Fatigue performance of reinforced concrete beams strengthened with CFRP sheets," *Construction and Building Materials*, vol. 25, no. 8, pp. 3520–3529, 2011.

[10] S. Hashemi and R. Al-Mahaidi, "Flexural performance of CFRP textile-retrofitted RC beams using cement-based adhesives at high temperature," *Construction and Building Materials*, vol. 28, no. 1, pp. 791–797, 2012.

[11] J. R. Correia, F. A. Branco, and J. G. Ferreira, "Flexural behaviour of GFRP-concrete hybrid beams with interconnection slip," *Composite Structures*, vol. 77, no. 1, pp. 66–78, 2007.

[12] T. H. Almusallam, "Load-deflection behavior of RC beams strengthened with GFRP sheets subjected to different environmental conditions," *Cement and Concrete Composites*, vol. 28, no. 10, pp. 879–889, 2006.

[13] J. R. Correia, L. Valarinho, and F. A. Branco, "Post-cracking strength and ductility of glass-GFRP composite beams," *Composite Structures*, vol. 93, no. 9, pp. 2299–2309, 2011.

[14] N. F. Grace, W. F. Ragheb, and G. Abdel-Sayed, "Development and application of innovative triaxially braided ductile FRP fabric for strengthening concrete beams," *Composite Structures*, vol. 64, no. 3-4, pp. 521–530, 2004.

[15] J. Sim, C. Park, and D. Y. Moon, "Characteristics of basalt fiber as a strengthening material for concrete structures," *Composites B*, vol. 36, no. 6-7, pp. 504–512, 2005.

[16] H. S. Kim and Y. S. Shin, "Flexural behavior of reinforced concrete (RC) beams retrofitted with hybrid fiber reinforced polymers (FRPs) under sustaining loads," *Composite Structures*, vol. 93, no. 2, pp. 802–811, 2011.

[17] A. Peled and A. Bentur, "Geometrical characteristics and efficiency of textile fabrics for reinforcing cement composites," *Cement and Concrete Research*, vol. 30, no. 5, pp. 781–790, 2000.

[18] Y. Li, Y.-W. Mai, and L. Ye, "Sisal fibre and its composites: a review of recent developments," *Composites Science and Technology*, vol. 60, no. 11, pp. 2037–2055, 2000.

[19] S. V. Joshi, L. T. Drzal, A. K. Mohanty, and S. Arora, "Are natural fiber composites environmentally superior to glass fiber reinforced composites?" *Composites A*, vol. 35, no. 3, pp. 371–376, 2004.

[20] A. V. Ratna Prasad and K. Mohana Rao, "Mechanical properties of natural fibre reinforced polyester composites: jowar, sisal and bamboo," *Materials and Design*, vol. 32, no. 8-9, pp. 4658–4663, 2011.

[21] A. C. Milanese, M. O. H. Cioffi, and H. J. C. Voorwald, "Mechanical behavior of natural fiber composites," *Procedia Engineering*, vol. 10, pp. 2022–2027, 2011.

[22] G. Hota and R. Liang, "Advanced fiber reinforced polymer composites for sustainable civil infrastructures," in *Proceedings of the International Symposium on Innovation & Sustainability of Structures in Civil Engineering*, Xiamen University, Nanjing, China, 2011.

[23] K. Begum and M. A. Islam, "Natural fiber as a substitute to synthetic fiber in polymer composites: a review," *Research Journal of Engineering Sciences*, vol. 2, no. 3, pp. 46–53, 2013.

[24] Laney and M. Langford, *Sustainable composites from natural materials [M.S. thesis]*, North Carolina State University, 2011.

[25] G. Cristaldi, A. Latteri, G. Recca, and G. Cicala, "Composites based on natural fibre fabrics," in *Woven Fabric Engineering*, chapter 17, InTechOpen, 2010, http://www.intechopen.com/.

[26] M. M. Kabir, H. Wang, T. Aravinthan, F. Cardona, and K. T. Lau, "Effects of natural fibre surface on composite properties: a review," in *Proceedings of the 1st International Postgraduate Conference on Engineering, Designing and Developing the Built Environment for Sustainable Wellbeing (eddBE '11)*, pp. 94–99, 2011.

[27] M. J. John and S. Thomas, "Biofibres and biocomposites," *Carbohydrate Polymers*, vol. 71, no. 3, pp. 343–364, 2008.

[28] P. D. Dubrovski, Ed., *Woven Fabric Engineering*, Sciyo, Rijeka, Croatia, 2010.

[29] *Textile Biocomposites*, Shodhganga, http://shodhganga.inflibnet.ac.in/bitstream/10603/509/12/12_part_3.pdf.

[30] M. Z. Rong, M. Q. Zhang, Y. Liu, G. C. Yang, and H. M. Zeng, "The effect of fiber treatment on the mechanical properties of unidirectional sisal-reinforced epoxy composites," *Composites Science and Technology*, vol. 61, no. 10, pp. 1437–1447, 2001.

[31] M. Ramesh, K. Palanikumar, and K. Hemachandra Reddy, "Mechanical property evaluation of sisal-jute-glass fiber reinforced polyester composites," *Composites B*, vol. 48, pp. 1–9, 2013.

[32] A. Campos, J. M. Marconcini, S. M. Martins-Franchetti, and L. H. C. Mattoso, "The influence of UV-C irradiation on the properties of thermoplastic starch and polycaprolactone biocomposite with sisal bleached fibers," *Polymer Degradation and Stability*, vol. 97, no. 10, 2012.

[33] P. A. Sreekumar, S. P. Thomas, J. M. Saiter, K. Joseph, G. Unnikrishnan, and S. Thomas, "Effect of fiber surface modification on the mechanical and water absorption characteristics of sisal/polyester composites fabricated by resin transfer molding," *Composites A*, vol. 40, no. 11, pp. 1777–1784, 2009.

[34] S. Kaewkuk, W. Sutapun, and K. Jarukumjorn, "Effect of heat treated sisal fiber on physical properties of polypropylene composites," *Advanced Materials Research*, vol. 123–125, pp. 1123–1126, 2010.

Hindawi Publishing Corporation
Advances in Materials Science and Engineering
Volume 2013, Article ID 932636, 6 pages
http://dx.doi.org/10.1155/2013/932636

Research Article

Nanofibre Electrospinning Poly(vinyl alcohol) and Cellulose Composite Mats Obtained by Use of a Cylindrical Electrode

Anna Sutka,[1] Silvija Kukle,[1] Janis Gravitis,[2] Rimvydas Milašius,[3] and Jolanta Malašauskienė[3]

[1] *Institute of Textile Materials Technologies and Design, Riga Technical University, Riga 1048, Latvia*
[2] *Laboratory of Biomass Eco-Efficient Conversation, Latvian State Institute of Wood Chemistry, Riga 1006, Latvia*
[3] *Department of Textile Technology, Kaunas University of Technology, 51424 Kaunas, Lithuania*

Correspondence should be addressed to Anna Sutka; anna.putnina@rtu.lv

Received 30 May 2013; Revised 6 August 2013; Accepted 14 August 2013

Academic Editor: Yu Dong

A study of nanofibre composites obtained by electrospinning from poly(vinyl alcohol) (PVA) solutions of steam exploded hemp fibres and shives is reported. A combined treatment of steam explosion (SE), ball milling, and high-intensity ultrasound (HIUS) is applied to prepare cellulose nanofibres (CNF) from hemp fibres (CNF-F) and shives (CNF-S). The reflectance Fourier transform infrared (FTIR ATR) spectroscopy is used to analyze the obtained PVA/CNF composite mats. Morphology of the PVA/CNF composites was studied by scanning electron microscopy (SEM).

1. Introduction

Nanofibres based on poly(vinyl alcohol) (PVA) have numerous applications in various fields such as filtration materials, biomedical applications, membranes, drug release, optics, and protective clothing [1–3]. PVA is a semicrystalline, completely biodegradable, nontoxic, water-soluble, and biocompatible polymer produced industrially by hydrolysis of poly(vinyl acetate) [4–6].

Recently, attention has been paid to modification of the PVA nanofibres by different materials, such as carbon nanotubes [7], titanium [8], silica [9], chitosan [10], collagen [11], cellulose nanocrystals [12, 13], and others. Reinforcement of PVA with cellulose nanocrystals (CNC) improves thermomechanical properties and reduces water absorption [12]. Development of CNC-filled nanocomposite fibres/mats generates new and specific applications such as energy-related materials, sensors, barrier films, and tissue engineering scaffolds [14].

In the present work, we combine PVA with cellulose nanofibres (CNF) obtained from hemp by electrospinning technique. To our knowledge, there has no report on the preparation of nanofibers of PVA/CNF composite. In this paper, we use CNF obtained from hemp fibers and hemp shives by combination of steam explosion (SE), ball milling, and high-intensity ultrasonication (HIUS) processing.

In recent years, much attention has been focused on reinforced PVA nanofibre production by needle electrospinning [8, 12, 14–17]. Electrospinning from needle-shaped electrode has low production rate and can be used only in laboratory scale [18]. In this research, electrospinning technique by using circular cylindrical electrode has been used for PVA/CNF composite preparation. Circular electrode has main advantage—larger production rate compared to the conventional needle electrospinning [18], and equipment modules for nanofiber production in small or high volumes are available [19].

2. Materials and Methods

Dew-retted hemp fibers of local variety "Purini" and shives of variety "Bialobrzeskie" grown on the experimental fields of the Latgalian Agriculture Research Center LLZC (district Vilani, Latvia) are used in this research.

Hemp fibres and shives were treated using steam explosion treatment from previous researches [20, 21], milling treatment, and high-intensity ultrasonication technique.

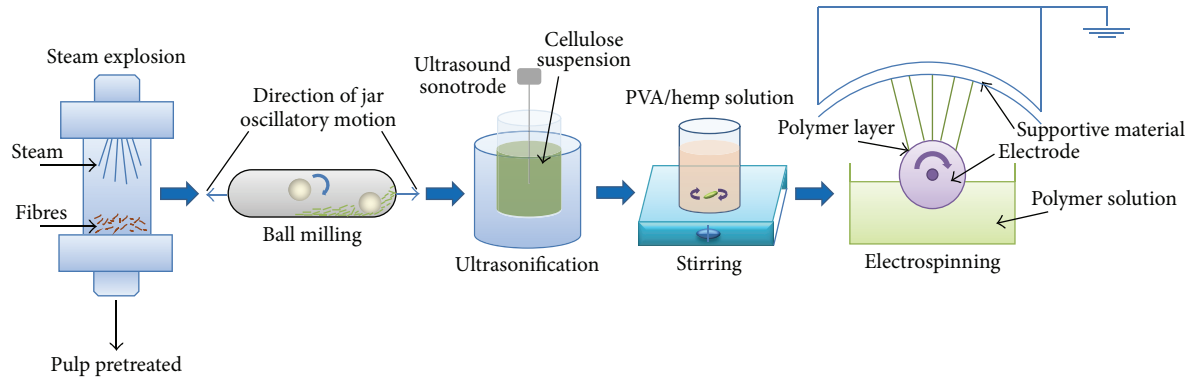

Figure 1: Schematic illustration of the treatment sequence of hemp fibres and shives.

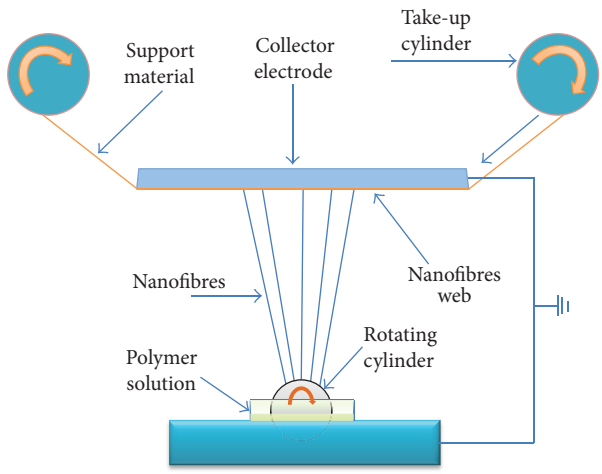

Figure 2: Scheme of electrospinning setup—"Nanospider."

Schematic illustration of fibers and shives treatments is shown in Figure 1.

2.1. Steam Explosion Treatment (SE). Steam explosion autohydrolysis is process which includes fast impregnation of the plant material with saturated steam in a closed reactor. The treatment proceeds at moderate temperature and pressure for a desired period of time (from some seconds to some minutes).

Severity parameter or the reaction ordinate R_0 of SE is defined by

$$R_0 = t * \exp\left[\frac{(T - 100)}{14.75}\right], \quad (1)$$

where duration of treatment (t, minutes), and the temperature (T, °C) express the SE severity against the base or reference temperature $T_{\text{base}} = 100°\text{C}$ [22].

2.2. Milling. For hemp pulp homogenization and agglomerate crushing, ball milling was performed. A Mixer Mill Retsch MM200 (Germany) at frequency 30 s^{-1} for 10 minutes was used.

2.3. High-Intensity Ultrasonic Treatment. The powdered fibers or shives were suspended in distilled water and treated with ultrasound (ultrasonic processor UP 200 Hp, 200 W, frequency 26 kHz, amplitude 90%, sonotrode S26d14, and Ø14 mm) (HIUS) for 30 min. HIUS produces very strong mechanical oscillating power, so cellulose fibrils can be isolated from cellulose fibers by the action of hydrodynamic forces of ultrasound [23]. In order to control the process temperature, the beaker with the cellulose fiber solution was put in a water bath. The suspensions of fibers and shives after ultrasonification was mixed with PVA 8 wt% solution and stirred for 1 h. PVA solution was prepared before at 70°C by dissolving PVA granules in distilled water and gently stirred for 2 h. Poly(vinyl alcohol) JP-24 with degree of hydrolysis of 88% was supplied by Vam and Poval Co., Ltd. (Japan).

2.4. Viscosity Measurements. The viscosity of PVA/cellulose solutions was measured by HAAKE Viscotester 6 plus (Germany) at the temperature 20 ± 0.5°C.

2.5. Electrospinning. Fibers from PVA suspensions (without or with shives or fibers added) were obtained by electrospinning equipment—"Nanospider" (Elmarco, Czech Republic). While cylindrical electrode rotating, it is covered by a film of the polymer solution. When the electrostatic force overcomes the surface tension of the polymer solution, jet of polymer solution ejected from the Taylor cone. The jet moves towards the upper electrode and sets down on the spunbonded polypropylene substrate material (surface density $Q = 21.5 \pm 3\ \text{g/m}^2$). Meanwhile, the nanofibre becomes thinner; the solvent evaporates and then solidifies [24]. Scheme of electrospinning setup—"Nanospider" is shown in Figure 2.

Distance between rotating cylinder and collector electrode was 13 cm, applied voltage was 70 kV, the temperature of the electrospinning environment was $t = 20 \pm 2°\text{C}$, and the humidity was $\gamma = 45 \pm 2\%$.

2.6. Scanning Electron Microscopy (SEM). Microstructural features of the electrospun fiber samples were detected by SEM using a Field Emission Gun SEM (Tescan Mira/LMU, Czech Republic). Prior to SEM evaluation, the samples were coated with gold by means of a plasma sputtering apparatus.

2.7. Static Image Analysis. CorelDRAW Graphics Suite X6 software was used to measure the diameter and diameter

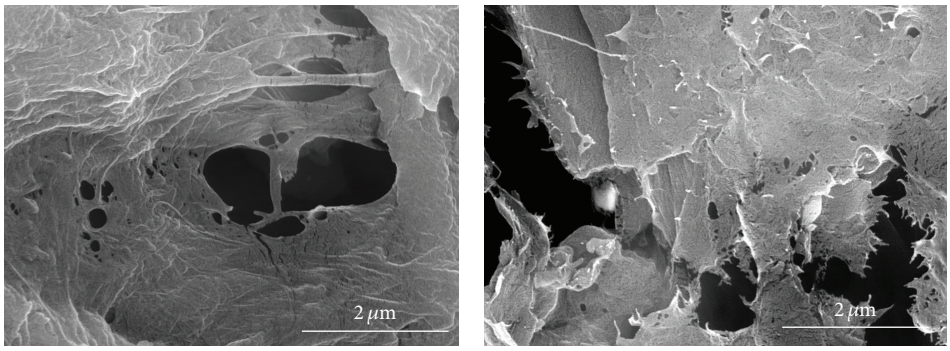

(a) (b)

Figure 3: SEM micrographs of the (a) hemp fibres (CNF-F), and (b) hemp shives (CNF-S).

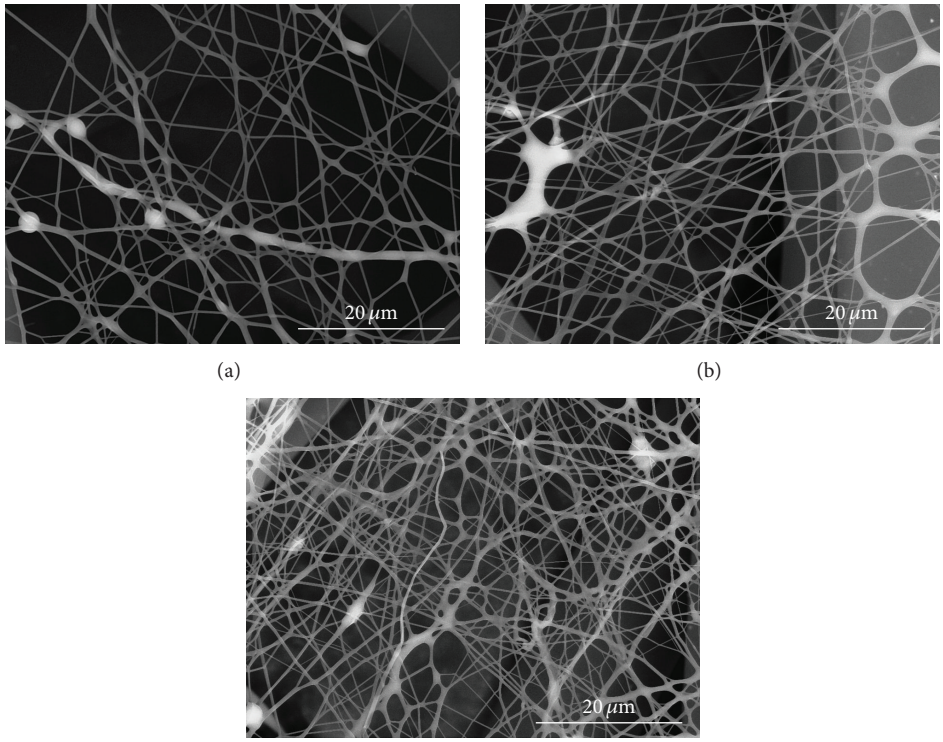

(a) (b)

(c)

Figure 4: SEM micrographs of the (a) neat PVA fibres, (b) PVA/CNF-S 2%, and (c) PVA/CNF-F 2%.

distribution of electrospun fibres from two-dimensional images obtained from SEM micrographs.

2.8. Attenuated Total Reflection Fourier Transform Infrared (ATR-FTIR) Spectroscopy. ATR-FTIR was used to chemically confirm the presence of the MCC or shives cellulose inside the PVA nanofibre matrix. All spectra of the samples under investigation were recorded by Spectrum One (Perkin Elmer, UK) FTIR spectrometer in the range of 4000–400 cm^{-1} (resolution: 4 cm^{-1}).

3. Results and Discussion

Steam explosion treatment conditions are shown in Table 1. After SE treatment fibres or shives were additionally washed with distilled water to remove water-soluble components and with NaOH 0.4 wt% solution in water to remove hemicelluloses, pectins/waxes, lignin, and oils. Then, solution was neutralized with HCl to precipitate lignin, filtered and additionally washed with water, and dried in air at room temperature. After drying, forms of dense pulp were made from agglomerates of the nonuniformly sized fibres.

The loss of mass during the SE treatment was found to be ~14% and ~23% in case of fibres and shives, respectively. A higher evaporation intensity of shives is attributed to a higher content of lignin stability which is lower during the SE treatment compared with cellulose. The mass of water-soluble components removed from fibre samples equals to ~25% and ~33%—from shive samples. About 68% of mass is recovered

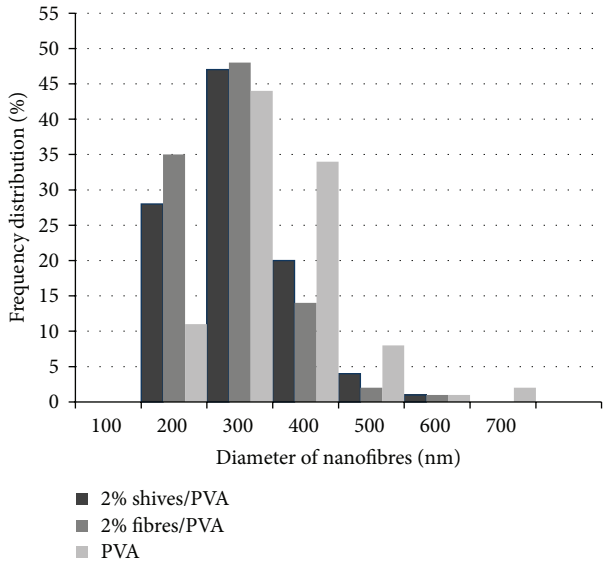

Figure 5: Diameter distribution of nanofibres from PVA, shives/PVA, and fibers/PVA.

Table 1: Parameters of steam explosion treatment.

Variety	SE parameters			
	Temperature, °C	Pressure, bar	Time, min	$\log R_0$
Fibres ("Purini")	235	32	3	4.45
Shives ("Bialobrzeskie")	235	32	3	4.45

in the cellulose residues of fiber samples and about 42%—in case of shives (Table 2).

As found by SEM (Figure 3) studies, cellulose nanofibres (CNF) of average diameter below 100 nm are successfully obtained from hemp fibers and shives after combined treatment by SE, ball milling, and HIUS.

When adding CNF to the PVA polymer solution, its viscosity increases (Table 3). The remarkable variation in the rheological behaviour of the solutions used in our work could be due to the shear stress between fibres and polymer macromolecules. Viscosity of the solutions influences applied voltage threshold [25]. It was found that for higher polymer solution concentration higher applied voltage is necessary. In our case, viscosity for all solutions lies within the limits of the equipment for nanofibre spinning.

The morphology of electrospun fibres was studied by SEM. Figure 4 shows typical SEM micrographs for fibers obtained from PVA (a) and from PVA with 2% concentration of shives (b) and fibers (c). It was found that it is possible to obtain electrospun submicrometer fibres from used solutions. The morphology of submicrometer fibres, for example, defect concentration, shape of the fibers, and their average diameters, was not influenced by the composition of the spinning solution. However, it was found that coverage of the nanowires on the substrate material is higher for PVA/CNF composites than neat PVA.

From SEM images (Figure 4), it also can be seen that electrospun PVA and PVA/CNF melts together, thus making fraction of the composite fibres with higher diameter. This can be explained by the fact that the collecting distance was not large enough for sufficient solvent evaporation from the jet before deposition [26].

As we already concluded there is no remarkable difference between modal diameters of the PVA and PVA/CNF composite fibres, and their diameter is found to be 250 nm for both shives and cellulose fibres. The second modal diameters of fibres/PVA and shives/PVA correspond to the diameter range 100–200 nm but for PVA move to the diameter range 300–400 nm. It means that the PVA fibres are formed with average diameters above 300 nm (Figure 5). The addition of shives or fibers led to decreasing the average diameter of the electrospun fibers which is explained by the change in the ionic strength and conductivity of the spinning solution produced by the negatively charged cellulose. An increased electrostatic charge density of the spinning solution induced more extensive filament stretching during jet whipping [13].

To confirm the presence of hemp fibres and shives in the PVA submicrometer fibre mats, they were subjected to analysis with Attenuated total reflection Fourier transform infrared (ATR-FTIR) spectroscopy. Spectra of neat PVA polymer and combined with 1% and 2% of fibers are presented in Figure 6(a), but for shives Figure 6(b). All major peaks related to hydroxyl and acetate groups were evident in the spectra corresponding to the neat PVA. The large bands observed between 3550 and 3200 cm^{-1} were typical of the stretching O–H from the intermolecular and intermolecular hydrogen bonds [13]. The vibrational band observed between 2850 and 2940 cm^{-1} corresponds to the stretching C–H from alkyl groups, and the peak diapason between 1730 and 1710 cm^{-1} was assigned to the C–O and C–O stretching from residual acetate groups in the PVA matrix. The presence of the peak diapason between 1085 and 1126 cm^{-1}, corresponding to the C–O stretching of the alcohol groups of cellulose, was clearly visible from Figure 5 of electrospun fibers/PVA composite. Intensity of peaks between this diapason increases with an increase in the fibers content of the fibers/PVA solution and the same in shives case of the peaks diapason between 1115 and 1128 cm^{-1}, especially with the 2% shives content (Figure 6(b)), thus confirming formation of cellulose/PVA composites.

4. Conclusions

In this study, we have introduced the combination of the steam explosion, ball milling, and high-intensity ultrasonication treatments to ensure successful formation of the cellulose nanofibres with the average diameter below 100 nm from hemp fibres and shives. Submicron PVA fiber mats reinforced with cellulose nanofibres were prepared by electrospinning of aqueous PVA solutions using a circular cylinder as the emitting electrode. The obtained diameters of the PVA/CNF composite mats were ~0.250 μm (250 nm). The presence of the cellulose in the PVA matrix was confirmed by ATR-FTIR

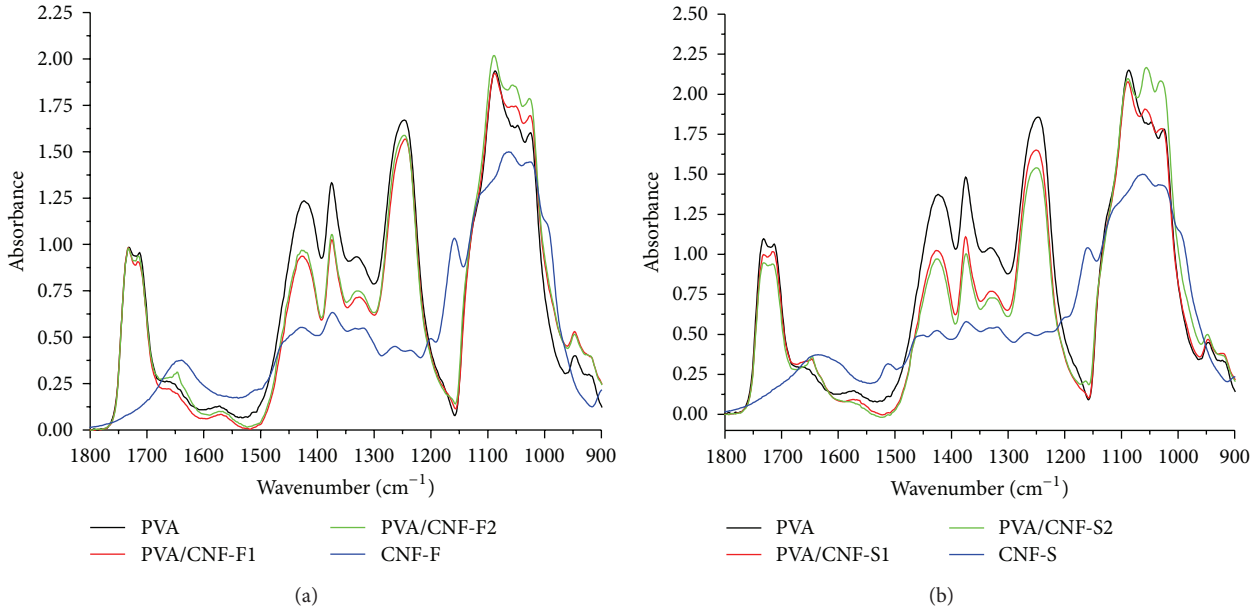

Figure 6: FTIR spectra corresponding to electrospun fibres and shives/PVA composites.

Table 2: Modes of hemp samples after SE and after treatment [21].

Sample	Evaporable fractions, %	Residue, %	Water solub., %	Resid. after wat., %	Alk. solub., %	Resid. after alk. extr., %
Fibres	13.8	86.2	10.8	75.3	7.1	68.3
Shives	22.5	77.5	10.2	67.4	25.5	41.8

Table 3: Viscosity of the polymer solutions.

Composition of polymer solution	Polymer concentration, %	Fibre concentration, %	Viscosity, mPa·s·10^{-3}
PVA	8	0	0.46
PVA/CNF-F1	8	1	0.69
PVA/CNF-F2	8	2	1.07
PVA/CNF-S1	8	1	0.86
PVA/CF-S2	8	2	1.8

spectra of the composites. Further experiments are necessary to study physical, mechanical, thermomechanical, and water absorption properties, as well as structural stability of obtained nanocomposites.

References

[1] A. F. Spivak, Y. A. Dzenis, and D. H. Reneker, "Model of steady state jet in the electrospinning process," *Mechanics Research Communications*, vol. 27, no. 1, pp. 37–42, 2000.

[2] A. Theron, E. Zussman, and A. L. Yarin, "Electrostatic field-assisted alignment of electrospun nanofibres," *Nanotechnology*, vol. 12, no. 3, pp. 384–390, 2001.

[3] L. Huang, K. Nagapundi, and E. L. Chaikof, "Engineered collagen-PEO nanofibers and fabrics," *Journal of Biomaterials Science Polymer Edition*, vol. 12, no. 9, pp. 979–993, 2001.

[4] X. Wang, C. Drew, S.-H. Lee, K. J. Senecal, J. Kumar, and L. A. Samuelson, "Electrospun nanofibrous membranes for highly sensitive optical sensors," *Nano Letters*, vol. 2, no. 11, pp. 1273–1275, 2002.

[5] W. J. Li, C. T. Laurencin, E. J. Caterson, R. S. Tuan, and F. K. Ko, "Electrospun nanofibrous structure: a novel scaffold for tissue engineering," *Journal of Biomedical Materials Research*, vol. 60, no. 4, pp. 613–621, 2002.

[6] J. A. Matthews, G. E. Wnek, D. G. Simpson, and G. L. Bowlin, "Electrospinning of collagen nanofibers," *Biomacromolecules*, vol. 3, no. 2, pp. 232–238, 2002.

[7] C. Fu and L. Gu, "Composite fibres from poly(vinyl alcohol) and poly(vinyl alcohol)-functionalized multiwalled carbon nanotubes," *Journal of Applied Polymer Science*, vol. 128, no. 2, pp. 1044–1053, 2013.

[8] P. Ahmadpoor, A. S. Nateri, and V. Motaghitalab, "The optical properties of PVA/TiO_2 composite nanofibres," *Journal of Applied Polymer Science*, vol. 130, no. 1, pp. 78–85, 2013.

[9] C. Shao, H.-Y. Kim, J. Gong, B. Ding, D.-R. Lee, and S.-J. Park, "Fiber mats of poly(vinyl alcohol)/silica composite via electrospinning," *Materials Letters*, vol. 57, no. 9-10, pp. 1579–1584, 2003.

[10] M. Ignatova, K. Starbova, N. Markova, N. Manolova, and I. Rashkov, "Electrospun nano-fibre mats with antibacterial properties from quaternised chitosan and poly(vinyl alcohol)," *Carbohydrate Research*, vol. 341, no. 12, pp. 2098–2107, 2006.

[11] S.-H. Teng, E.-J. Lee, P. Wang, and H.-E. Kim, "Collagen/hydroxyapatite composite nanofibers by electrospinning," *Materials Letters*, vol. 62, no. 17-18, pp. 3055–3058, 2008.

[12] M. S. Peresin, Y. Habibi, A.-H. Vesterinen, O. J. Rojas, J. J. Pawlak, and J. V. Seppälä, "Effect of moisture on electrospun nanofiber composites of poly(vinyl alcohol) and cellulose nanocrystals," *Biomacromolecules*, vol. 11, no. 9, pp. 2471–2477, 2010.

[13] M. S. Peresin, Y. Habibi, J. O. Zoppe, J. J. Pawlak, and O. J. Rojas, "Nanofiber composites of polyvinyl alcohol and cellulose nanocrystals: manufacture and characterization," *Biomacromolecules*, vol. 11, no. 3, pp. 674–681, 2010.

[14] C. Zhou and Q. Wu, *Recent Development in Applications of Cellulose Nanocrystals for Advanced Polymer-Based Nanocomposites by Novel Fabrication Strategies, Nanocrystals—Synthesis, Characterization and Applications*, 2012, Edited by Sudheer Neralla.

[15] H. Fong, I. Chun, and D. H. Reneker, "Beaded nanofibers formed during electrospinning," *Polymer*, vol. 40, no. 16, pp. 4585–4592, 1999.

[16] H. Niu, J. Zhang, Z. Xie, X. Wang, and T. Lin, "Preparation, structure and supercapacitance of bonded carbon nanofiber electrode materials," *Carbon*, vol. 49, no. 7, pp. 2380–2388, 2011.

[17] C. Huang, Y. Tang, X. Liu et al., "Electrospinning of nanofibres with parallel line surface texture for improvement of nerve cell growth," *Soft Matter*, vol. 7, no. 22, pp. 10812–10817, 2011.

[18] H. Niu and T. Lin, "Fiber generators in needleless electrospinning," *Journal of Nanomaterials*, vol. 2012, Article ID 725950, 13 pages, 2012.

[19] Elmarco, "Nanospider Technology," http://www.elmarco.cz/technology/nanospider%3Csup%3Etm%3Csup%3E-technology/.

[20] S. Kukle, J. Gravitis, and A. Putnina, "Processing parameters influence on disintegration intensity of technical hemp fibres," *Journal of Biobased Materials and Bioenergy*, vol. 6, no. 4, pp. 440–448, 2012.

[21] A. Putnina, S. Kukle, and J. Gravitis, "Steam explosion as the pretreatment method of lignocellulosic biomass," *Scientific Journal of RTU*, vol. 7, pp. 80–83, 2012.

[22] M. Heitz, E. Capek-Menard, P. G. Keoberle et al., "Fractionation of populus tremuloides at the pilot plant scale: optimization of steam pretreatment conditions using the STAKE II technology," *Bioresource Technology*, vol. 35, no. 1, pp. 23–32, 1991.

[23] Q. Cheng, *Fabrication and analysis of polymeric nanocomposites from cellulose fibrils [Ph.D. dissertation]*, University of Tennessee, 2007.

[24] E. Adomavičiūtė, M. Adomavičienė, R. Milašius, M. Leskovšek, and A. Demšar, Magic World of Textiles Book, pp. 37–41, Proceedings of the 4rd ITC & DC, 2008.

[25] D. Wu, X. Huang, X. Lai, D. Sun, and L. Lin, "High throughput tip-less electrospinning via a circular cylindrical electrode," *Journal of Nanoscience and Nanotechnology*, vol. 10, no. 7, pp. 4221–4226, 2010.

[26] H. Niu, X. Wang, and T. Lin, *Needleless Electrospinning: Developments and Performances, Nanofibres—Production, Properties and Functional Applications*, 2011, Edited by T. Lin.

Hindawi Publishing Corporation
Advances in Materials Science and Engineering
Volume 2013, Article ID 941617, 7 pages
http://dx.doi.org/10.1155/2013/941617

Research Article

Improvement of Mechanical Properties of Noil Hemp Fiber Reinforced Polypropylene Composites by Resin Modification and Fiber Treatment

Zili Yan,[1,2] Jianchun Zhang,[2,3] Hua Zhang,[2,3] and Hao Wang[1]

[1] *Centre of Excellence in Engineered Fibre Composites, University of Southern Queensland, Toowoomba, QLD 4350, Australia*
[2] *Special High Value Biomass Industry and Technology Innovation Strategic Alliance, Beijing 100082, China*
[3] *The Research Centre of China-Hemp Materials, Beijing 100082, China*

Correspondence should be addressed to Zili Yan; yan_zili@sina.com and Hao Wang; hao.wang@usq.edu.au

Received 31 May 2013; Revised 15 August 2013; Accepted 23 August 2013

Academic Editor: Hazizan Md Akil

The present study aims to improve the reinforcement of hemp fibre to polypropylene (PP) by simple resin modification and fibre treatment. Maleic anhydride grafted polypropylene (MAPP) was used as resin modifier by direct mixing with PP, and hydrophobically modified hydroxyethyl cellulose (HMHEC) was used as fibre treatment reagent by immersing fibre into its aqueous solution. The influences of fibre content, resin modification, and fibre treatment on the mechanical properties (tensile, flexural, and impact strengths) of composites were investigated. The change of interfacial bonding between fibre and resin in composites caused by MAPP and HMHEC was studied by scanning electron microscopy and dynamic mechanical analysis. Resin modification and fibre treatment were effective to enhance the mechanical properties of the composites. The improvement in interfacial bonding is quantitatively evaluated with adhesion factor.

1. Introduction

Glass fibres are the most widely used reinforcement to plastics due to their low cost and satisfactory effectiveness. However, their drawbacks are also evident, including the health risk when handling and nonbiodegradability when disposed [1, 2]. Using natural fibres, especially plant fibres, as replacement of glass fibres can overcome the above-mentioned problems with additional advantages, including cost-effectiveness, low density, high specific strength, and their availability as renewable resources [3–5]. So far, natural fibres have been used to replace glass fibres in automotive industry but mostly in nonstructural components [6, 7]. The first and most important reason for the limited application of natural fibre composites is due to the poor interfacial bonding between the hydrophilic natural fibres and the hydrophobic resins, which means the poor shear stress transferring ability at microscale and the unsatisfactory mechanical properties at macroscale in the composites [8, 9]. Additional disadvantages arisen from this drawback are apparent fibre breakage and unavoidable thermal degradation when internal mixing or extruding is used to fabricate compound of natural fibre and plastic because strong shearing force and long compounding time are necessary to realize homogeneous fibre distribution [10–12].

Many studies have been focused on resin modification and fibre treatment to improve interfacial bonding. For thermoplastic matrix composites, a lot of resin modifiers have been developed and shown positive effect on interfacial bonding and mechanical properties [13–15]. The most effective modifier is maleic grafted polymer in which the maleic anhydride can react with the hydroxygen group on natural fibre surface, and the main chain of modifier entangles with the matrix [15]. However, the overall mechanical properties of the composites are still lower than corresponding glass fibre reinforced composites [16]. Fibre surface treatment is another approach to achieve improved mechanical performance. Various fibre treatments have been developed using alkali, isocyanate, silane, and acrylic acids, permanganate, and so forth [17, 18]. Nevertheless, much water is consumed to wash

Table 1: The chemical composition of NHF.

Components	Cellulose, wt%	Lignin, wt%	Hemicellulose, wt%	Pectin, wt%	Others, wt%
NHF	91.9	1.7	3.5	1.2	1.7

Note: the chemical composition test was based on dry hemp fibre.

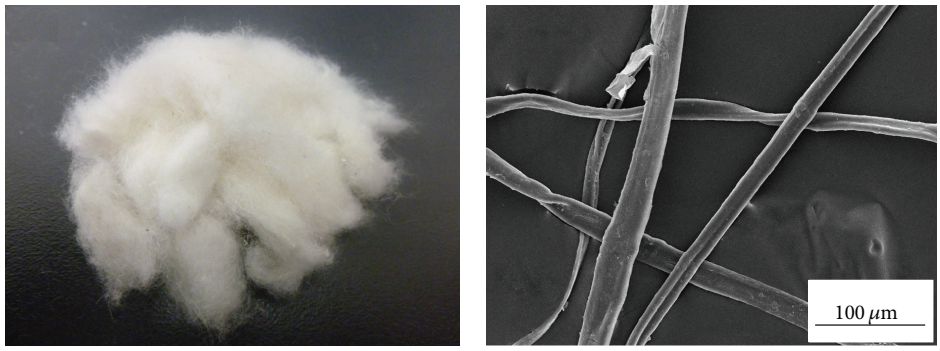

(a) (b)

Figure 1: Photo and micrograph of NHF.

the alkali treated fibre to neutral PH, and many of other treatments are undertaken in pure organic solvent or mixed solvent containing organic solvent, which have the problems of disposal of chemicals after treatment [19]. Caulfield et al. [20] used aqueous emulsion of paper sizing agents (alkyl ketene dimer and alkenyl succinic anhydride) to treat cellulose fibre. The treatment improved the hydrophobicity of the fibre and the compatibility between the fibre and the matrix but did not show any improvement in mechanical properties of the composites.

This research is an attempt aiming to develop simple resin modification and fibre treatment route to improve mechanical properties of hemp fibre reinforced polypropylene composites. The fibre treatment was carried out simply by immersing fibre into aqueous solution of hydrophobically modified hydroxyethyl cellulose (HMHEC) followed by oven drying. Resin modification was achieved by applying maleic anhydride grafted polypropylene (MAPP) to Polypropylene (PP).

2. Experimental Section

2.1. Raw Materials. Noil hemp fibre (NHF) was obtained from China-Hemp Industrial Investments and Holding Co., Ltd. (Yunnan Province, China). It is an overdegummed hemp fibre by-product in hemp fibre production for textile purpose, with a length shorter than the requirement for textile industry. The chemical composition and microstructure of NHF are shown in Table 1 and Figure 1, respectively. It mainly consists of cellulose (91.9 wt%) and has low content of pectin, hemicellulose, and lignin. The fibre has smooth surface and an average diameter of 20–30 μm.

Polypropylene (PP, M800E, Sinopec Shanghai petrochemical Co. Ltd., China) with melt flow index of 8.0 ± 1.5 g/10 min was chosen as a matrix. MAPP with MA content of 1.0 wt% (Bondyram 1001, Polyram Ram-On Industries, Israel) was used as a modifier to the resin. HMHEC (NATROSOL Plus 330, Hercules Chemicals Co. Ltd., China) was used as a fibre treatment reagent. Antioxidant and anti-UV agents were applied as additives to the composites.

2.2. Composites Preparation. HMHEC powder was added into stirred water and then kept for 24 h to get a semitransparent aqueous solution with 0.5 wt% of HMHEC. Then NHF was immersed in the solution for 0.5 h with a fibre/solution weight ratio of 1/5. After that, the treated NHF was taken out and heated to 60°C for 12 h and then to 105°C for 8 h to remove water/moisture before it was used for composite fabrication. When no fibre treatment was applied to NHF, it was heated to 105°C and kept for 8 h to remove moisture before mixing with PP.

After the internal mixer was preheated to 170–180°C, PP, antioxidants (0.3%), and an anti-UV agent (0.3%) were added into it and mixed for 15 min to make the resin melt with a rotor speed of 50 rpm. Then NHF was added into the mixer to mix with resin melt for 10–15 min at the same temperature and rotor speed. After that, the composite melt was sheeted using an open mill. The cooled sheets were then crushed into granule of 3–7 mm in size by a crusher. The granules were finally moulded into specimens at 170–175°C for mechanical tests by an injection moulding machine. Composites with 10–40 wt% NHF were fabricated to evaluate the influence of fibre content on the mechanical properties of composites. Composites with MAPP modification to PP and HMHEC treatment to NHF were also fabricated. For those two composites, MAPP was added into the internal mixer together with PP, and the contents of MAPP and NHF were fixed at 5 wt% and 30 wt%, respectively.

2.3. Characterizations. In accordance with ISO 527-2-1993, the tensile strength test was performed on dumbbell-shaped specimens of Type 1A using a multifunctional machine (AG-2000A, Shimadzu Corp., Japan) with a loading rate

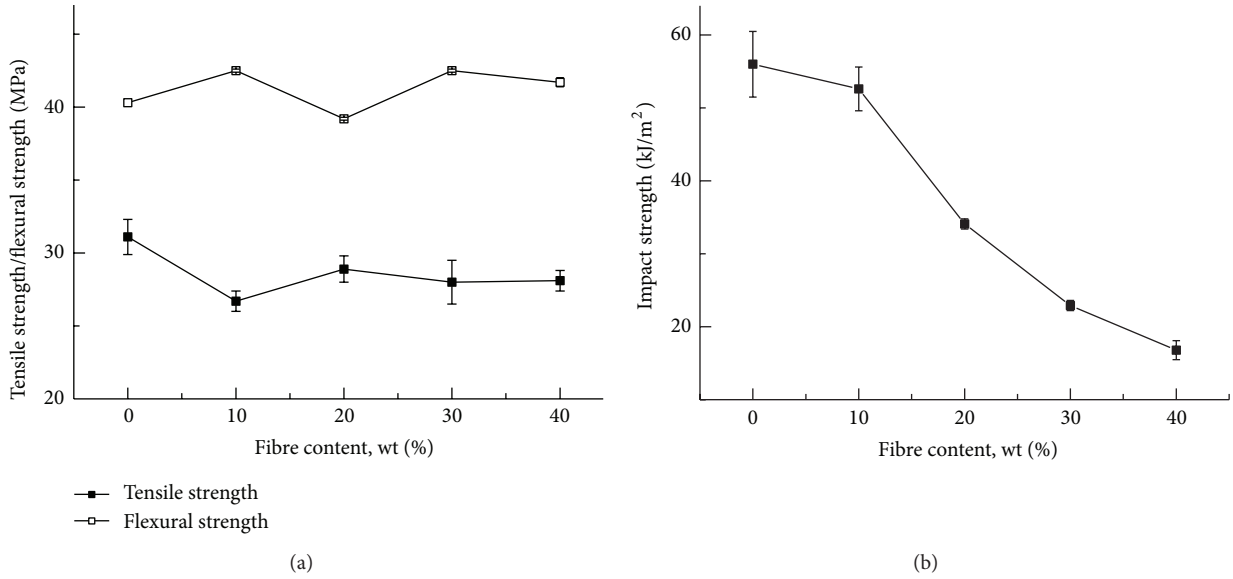

Figure 2: The influence of fibre content on mechanical properties of NHF/PP composites.

of 10 mm/min and a 10 kN load cell at room temperature. The standard samples with nominal dimensions of 80 mm × 10 mm × 4 mm were used to measure the flexural strength using the above-mentioned MPa multifunctional machine according to ISO 178-2001 with a loading rate of 3 mm/min. The unnotched Charpy impact strength test was conducted on standard samples with nominal dimensions of 80 mm × 10 mm × 4 mm with an impact tester (XCJ24, Chengde Testing Machine Co., Ltd., China) in accordance with ISO 179-2000. All the results were based on average value of at least five specimens.

A scanning electron microscopy (SEM, JSM-646-LV, Shimadzu Corp., Japan) was used to observe the microstructure of the fracture surface of tensile test specimens and fibre-matrix interface adhesion. The acceleration voltage is 20 kV. The fracture surface of the specimens was lightly sputter coated with carbon before SEM observation. Dynamic mechanical analyzer (DMA, Q-800, TA instrument, USA) was used to evaluate the damping coefficient and the adhesion factor of different composites. Rectangular specimens of 60 mm × 10 mm × 3.5 mm were used for this test, which were cut and sanded from injection moulded specimens for flexural/impact strength tests. The tests were carried out under a dual cantilever mode at a fixed frequency of 1 Hz in a temperature range of 30–145°C. The deflection amplitude was 15 μm, and the heating ramp rate was 3°C/min.

3. Results and discussion

3.1. Effect of Fibre Content on Mechanical Properties of the Composites. Fibre content has important influence on the overall performance of composites. Figure 2 shows the effect of NHF content on mechanical properties of the composites without resin modification and fibre treatment. Tensile strength is decreased to 26.7 MPa, when fibre content is 10 wt% compared with neat PP (31.1 MPa). Further increasing fibre content to 40 wt% has negligible effect on tensile strength of the composites. Flexural strength in NHF/PP almost keeps constant with increasing the NHF from 0 to 40 wt%. Comparing to the tensile strength of composites, the standard deviation of flexural strength is so small that it is invisible. The impact strength of PP/NHF decreases with increasing the fibre from 56 KJ/m^2 in neat PP to 16.8 KJ/m^2 in PP/NHF (40 wt%). The overall mechanical properties of the composites are lower than neat PP. As has been stated in the pieces of literature [21, 22], the low adhesion between the hydrophilic natural fibre and hydrophobic PP is the reason why direct compounding of fibre and PP cannot exhibit fibre reinforcement.

3.2. Effect of Resin Modification and Fibre Treatment. Fibre treatment and resin modification are necessary to achieve the benefit from fibre to reinforce plastics [15, 23]. Figure 3 shows the influence of resin modification with MAPP and fibre treatment with HMHEC on the mechanical properties of the composites with 30 wt% fibre. Tensile, flexural, and impact strengths of the composites with MAPP (NHF/PP/MAPP) are 39.3 MPa, 62.6 MPa, and 33 KJ/m^2, respectively. Compared to the composites without MAPP (NHF/PP), the improvements by MAPP addition are 40%, 47%, and 44%, respectively. The combination of fibre treatment and resin modification (HMHEC/NHF/PP/MAPP) leads to further improvement in tensile strength and impact strength but shows minimal effect on flexural strength. The finial composites show a tensile strength of 44.5 MPa (13% improvement compared to resin modified composites), a flexural strength of 60.9 MPa (3% decrease), and an impact strength of 39.3 kJ/m^2 (19% improvement).

3.3. Fracture Surface of Composites. Figure 4 shows fracture surfaces of the three composites, unmodified, resin modified,

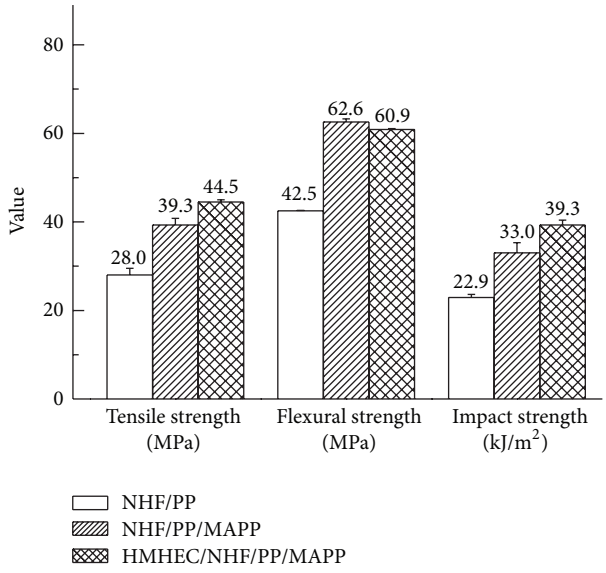

Figure 3: Influence of resin modification with MAPP and fibre treatment with HMHEC on the mechanical properties of the composites.

and resin modified plus fibre treated. There is a visible difference in fracture surface between the three composites. When no resin modification and no fibre treatment were conducted to the composites (NHF/PP), fibre has a tendency to be pulled out from the matrix, and the extracted fibre length is long (Figure 4(a)). For the composites with 5 wt% MAPP resin modification (NHF/PP/MAPP) (Figure 4(b)), fibre breakage is the main fracture mechanism, and the extracted fibre is shorter than that in NHF/PP. The fracture surface of composites with both resin modification and fibre treatment (HMHEC/NHF/PP/MAPP) shows similar appearance with NHF/PP/MAPP but less fibre pullout (Figure 4(c)).

The previous difference demonstrates the enhanced interfacial bonding in composites by resin modification and fibre treatment. MAPP has been used as modifier in wood plastic composites to improve interfacial bonding because of the reaction between maleic anhydride of MAPP and hydrogen on fibre surface, together with the entanglement of the PP chain between MAPP and the matrix [24–26]. HMHEC for fibre treatment has hydroxyethylcellulose (HEC) as hydrophilic main chain and long-chain alkyl group as hydrophobic graft chain (Figure 5) [27]. The similar structure between HEC and cellulose in NHF allows Van der Waals forces and hydrogen bond between the modifier and NHF. The olefinic structure of the graft chain is miscible with polypropylene. Both the graft chain and the main chain of HMHEC contributed to the improvement of the interfacial bonding of the composites.

3.4. Fibre Matrix Adhesion Factor. Dynamic mechanical analysis (DMA) is a powerful technique to characterize transition and relaxation process of matrix resin and the effect from fibre [28]. tan δ, damping coefficient from DMA test, is to characterize the energy dissipation of polymers and their composites. It has been commonly employed to determine the interfacial characteristics of composites because interfacial bonding is one of the most significant sources of damping in composites [29]. In general, a perfect interface will transfer the entire load from matrix to fibre and does not therefore contribute to the damping characteristics. Based on previous research with DMA, an adhesion factor (A) is adopted to evaluate the interfacial bonding of composites [30], which can be expressed as

$$A = \frac{1}{1 - V_f} \frac{\tan \delta_c}{\tan \delta_m} - 1, \quad (1)$$

in which V_f is fibre volume fraction and $\tan \delta_c$ and $\tan \delta_m$ represent the damping coefficients of the composite and the matrix, respectively. A low value of adhesion factor is an indication of good interfacial bonding between the fibre and the matrix.

The damping coefficients of neat PP and three composites are shown in Figure 6. $\tan \delta$ of neat PP and its composites increases with the rising of temperature. However, there is an apparent difference between them. Compared with neat PP, NHF/PP has lower $\tan \delta$ at low temperature but higher $\tan \delta$ at high temperature, whereas the composites with resin modification and fibre treatment, NHF/PP/MAPP and HMHEC/NHF/PP/MAPP, have lower $\tan \delta$ in the whole temperature range of the DMA test, which means that the resin modification and the fibre treatment improve the interfacial bonding in composites. Furthermore, the fibre treatment leads to even lower $\tan \delta$ of the composites (HMHEC/NHF/PP/MAPP) at high temperature. Figure 7shows the calculated adhesion factors of three composites. Unmodified composites (NHF/PP) have higher adhesion factor in the whole temperature range. The MAPP resin modification brings about a significant decrease in adhesion factor. When the fibre treatment is combined with resin modification, the adhesion factor is slightly increased at low temperature but noticeably decreased at high temperature.

The results are consistent with the molecular movement theory and the previous research on the dynamic mechanical analysis of composites [31, 32]. Different from single phase of neat resin, the composite is consists of three phases: matrix, fibre, and interfacial phases. Therefore, besides the matrix, both the fibre and the interface affect the comprehensive properties of the composites, including the damping behavior. The fibre behaves more elastically than the matrix resin [31], which leads to the reduced energy dissipation of composites in the whole temperature range of the DMA test. The interfacial bonding in composites affects $\tan \delta$ by restricting the molecular movement of the resin on the fibre surface. In NHF/PP, the poor interfacial bonding between NHF and PP shows limited restriction to the molecular movement of matrix, especially at high temperature. Due to the combined influence by fibre and the interfacial bonding, NHF/PP has lower $\tan \delta$ at low temperature and higher $\tan \delta$ at low temperature than PP. The effect of MAPP in enhancing interfacial bonding has been repeatedly testified in this study and leads to the lower $\tan \delta$ of NHF/PP/MAPP than that of NHF/PP.

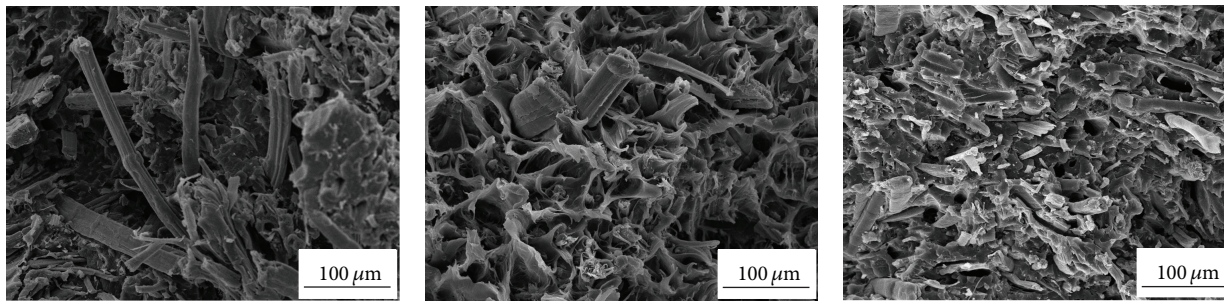

Figure 4: SEM images of fracture surface of (a) NHF/PP; (b) NHF/PP/MAPP; (c) HMHEC/NHF/PP/MAPP.

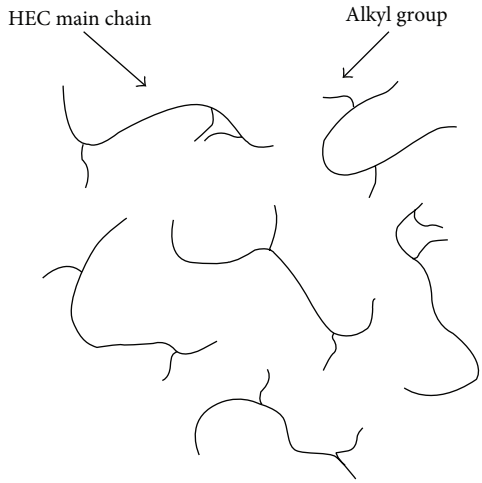

Figure 5: Illustration of HMHEC in aqueous solution.

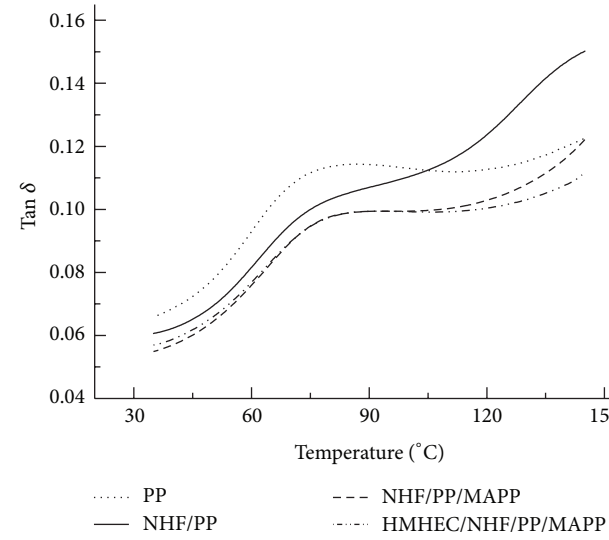

Figure 6: Plots of tan δ versus temperature of neat PP and its composites.

The further decreased tan δ in HMHEC/NHF/PP/MAPP at high temperature suggests the effectiveness of fibre treatment in improving the interfacial bonding. Based on the previous discussion, it suggests that tan δ of composites at high temperature is more related with interfacial bonding. Figure 7 shows an adhesion factor sequence of NHF/PP > NHF/PP/MAPP > HMHEC/NHF/PP/MAPP at high temperature, which means increased interfacial bonding by resin modification and fibre treatment. Slightly high adhesion factor of HMHEC/NHF/PP/MAPP at low temperature (less than 65°C) compared to NHF/PP/MAPP is also observed Figure 7. Similar result was reported in the research of glass sphere/polyethylene composites [32]. It could be attributed to high molecular mobility of HMHEC due to its small molecular weight compared with PP. It is also noticed that MAPP addition results in more significant reduction of adhesion factor, which indicates that resin modification is more effective in improving the mechanical properties of the hemp/PP composites.

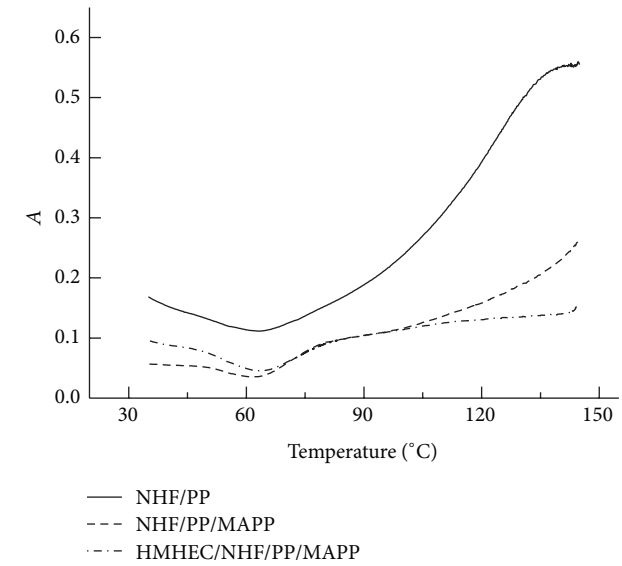

Figure 7: Adhesion factor of different composites.

4. Conclusions

The incompatibility of hydrophilic hemp fibre and hydrophobic polypropylene leads to poor interfacial bonding between

the fibre and the matrix. Resin modification and fibre treatment are effective in improving the interfacial bonding, which results in improved mechanical properties. MAPP resin modification leads to 40% improvement in tensile strength, 47% in flexural strength, and 44% in impact strength. When combining fibre treatment with resin modification, the mechanical properties are further improved, and the resulted hemp/PP composites achieved a tensile strength of 44.5 MPa, a flexural strength of 60.9 MPa, and an impact strength of 39.3 KJ/m^2. The fracture surface observation indicates that the fracture mechanism is changed from fibre pullout to fibre breakage after the resin modification and fibre treatment. The improvement of interfacial bonding can be quantitatively evaluated by fibre matrix adhesion.

Acknowledgments

This work has been partially supported by Australia Cooperative Research Centre in Advanced Composite Structures. The authors would like to thank Wenzhou Lisen Enterprises Co., Ltd., for its help in carrying out the experimental work.

References

[1] P. Asokan, M. Osmani, and A. D. F. Price, "Assessing the recycling potential of glass fibre reinforced plastic waste in concrete and cement composites," *Journal of Cleaner Production*, vol. 17, no. 9, pp. 821–829, 2009.

[2] M. J. John and S. Thomas, "Biofibres and biocomposites," *Carbohydrate Polymers*, vol. 71, no. 3, pp. 343–364, 2008.

[3] F. P. La Mantia and M. Morreale, "Green composites: a brief review," *Composites Part A*, vol. 42, no. 6, pp. 579–588, 2011.

[4] S. N. Monteiro, F. P. D. Lopes, A. S. Ferreira, and D. C. O. Nascimento, "Natural-fiber polymer-matrix composites: cheaper, tougher, and environmentally friendly," *JOM*, vol. 61, no. 1, pp. 17–22, 2009.

[5] K. G. Satyanarayana, G. G. C. Arizaga, and F. Wypych, "Biodegradable composites based on lignocellulosic fibers: an overview," *Progress in Polymer Science*, vol. 34, no. 9, pp. 982–1021, 2009.

[6] H. Y. Cheung, M. P. Ho, K. T. Lau, F. Cardona, and D. Hui, "Natural fibre-reinforced composites for bioengineering and environmental engineering applications," *Composites Part B*, vol. 40, no. 7, pp. 655–663, 2009.

[7] M. S. Huda, L. T. Drzal, D. Ray, A. K. Mohanty, and M. Misra, "Natural-fibre composites in the automotive sector," in *Properties and Performance of Natural-Fibre Composites*, K. L. Pickering, Ed., pp. 256–261, CRC Press, Washington, DC, USA, 2008.

[8] D. Puglia, J. Biagiotti, and J. M. Kenny, "A review on natural fibre-based composites. Part II: application of natural reinforcements in composite materials for automotive industry," *Journal of Natural Fibers*, vol. 1, no. 3, pp. 23–65, 2004.

[9] M. P. Ho, J. H. WangH Lee, C. K. Ho, K. T. Lau, J. S. Leng, and D. Hui, "Critical factors on manufacturing processes of natural fibre composites," *Composites Part B*, vol. 43, no. 8, pp. 3549–3562, 2012.

[10] N. L. Moigne, M. V. D. Oever, and T. Budtova, "A statistical analysis of fibre size and shape distribution after compounding in composites reinforced by natural fibres," *Composites Part A*, vol. 42, no. 10, pp. 1542–1550, 2011.

[11] A. Etaati, H. Wang, S. Pather, Z. L. Yan, and S. Mehdizadeh A, "3D X-ray microtomography study on fibre breakage in noil hemp fibre reinforced polypropylene composites," *Composites Part B*, vol. 50, pp. 239–246, 2013.

[12] A. Alemdar, H. Zhang, M. Sain, G. Cescutti, and J. Müssig, "Determination of fiber size distributions of injection moulded polypropylene/natural fibers using X-ray microtomography," *Advanced Engineering Materials*, vol. 10, no. 1-2, pp. 126–130, 2008.

[13] T. T. Doan, S. L. Gao, and E. Mäder, "Jute/polypropylene composites I. Effect of matrix modification," *Composites Science and Technology*, vol. 66, no. 7-8, pp. 952–963, 2006.

[14] J. Qian, L. Zhu, J. Zhang, and R. S. Whitehouse, "Comparison of different nucleating agents on crystallization of poly(3-hydroxybutyrate-co-3-hydroxyvalerates)," *Journal of Polymer Science B*, vol. 45, no. 13, pp. 1564–1577, 2007.

[15] T. J. Keener, R. K. Stuart, and T. K. Brown, "Maleated coupling agents for natural fibre composites," *Composites Part A*, vol. 35, no. 3, pp. 357–362, 2004.

[16] J. L. Thomason, "Why are natural fibres failing to deliver on composite performance?" in *Proceedings of the 17th International Conference on Composite Materials (ICCM '17)*, Edinburgh, UK, July 2009.

[17] X. Li, L. G. Tabil, and S. Panigrahi, "Chemical treatments of natural fiber for use in natural fiber-reinforced composites: a review," *Journal of Polymers and the Environment*, vol. 15, no. 1, pp. 25–33, 2007.

[18] J. George, M. S. Sreekala, and S. Thomas, "A review on interface modification and characterization of natural fiber reinforced plastic composites," *Polymer Engineering and Science*, vol. 41, no. 9, pp. 1471–1485, 2001.

[19] X. Yuan, K. Jayaraman, and D. Bhattacharyya, "Effects of plasma treatment in enhancing the performance of woodfibre-polypropylene composites," *Composites Part A*, vol. 35, no. 12, pp. 1363–1374, 2004.

[20] D. F. Caulfield, J. A. Koutsky, and D. T. Quillen, "Cellulose/polypropylene composites: the use of AKD and ASA sizes as compatibilizers," in *Wood-Fiber/Polymer Composites: Fundamental Concepts, Processes, and Material Options*, pp. 128–134, 1993.

[21] B. Nyström, R. Joffe, and R. Långström, "Microstructure and strength of injection molded natural fibre composites," *Journal of Reinforced Plastics and Composites*, vol. 26, pp. 579–599, 2007.

[22] G. W. Beckermann, K. L. Pickering, and N. J. Foreman, "Evaluation of the mechanical properties of injection moulded hemp fibre reinforced polypropylene composites," *Advanced Materials Research*, vol. 29-30, pp. 303–306, 2007.

[23] J. George, M. S. Sreekala, and S. Thomas, "A review on interface modification and characterization of natural fiber reinforced plastic composites," *Polymer Engineering and Science*, vol. 41, no. 9, pp. 1471–1485, 2001.

[24] P. Niu, B. Liu, X. Wei, X. Wang, and J. Yang, "Study on mechanical properties and thermal stability of polypropylene/hemp fiber composites," *Journal of Reinforced Plastics and Composites*, vol. 30, no. 1, pp. 36–44, 2011.

[25] Z. Y. Sun, H. S. Han, and G. C. Dai, "Mechanical properties of injection-molded natural fiber-reinforced polypropylene composites: formulation and compounding processes," *Journal of Reinforced Plastics and Composites*, vol. 29, no. 5, pp. 637–650, 2010.

[26] P. Mutjé, M. E. Vallejos, J. Gironès et al., "Effect of maleated polypropylene as coupling agent for polypropylene composites reinforced with hemp strands," *Journal of Applied Polymer Science*, vol. 102, no. 1, pp. 833–840, 2006.

[27] http://www.in-cosmetics.com/__novadocuments/2234.

[28] P. A. Sreekumar, R. Saiah, J. M. Saiter et al., "Effect of chemical treatment on dynamic mechanical properties of sisal fiber-reinforced polyester composites fabricated by resin transfer molding," *Composite Interfaces*, vol. 15, no. 2-3, pp. 263–279, 2008.

[29] R. Chandra, S. P. Singh, and K. Gupta, "Damping studies in fiber-reinforced composites: a review," *Composite Structures*, vol. 46, no. 1, pp. 41–51, 1999.

[30] I. Ghasemi and M. Farsi, "Interfacial behaviour of wood plastic composite: effect of chemical treatment on wood fibres," *Iranian Polymer Journal*, vol. 19, no. 10, pp. 811–818, 2010.

[31] M. Tajvidi, R. H. Falk, and J. C. Hermanson, "Effect of natural fibers on thermal and mechanical properties of natural fiber polypropylene composites studied by dynamic mechanical analysis," *Journal of Applied Polymer Science*, vol. 101, no. 6, pp. 4341–4349, 2006.

[32] J. Kubat, M. Rigdahl, and M. Welander, "Characterization of interfacial interactions in high density polyethylene filled with glass spheres using dynamic-mechanical analysis," *Journal of Applied Polymer Science*, vol. 39, no. 7, pp. 1527–1539, 1990.